ABSTRACT

Title of Dissertation: RECOVERY AND RECONSTRUCTION IN QUANTUM SYSTEMS

Yixu Wang
Doctor of Philosophy, 2022

Dissertation Directed by: Professor Brian Swingle
Department of Physics

Quantum systems are prone to noises. Accordingly, many techniques are developed to cancel the action of a quantum operation, or to protect the quantum information against the noises. In this dissertation, I discuss two such schemes, namely the recovery channel and the quantum error correction, and various scenarios in which they are applied.

The first scenario is perfect recovery in the Gaussian fermionic systems. When the relative entropy between states ρ and σ remains unchanged under a channel, then perfect recovery of state ρ can be achieved, using σ as the reference state. It is realized by the Petz recovery map. We study the Petz recovery map in the case where the quantum channel and input states are fermionic and Gaussian. Gaussian states are convenient because they are totally determined by their covariance matrix and because they form a closed set under so-called Gaussian channels. Using a Grassmann representation of fermionic Gaussian maps, we show that the Petz recovery map is also Gaussian and determine it explicitly in terms of the covariance matrix of the reference

state and the data of the channel. As a by-product, we obtain a formula for the fidelity between two fermionic Gaussian states. This scenario is based on the work [1].

The second scenario is approximate recovery in the context of quantum field theory. When perfect recovery is not achievable, the existence of a universal approximate recovery channel is proven. The approximation is in the sense that the fidelity between the recovered state and the original state is lower bounded by the change of the relative entropy under the quantum channel. This result is a generalization of previous results that applied to type-I von Neumann algebras in [2]. To deal with quantum field theory, the type of the von Neumann algebras is not restricted here. This induces qualitatively new features and requires extra proving techniques. This result hinges on the construction of certain analytic vectors and computations/estimations of their Araki-Masuda L_p norms. This part is based on the work [3].

The third scenario is applying quantum error correction codes on tensor networks on hyperbolic planes. This kind of model is proposed to be a toy model of the AdS/CFT duality, thus also dubbed holographic tensor network. In the case when the network consists of a single type of tensor that also acts as an erasure correction code, we show that it cannot be both locally contractible and sustain power-law correlation functions. Motivated by this no-go theorem, and the desirability of local contractibility, we provide guidelines for constructing networks consisting of multiple types of tensors which are efficiently contractible variational ansatze, manifestly (approximate) quantum error correction codes, and can support power-law correlation functions. An explicit construction of such networks is also provided. It approximates the holographic HaPPY pentagon code when variational parameters are taken to be small. This part is based on the work [4].

Supplementary materials and technical details are collected in the appendices.

RECOVERY AND RECONSTRUCTION IN QUANTUM SYSTEMS

by

Yixu Wang

Dissertation submitted to the Faculty of the Graduate School of the
University of Maryland, College Park in partial fulfillment
of the requirements for the degree of
Doctor of Philosophy
2022

Advisory Committee:
Professor Theodore Jacobson, Chair
Professor Brian Swingle, Advisor/ Co-chair
Professor Victor Albert
Professor Raman Sundrum
Professor Jonathan Rosenberg

Dedication

This dissertation is dedicated to my parents, who raised me, shaped me and are always supporting me.

Acknowledgments

I am grateful to many people I meet and interact with in my life.

First of all, I would like to thank my advisor Brian Swingle. He is always optimistic, encouraging and supportive. He always tries to provide the most comfortable and unrestrained research environment for me. He is always available when I need suggestions or support. It was him who consolidated my confidence when I was most depressed and self-doubting. I feel fortunate to be his student and I wish to live upto his expectations with my efforts.

I wish to express my appreciation to the people who assist my academic career. I wish to thank my undergraduate advisor Ling-Yan Hung. Were it not for her assistance, I would hardly have had the chance to start the journey of PhD. I wish to thank my collaborators Thomas Faulkner, Stefan Hollands, ChunJun Cao, Jason Pollack and Zhou Shangnan. They share their knowledge and inspirations selflessly. Without their help, many works presented here can hardly be accomplished. I would also like to thank my fellow researchers Gong Cheng, Stefano Antonini, Subhayan Sahu, Rodrigo Silva, Batoul Banihashemi, Alireza Parhizkar and others. Your sharp insights broadened my horizons and deepened my understanding. The time spent on discussing with you will be a nice memory of my life.

I owe a lot to my friends in many dimensions. I am most grateful to my roommates Sun-Ting Tsai and Yihang Wang. It is via their support in my everyday life and my mentality that I was able to maintain a relatively stable body and mental health during this highly pressive time of PhD research and this unexpected extremely uncertain period of Covid-19 pandemic. I would like to thank Yiming Cai, Neill Warrington, Yukari Yamauchi and Dan Zhang for providing a friendly and supportive office atmosphere. I wish to express my gratitude to my old friends Chenxi Huang, Yikun Jiang, Yifu Yang, Yimei Zheng, Yang Wang, Xucheng Gan, Wentao Guan, Wei Zhang, Haoyang Gu, Xudong Zhu, Lingyao Zhou, as well as new friends Yijia Xu, En-Jui Kuo, Vu Tran Dinh Duy, Zhiyu Yin, Yalun Yu and many many others. No matter whether they provided valuable advice when I had to make decisions, or they just patiently listened to my daily complaints, minor worries, or trivial opinions, their support and influence on me are tremendous.

Lastly, I wish to express my gratitude to my family members. My parents provided all their efforts and resources to support my growth, my development and my dream. If I had any achievements, they should be attributed to them. I want to express my special gratitude to my grandfather. As a teacher himself, I cannot remember any concrete knowledge learnt from him. But my curiosity of nature, my passion for the research and my attitude towards the world, are all inherited from him. Without his influence, it would be very unlikely for me to dream of pursuing a doctor degree.

Table of Contents

List of Figures

List of Abbreviations

AdS	Anti de Sitter spacetime
(A)QECC	(Approximate) Quantum Error Correction Code
ANEC	Averaged Null Energy Condition
CFT	Conformal Field Theory
CP	Completely Positive
EP	Edge Polygon
HaPPY code	Harlow-Pastawski-Preskill-Yoshida code
HMERA	Hyper-invariant Multiscale Entanglement Renormalization Ansatz
LHS	Left Hand Side
MERA	Multiscale Entanglement Renormalization Ansatz
MMI	Monogamy of Mutual Information
RHS	Right Hand Side
TP	Trace Preserving
QNEC	Quantum Null Energy Condition
VP	Vertex Polygon

Chapter 1: Introduction

Quantum systems are delicate and prone to various kinds of noises from the environment. Systems of our interest are usually idealized to be isolated, so that their evolution is determined solely by the system Hamiltonian as designed. However, in nature any system is inevitably coupled to the environment. Coupling to the environment on the one hand enables controls over the system, so that quantum channels can be performed on a system. On the other, it is also this coupling to the environment that introduces unavoidable noise to the system. Therefore, to make practical use of quantum systems, we need to deal with undesired quantum operations when they occur, which amounts to studying whether or in what circumstances they could be undone. This naturally introduces the idea of quantum recovery channels. Or, we wish to develop methods to store quantum information in a noise-resistant way. This idea leads to the theory of quantum error correction code(QECC) [5]. Under certain conditions, a perfect recovery channel does exist. It is named Petz recovery channel and will be better introduced in Section (1.1.1). QECCs are an important class of examples where perfect recovery is achievable and the Petz recovery channel can be constructed explicitly [6].

In this dissertation, I present three scenarios where the above frameworks are applied or extended. The form of the Petz recovery channel is in general complicated. To get a better understanding, in Chapter (2) I study the relatively simple system of Gaussian fermions and obtain an explicit form of the Petz recovery channel. In Chapter (3), I extend my study from systems with finite degrees of freedom to those with infinite ones, i.e. quantum field theory (QFT). and from perfect recovery to the more realistic approximate recovery. In Chapter (4), I study the approximate QECC in the context of anti de Sitter spacetime/ conformal field theory duality (AdS/CFT).

These three scenarios are chosen in line with my long term goal of studying the reconstruction problem in AdS/CFT. It was suggested in [7] that the duality can be viewed as a quantum channel so the reconstruction in AdS/CFT is a problem of finding an appropriate recovery channel. Most of the concrete AdS/CFT models are based on the large N limit of gauge theories, where the physical fields are approximately free. So I start my research with Gaussian fermion systems in (2), which are also known as generalized free fermions. To treat quantum gravity properly, it is necessary to deal with quantum field theories as the proper description of matter in curved spacetime. Therefore, in Chapter (3) I try to extend the theory of approximate recovery to QFTs. The approximate QECC studied in Chapter (4) are toy models of AdS/CFT duality. My effort concentrates in trying to capture more realistic features of AdS/CFT, especially the power-law decay of the primary opeartors two-point functions in the boundary CFT. They are steps towards my final goal.

1.1 Perfect recovery in finite system: Petz recovery channel of Fermionic Gaussian systems

The motivation for studying recovery channels comes not only from the intrinsic delicate nature of quantum systems, but also from the intensive interaction between quantum information and many other fields of physics, such as quantum field theory and topological quantum matter. The Petz recovery map has important applications in many of these circumstances. For example, one can show that strong subadditivity of the von Neumann entropy implies the averaged null energy condition (ANEC) in relativistic quantum field theories in Minkowski spacetime [8]. The strong subaddativity can be written in terms of the monotonicity of relative entropy, $S(\rho_{ABC}\|\rho_A\otimes\rho_{BC}) \geq S(\rho_{AB}\|\rho_A \otimes \rho_B)$, under the channel of tracing out part C. The saturation of the ANEC bound requires achieving the equality in the above inequality, which is the same condition as the existence of a perfect recovery map, whose forward channel is an inclusion in the null direction. This is the same setup as the example studied in Section (3.4.2) of Chapter (3). Another example is provided by quantum error correction, say in the context of topological quantum matter, where the Petz map serves as a universal reversal operation that generates no more than twice the error of the optimal reversal operation[6]. The Petz map also arises in the structure of quantum Markov states [9], and such Markov states have been used to construct thermal states of quantum many-body systems [10]. These examples make an explicitly calculable form of the Petz recovery map important in its own right. In Chapter (2), we solve this problem for the special case of Gaussian fermionic states and channels, they are together collectively called fermionic Gaussian systems.

1.1.1 Perfect recovery channel and its existence

We start by stating what a legitimate quantum operation is. Rotating a rigid body or breaking a chinaware plate are examples of classical operations. They can be reversed or not for obvious reasons. On the quantum level, an operation needs to satisfy the complete positivity (CP) condition and the trace preserving (TP) condition to be compatible with the principles of quantum mechanics. Such a compatible operation is called a quantum channel or a CPTP map. Given only this abstract definition, it is less obvious under what conditions we can reverse a given quantum channel. It turns out that for certain channels and input states satisfying an information theoretic criterion, it is possible to perfectly reverse the channel and recover the initial state. The operation that implements this perfect reversal is called Petz recovery channel [11, 12].

Mathematically, recovering one particular state is trivial. Let $\mathcal{N}$ be a channel and ρ a state. We just need to discard $\mathcal{N}(\rho)$, the state contaminated by errors, and replace it with a fresh new state ρ. This is a legitimate quantum channel but is too specific to be practical. At the same time, when we perform the recovery, we wish to preserve the entanglement between the system to be recovered and the environment, if there initially were entanglement between them. The naive state substitution recovery clearly breaks the entanglement. What we really want is to develop a recovery method that can apply to a set of states we are interested in. In this process we do not want to mess up one state in this set with another. This is why in the discussion of recovery channels, we need to introduce a reference state, rather than just focusing on one state. It is in the same set as the interested state ρ. We need the presence of another state to compare with so that we can determine whether the error channel harms the distinguishability between the states ρ and σ.

The quantum error correction is a concrete example of a recovery channel. There, the family of the interested states is the so-called "code subspace", i.e. the states that represent the logical information. The reference state in the QECC context is another state in the code subspace. It is sometimes taken as the maximally mixed state in the code subspace. To see this, we note that the quantum error correction condition, $\langle\psi_i|E_a^\dagger E_b|\psi_j\rangle = C_{ab}\delta_{ij}$, imposes a similar requirement. That is, if two states were initially orthogonal to each other, they should be still orthogonal after errors occur. So that this set of errors will not mix up different states, thus can be corrected with respect to this set of states. The very non-trivial mathematical result of quantum recovery is that, if the states in a set all satisfy the perfect recovery condition, then the form of the recovery map, though explicitly dependent on the reference state, is actually independent of the choice of reference states. Also, this recovery map can recover any state in this set. This is exactly the more practical recovery method we look for.

The Petz recovery channel first originated from considering the notion of sufficiency of channels over von Neumann algebras[11, 12]. A channel $\mathcal{N}$ between two algebras $\mathcal{N}: M \to N$ is called "sufficient" with respect to a family of states θ, if there exists a channel $\mathcal{R}: N \to M$ such that for any $\phi \in \theta$, $\mathcal{R} \circ \mathcal{N}(\phi) = \phi$.[1] $\mathcal{R}$ is called a recovery channel because it recovers the initial state from the action of the channel $\mathcal{N}$. It turns out that sufficiency over θ is equivalent to sufficiency over any pair of the states in θ. A channel $\mathcal{N}$ is sufficient for a pair of states $\{\rho, \sigma\} \in \theta$ if and only if

$$S(\rho||\sigma) = S(\mathcal{N}(\rho)||\mathcal{N}(\sigma)). \tag{1.1}$$

$S(\rho||\sigma)$ is the relative entropy defined as

$$S(\rho||\sigma) = \text{tr}(\rho \log \rho) - \text{tr}(\rho \log \sigma) \tag{1.2}$$

[1]The notion of "sufficiency" is inherited from the literature of mathematical statistics. A statistic is any quantity computed from a given sample of probabilistic distribution. A set of statistics is sufficient with respect to a statistical model and its unknown parameter if no other statistic that can be calculated from the same sample provides any additional information as to the value of the parameter. A set of statistics R is sufficient for a parameterized family of distributions if and only if for each pair of probability distributions μ and ν from the family, the classical relative entropy obeys $S(\mu\|\nu) = S(\mu_R\|\nu_R)$, where μ_R, ν_R are these distributions restricted to R. To draw analogy to quantum cases, the samples of the distribution are analogous to density matrices. The concept of statistic is thought of as a manipulation of a given sample. So its quantum analogy is a quantum channel. The analog of classical relative entropy is the quantum relative entropy.

if supp(ρ) $\subseteq$ supp(σ), and $+\infty$ otherwise. The intuition is that the relative entropy measures the difference between two states. If such a channel $\mathcal{N}$ does not lose this distinguishability, then a perfect recovery channel is achieveable, this channel is called "Petz recovery channel". Mathematically, the relative entropy is non-increasing under any quantum channel. So if $\mathcal{N}$ is recoverable, the relative entropy should be unchanged under $\mathcal{N}$, as well as its recovery channel.

When the perfect recovery condition is satisfied, for density matrices of finite dimensional Hilbert space and a quantum channel $\mathcal{N} : M \to N$, Petz recovery channel takes the following explicit form on the support of $\mathcal{N}(\sigma)$: [9]

$$\mathcal{P}_{\sigma,\mathcal{N}}(X) = \sigma^{\frac{1}{2}}\mathcal{N}^* \left(\mathcal{N}(\sigma)^{-\frac{1}{2}} X \mathcal{N}(\sigma)^{-\frac{1}{2}}\right) \sigma^{\frac{1}{2}}. \tag{1.3}$$

Here supp($\mathcal{N}(\sigma)$) $= \{O|\text{tr}(O\mathcal{N}(\sigma)) \neq 0\}$. $\mathcal{N}^* : N \to M$ is defined to be the adjoint map of $\mathcal{N}$ such that $\langle A, \mathcal{N}(B)\rangle = \langle \mathcal{N}^*(A), B\rangle$ for any $A \in N, B \in M$. When the channel is in its Krauss representation $\mathcal{N}(\cdot) = \sum_a E_a^\dagger(\cdot)E_a$, the adjoint map takes the explicit form $\mathcal{N}^*(\cdot) = \sum_a E_a(\cdot)E_a^\dagger$. The inner product here takes the usual Hilbert-Schmidt form: $\langle A, B\rangle = \text{tr}(A^\dagger B)$. Note that if we restrict the input to $\mathcal{P}_{\sigma,\mathcal{N}}$ to be in supp $(\mathcal{N}(\sigma))$, then the operator inverse $\mathcal{N}(\sigma)^{-\frac{1}{2}}$ is well defined. Eq. (1.1) is obtained if and only if $\mathcal{P}_{\sigma,\mathcal{N}} \circ \mathcal{N}(\sigma) = \sigma$ and $\mathcal{P}_{\sigma,\mathcal{N}} \circ \mathcal{N}(\rho) = \rho$.

A variant of the Petz recovery man, named "rotated recovery map" was introduced in [13]. It is defined as

$$\mathcal{R}^t_{\sigma,\mathcal{N}}(X) \equiv \left(\mathcal{U}_{\sigma,t} \circ \mathcal{P}_{\sigma,\mathcal{N}} \circ \mathcal{U}_{\mathcal{N}(\sigma),-t}\right)(X), \tag{1.4}$$

where $\mathcal{P}_{\sigma,\mathcal{N}}$ is the Petz recovery map and $\mathcal{U}_{\sigma,t}(\cdot) \equiv \sigma^{it}(\cdot)\sigma^{-it}$ is a one-parameter group, where σ^{it} is a partial isometry. This means that if $X \in$ supp(σ), then σ^{it} is an isometry, if $X \notin$

supp(σ), then $\sigma^{it}X\sigma^{-it} = 0$. Especially, $\sigma^{i0} = P_\sigma$, which is the support projector of the state σ. This rotated recovery map is of interest because it appears in several works that strengthen the monotonicity of the relative entropy(e.g. [2, 13]), and helps to give a refined description of the recoverablity. It is physically interesting to investigate as it might give a stronger constraint for energy conditions in quantum field theory[14].

1.1.2 Fermionic Gaussian systems

The main effort of Chapter (2) is to characterize the Petz recovery map $\mathcal{P}_{\sigma,\mathcal{N}}$ for fermionic Gaussian channels and states via the Grassmann representation for fermionic Gaussian channels. It turns out that in this case $\mathcal{P}_{\sigma,\mathcal{N}}$ is also a Gaussian channel. The same result is established for $\mathcal{R}^t_{\sigma,\mathcal{N}}$ as well. We provide an explicitly calculable expression which might be useful, for example, for studying error correction in Majorana fermion systems or for studying free fermionic field theories.

Gaussian states are thermal states of Hamiltonians which are quadratic in creation and annihilation operators for both bosonic and fermionic operators. More precisely, a state ρ is Gaussian if it has the form $\rho = e^{-\beta H}/\mathrm{tr}(e^{-\beta H})$ for some quadratic H and inverse temperature β. The ground state of H, which is the limiting case as $\beta \to \infty$, is considered a Gaussian state as well. We denote canonical creation and annihilation operators by $c^\dagger, c$. They can be either bosonic or fermionic. The bosonic case could represent, for example, a system of photons, to which the subject of quantum optics is dedicated (e.g.[15]). The fermionic case could describe, for example, electrons or quarks. Here we consider the fermionic case. In either case, Gaussian states have a closure property such that certain so-called Gaussian channels send Gaussian input states to

Gaussian output states. The set of Gaussian channels includes many common operations such as tracing over subsystems and evolving under quadratic Hamiltonians. Furthermore, Gaussian states can be conveniently prepared in experiments [16] and described by the covariance matrix G. A more detailed discussion is presented in Section (2.1.1).

1.1.3 Main result

To state the main result, let $G^{(\sigma)}$ denote the covariance matrix of the reference state σ. Let a Gaussian channel $\mathcal{N}$ act on a Gaussian state with covariance matrix $G^{(\rho)}$. The covariance matrix of the output Gaussian state takes the form $G^{(\mathcal{N}(\rho))} = BG^{(\rho)}B^T + A$, where A, B are matrices encoding the action of channel $\mathcal{N}$ (see Section (2.1.2) for details). Our main result is that the corresponding A, B matrices for the recovery channel $\mathcal{P}_{\sigma,\mathcal{N}}$ are

$$\begin{aligned} B_{\mathcal{P}} &= \sqrt{I_{2n} + (G^{(\sigma)})^2} B^T \left(\sqrt{I_{2n} + (G^{(\mathcal{N}(\sigma))})^2} \right)^{-1}, \\ A_{\mathcal{P}} &= G^{(\sigma)} - B_{\mathcal{P}} G^{(\mathcal{N}(\sigma))} B_{\mathcal{P}}^T. \end{aligned} \tag{1.5}$$

Based on the above result, the rotated recovery map can be characterized by the matrices

$$A_{\mathcal{R},t} = B_{\sigma,t} A_{\mathcal{P}} B_{\sigma,t}^T, \quad B_{\mathcal{R},t} = B_{\sigma,t} B_{\mathcal{P}} B_{\mathcal{N}(\sigma),-t}, \tag{1.6}$$

in which $B_{\sigma,t} = e^{-2t \arctan G^{(\sigma)}}, B_{\mathcal{N}(\sigma),-t} = e^{2t \arctan G^{(\mathcal{N}(\sigma))}}$. It is noteworthy that Eq. (1.5) is analogous to that for bosonic Gaussian states[17].

The work introduced in this section is based on [1]. The full derivation is in Chapter (2). The corresponding supplementary materials are collected in Appendix (A). I performed the full derivations and analysis presented in the corresponding sections.

1.2 Approximate recovery in infinite systems: universal approximate recovery channel in quantum field theory

Although the perfect recovery in Chapter (2) gives compact elegant results, nature is not always perfect. When the relative entropy does change under a certain channel, perfect recovery is no longer achievable. In this case, we want to find a universal formula, to recover the channel approximately. At the same time, approximate recovery does have both theoretical and practical vaule. Consider the case in which one logical qubit is encoded into n physical qubits. If we restrict to the perfect recovery, no QECC can correct more than $n/4$ arbitrary errors happening on the physical qubits[18]. However, if approximate recovery is allowed, the logical qubit information can still be approximately achieved until up to $\lfloor (n-1)/2 \rfloor$ physical qubits have arbitrary errors [19]. Another scenario of interest, the AdS/CFT duality, is approximate if only finite order in the gravitational constant G is considered. So if recovery channels are applied in this context, they have to be approximate.

It turns out that for finite systems, a universal approximate recovery channel does exist. It was proven in [2] that

$$S(\rho\|\sigma) - S(\mathcal{N}(\rho)\|\mathcal{N}(\sigma)) \geq -2\log F(\rho, (\mathcal{R}_{\sigma,\mathcal{N}} \circ \mathcal{N})(\rho)). \tag{1.7}$$

Here $S(\rho\|\sigma)$ is the relative entropy between ρ and σ. F is the fidelity. It is a measurement of how close two quantum states are. For finite dimensions, it is defined in Eq. (2.42). Fidelity in infinite dimensions is defined in Eq. (3.23). Lemma (3.2.1) collects some important properties and other forms of fidelity. $\mathcal{R}_{\sigma,\mathcal{N}}$ is the desired approximate recovery channel that will be specified in Chapter (3). To characterize the deviation from perfect recovery, the natural parameter is the relative entropy difference before and after applying the channel, the LHS of the inequality. This lower bounds the fidelity between the original state and the recovered state, thus also characterizes the extent of the approximation of the recovery channel.

The main effort of Chapter (3) is to generalize the result Eq.(1.7) from finite dimensional Hilbert spaces to the uncountably infinite dimensional Hilbert spaces of quantum field theory. While quantum computers typically manipulate finite dimensional Hilbert spaces, many applications of error correction to field theory and gravity go beyond this simple setting and a general treatment requires more sophisticated tools, including tools from the theory of operator algebras. Operator algebraic approaches have a long tradition in treating quantum field theory, see e.g. [20]. One might hope to approximate any of these physical systems by finite quantum systems, but this point of view can obscure crucial physical features that are more naturally expressed in a less restrictive approach. At the same time, the operator algebra approach is so general that expressing proofs of fundamental quantum information results in this language exposes the core nature of such proofs and ends up simplifying the approach in many situations. Indeed, many of the original theorems in quantum information have their origin in the study of operator algebras.

1.2.1 Main result

In Chapter (3), the results of [2], pertaining to the approximate reversibility of quantum channels, are generalized from a type-I von Neumann algebra[2] setting to general von Neumann

[2]Direct sums of matrix algebras or the algebra of all bounded operators on a separable Hilbert space.

algebras, stated as Theorem (3.1.2). At the heart of these results is a strengthened version of the monotonicity [21] of relative entropy (Theorem (3.1.1)). Chapter (3) deals with the sub-algebra case which involves a simple quantum channel called an inclusion. General quantum channel cases are treated in a different work [22].

Along the way, we prove two theorems that might be of independent interest. Theorem (3.2.1) concerns the computations of the derivatives of the "sandwiched" and "Petz" relative Renyi entropies for two nearby states. We call this result a first law because of its similarity to the first law of entanglement entropy in the setting of AdS/CFT [23, 24]. Theorem (3.2.2) pertains to a regularization procedure for relative entropy that produces states with finite relative entropy and also allows for continuous extrapolation of relative entropy when removing the regulator. The vectors that result from this procedure are important here because they lead to extended domains of holomorphy that allow us to proceed towards the proof of strengthened monotonicity with a similar argument as in the finite dimensional setting.

We will also discuss an application to the study of the quantum information aspects of quantum field theory that require this general von Neumann algebra setting. In the field theory context, new results using operator algebra methods have made it possible to make rigorous statements about the dynamics of interacting theories. For example, in Section (3.4.2), we conjecture that the quantum null energy condition, a bound on the local null energy density (proven in [25, 26]), can be derived from the strengthened monotonicity result that we derive in Chapter (3).

The work introduced in this section is based on [3]. The corresponding supplementary materials are collected in Appendix (B). I independently proposed this research topic and developed my approach of the proof in Section (3.3).

1.3 Approximate quantum error correction model of AdS/CFT: a model with power-law correlations

Chapter (4) presents a model of approximate quantum error correction codes, aiming to characterize some features of the AdS/CFT duality, especially the power-law decay of the two-point correlation functions of primary operators in CFT. QECC is actually an important class of quantum recovery channels. To see this connection, it is worthwhile to point out that the quantum error condition[5], $\langle\psi_i|E_a^\dagger E_b|\psi_j\rangle = C_{ab}\delta_{ij}$, is a sufficient condition the perfect recovery condition [11, 12]. Also, the standard error correction protocol, where we perform the syndrome measurement, then do the correcting operation depending on the syndrome measurement outcome, is equivalent to the Petz recovery channel [6]. So the AQEC model in this chapter is a concrete example of the approximate recovery presented in Chapter (3). The model is built on a tensor network that tiles the hyperbolic spatial surface of the AdS_3 spacetime.

1.3.1 Tensor network models of AdS/CFT

Tensor networks are powerful tools to elucidate many-body physics [27, 28] and quantum gravity[29, 30]. More recently, they have also been used to study quantum error correction both in the context of holography[31, 32, 33] and beyond[34, 35, 36, 37]. For the former category, it was proposed that the Multiscale Entanglement Renormalization Ansatz (MERA) [38] resembles a discretized version of the AdS/CFT correspondence [29]. At the same time, the AdS/CFT correspondence itself is believed to implement semi-classical bulk physics as a quantum error correction code (QECC) [39], where the bulk low-energy subspace defines a code subspace. A number of models of this correspondence have been given using tensor networks [31, 32, 33, 40, 41, 42, 43]. See [44] for a recent review.

While these constructions (MERA[38], HaPPY [31], random tensor networks [32], etc.) all capture some desirable features of the AdS/CFT correspondence, it is somewhat unclear how to unify these features under a single framework. MERA is an efficient variational ansatz capable of capturing the correlations and entanglement of the ground state while realizing an approximate quantum error correction code [45]. However, it does not fully capture the correct symmetries [46, 47, 48] of AdS/CFT and is somewhat at odds with gravitational expectations for entropy bounds [49]. These flaws are amended in the hyper-invariant tensor network [50]. However, in neither construction is there a clear physical picture of entanglement wedge reconstruction or code properties. For example, in MERA it is not clear how explicit logical operations can be realized on the boundary, or, equivalently, how to reconstruct some bulk operator from boundary operators. Although one can study cursory properties of the code[45], its decoding and error correction properties are far from manifest. As for the hyper-invariant tensor network, it is not clear how it should be interpreted as a QECC.

The HaPPY code [31] on the other hand, being a stabilizer code, is a clear-cut QECC with well-defined logical and decoding operations[33, 35, 37]. It also excels in reproducing the desirable features of subregion duality and bulk reconstruction. However, it is very limited as a variational ansatz for studying many-body quantum states. Even with interacting bulk Hamiltonians, the boundary correlations cannot be made consistent with those of a CFT[51]. In most cases, boundary connected two-point functions are vanishing. Nevertheless, it is possible to produce some non-trivial correlations with localized operators only on some specific locations on the boundary. The fraction of these locations on the boundary goes to 0 as the boundary of this network extends outward [52]. In the limit of large bond dimension, random tensor networks [32] can also produce a QECC and can sustain power-law decaying correlations. In principle, given a suitably chosen tessellation of the (hyperbolic) bulk, they also capture the symmetries of an underlying geometry. However, the randomness and the large bond-dimension limit inherent in their definition make it difficult for these networks to function as variational ansatze usable for many-body physics. Code properties and decoding also remain underexplored in this picture.

1.3.2 Main result

In Chapter (4), we bridge these gaps by creating what we call a hyper-invariant MERA (HMERA) tensor network that combines the features of MERA and those of a holographic QECC. The HMERA inherits some nice features of MERA. HMERA serves as a variational ansatz for wavefunctions on quantum many-body systems. Each external leg on a HMERA represents a qubit. When calculating the norm of the wavefunction, we need two copies of tensor networks, as ket and bra (its dual tensor). The inner product is then calculated by performing the tensor contraction. Similarly, correlation functions can be calculatead by contracting two copies of tensor networks, with operators inserted on the corresponding legs. HMERA is a type of tensor network whose index contractions with its dual tensor can be efficiently performed, just as MERA. [3] As a(n approximate) QECC, the network is able to support the correct power-law behaviour for the two-point function, as well as features of subregion duality/bulk reconstruction. We provide a set of general construction guidelines for building these HMERA networks

[3] Usually a (m, n) tensor $T^{\nu_1 \dots \nu_n}_{\mu_1 \dots \mu_m}$ can be viewed as a map from n sites to m sites. Its dual tensor is $T^{*\mu_1 \dots \mu_m}_{\nu_1 \dots \nu_n}$, obtained from T by upper indices lowered, lower indices uppered and each entry complex conjugated. It is a map from m sites to n sites. Doing the tensor contraction $T^{*\mu_1 \dots \mu_m}_{\nu'_1 \dots \nu'_n} T^{\nu_1 \dots \nu_n}_{\mu_1 \dots \mu_m} = T^* T^{\nu_1 \dots \nu_n}_{\nu'_1 \dots \nu'_n}$ gives a n to n map. Specifically, a $(m, 0)$ tensor $T_{\mu_1 \dots \mu_m}$ defines a state on m sites. And its contraction with its dual $T^{*\mu_1 \dots \mu_m} T_{\mu_1 \dots \mu_m}$ gives a number, which corresponds to the norm squared of this state.

and provide one explicit example which is manifestly a quantum error correction code and well-approximates the HaPPY pentagon code[31] if we choose some of the variational parameters to be small. We also discuss some general constraints such codes follow. In particular, we prove a no-go theorem, which states that locally contractible HMERAs constructed from any single kind of quantum erasure correction code must contain trivial correlation functions. Hence our explicit construction, with two distinct types of tensors, is one of the simplest possible networks to exhibit power-law correlations.

The work introduced in this section is based on [4]. I proposed the idea of analyzing the constraints to the isometries on the tensor networks based on the tiling structure. This developed into the no-go theorem (4.2.1). I also performed the full detailed analysis of the explicit HMERA model, collected in Appendix (C).

Chapter 2: Petz recovery channel in Fermionic Gaussian systems

This chapter presents the full story of the Petz recovery channel of Fermionic Gaussian systems. It is organized as follows: Section (2.1) is a detailed introduction to Gaussian states and Gaussian channels with fermionic degrees of freedom. In Section (2.2), we construct the Petz recovery map and its rotated version explicitly using the Grassmann representation of the Gaussian map to get Eq. (1.5),(1.6). In Section (2.3), we present a result giving the fidelity between two fermionic Gaussian states, which is an application of the methods developed in Section (2.2) and provides a different formula from that in Ref.[53]. Section (2.4) is a brief summary of this chapter. The supplementary materials of this chapter are collected in Appendix (A). Some identities for Grassmann integrals are presented in Appendix (A.1). Appendix (A.2) is a collection of calculation details. Appendix (A.3) discusses the treatment of singular matrices involved in the derivation.

2.1 Fermionic Gaussian states and channels

We first give a brief introduction to the fermionic Gaussian state and fermionic Gaussian channels. Here we mainly follow the results of Ref. [54]. Some other reviews that introduce different aspects of Gaussian states and channels can be found in Refs. [55, 56, 57, 58]. Interested readers can refer to the references therein.

2.1.1 Fermionic Gaussian States

Dirac and Majorana Operators, Grassmann Variables

We start by considering a Hamiltonian quadratic in complex (Dirac) fermionic creation/ annihilation operators:

$$H = \sum_{i,j=1}^{n} c_i^\dagger K_{ij} c_j + c_i^\dagger A_{ij} c_j^\dagger + c_i A_{ij}^\dagger c_j. \tag{2.1}$$

Here $c^\dagger$'s and c's satisfy the canonical anti-communication relation

$$\{c_i^\dagger, c_j\} = \delta_{ij}, \quad \{c_i, c_j\} = \{c_i^\dagger, c_j^\dagger\} = 0. \tag{2.2}$$

The matrix K is Hermitian and A is anti-symmetric, so that the Hamiltonian is Hermitian.

It is standard to transform Eq. (2.1) into a basis of Majorana fermions:

$$\gamma_{2i-1} = (c_i + c_i^\dagger), \gamma_{2i} = i(c_i - c_i^\dagger), \tag{2.3}$$

which satisfy the anti-commutation relation

$$\{\gamma_i, \gamma_j\} = 2\delta_{ij}\hat{I}. \tag{2.4}$$

After ignoring the diagonal terms[1], Eq. (2.1) can be written as

$$H = \frac{i}{2} \sum_{i,j=1}^{2n} \gamma_i M_{ij} \gamma_j, \tag{2.5}$$

where

$$M = \frac{1}{4}\Im(K) \otimes I_2 + \frac{1}{2}\Re(A) \otimes \sigma_x - \frac{i}{4}\Re(K) \otimes \sigma_y + \frac{1}{2}\Im(A) \otimes \sigma_z. \tag{2.6}$$

Here σ's are the Pauli matrices and M is manifestly real and antisymmetric.

The most general form of the operators composed of $2n$ Majorana operators, denoted as $\mathcal{C}_{2n}$, should be the complex span of the monomials $\gamma_i \gamma_j ... \gamma_k$:

$$X = \alpha \hat{I} + \sum_{p=1}^{2n} \sum_{1 \le a_1 < a_2 < ... < a_p \le n} \alpha_{a_1 a_2 ... a_p} \gamma_{a_1} \gamma_{a_2} ... \gamma_{a_p}, \tag{2.7}$$

where $\alpha = 2^{-n} \mathrm{tr} X$ is fixed. For example, the Hamiltonian in Eq. (2.5) $H \in \mathcal{C}_{2n}$, where only the coefficients of order 2 terms are non-zero and purely imaginary.

To work efficiently with operators built from the Majorana fermions, it is convenient to utilize a Grassman calculus. Grassmann variables are mathematical objects following the anti-commutation rule

$$\theta_i \theta_j + \theta_j \theta_i = 0, \quad \theta_i^2 = 0. \tag{2.8}$$

For n Grassmann variables $\{\theta_1, \theta_2, ..., \theta_n\}$, denote the complex span of the monomials of these

[1] The diagonal terms contribute as a number which is the total self-energy of all the modes. It can be absorbed in a redefinition of the zero of energy.

variables as $\mathcal{G}_n$. A general element $f \in \mathcal{G}_n$ takes the form

$$f = \alpha + \sum_{p=1}^{n} \sum_{1 \leq a_1 < a_2 < \ldots < a_p \leq n} \alpha_{a_1 a_2 \ldots a_p} \theta_{a_1} \theta_{a_2} \ldots \theta_{a_p}. \tag{2.9}$$

The similarity between Eq. (2.7) and Eq. (2.9) indicates that there is a natural isomorphism $\omega : \mathcal{C}_{2n} \to \mathcal{G}_{2n}$ such that

$$\gamma_i \gamma_j \ldots \gamma_k \longmapsto \theta_i \theta_j \ldots \theta_k, \quad \hat{I} \longmapsto 1. \tag{2.10}$$

So each Majorana operator X can be mapped via ω to a polynomial of Grassmann variables $\omega(X, \theta)$. We will abbreviate $\omega(X, \theta)$ as $X(\theta)$ and call it the Grassmann representation of the operator X.

Majorana and Grassmann representation of Gaussian states

Fermionic Gaussian states are in general thermal states for some Hamiltonian of the form in Eq. (2.5),

$$\rho \equiv \mathrm{tr}\big(e^{-\beta H}\big)^{-1} e^{-\beta H} = Z_\rho^{-1} \exp\left(\frac{i}{2}\beta \sum_{i,j=1}^{2n} \gamma_i M_{ij} \gamma_j\right). \tag{2.11}$$

This is the Majorana representation of fermionic Gaussian states.

Any real $2n \times 2n$ antisymmetric matrix can be transformed into the following block-diagonal form:

$$M = O^T \left(B \otimes \begin{pmatrix} 0 & -1 \\ 1 & 0 \end{pmatrix} \right) O, \tag{2.12}$$

where $O \in SO(2n)$ and $B = \mathrm{diag}(\beta_1, \beta_2, \ldots \beta_n)$. The β_i's are the Williamson eigenvalues of the real antisymmetric matrix M.

The covariance matrix of a Gaussian state is defined as

$$G_{ij} = \frac{i}{2}\mathrm{tr}(\rho[\gamma_i, \gamma_j]). \tag{2.13}$$

Here G is antisymmetric and can be transformed into the block-diagonal form with the same matrix O as in Eq. (2.12). Its set of Williamson eigenvalues $\{\lambda_1, \lambda_2, ..., \lambda_n\}$ are related to β_i's via [59]

$$\lambda_i = -\tanh\left(\beta\beta_i\right). \tag{2.14}$$

This induces the matrix equation [2]

$$G = i\tanh\left(i\beta M\right). \tag{2.15}$$

Since Gaussian states represent the non-interacting limit of the corresponding fermionic degrees of freedom, all higher order correlation functions are totally determined by the matrix elements of G by Wick's theorem.

One can use the isomorphism Eq. (2.10) to get the Grassmann representation of the density operator in Eq. (2.11). [3] It turns out that the covariance matrix G plays a role in the Grassmann representation[4]:

$$\rho(\theta) = \frac{1}{2^n}\exp\left(\frac{i}{2}\theta^T G\theta\right). \tag{2.16}$$

[2]Eq. (2.15) can be found in e.g Ref [53]. We verify a generalization of it in Section (A.2.1) for the completion of the context. A bosonic version of this relation between covariance matrix and the Hamiltonian can be found in Ref. [60].

[3]The isomorphism Eq. (2.10) can only be used when the operator is written in the form of Eq. (2.7). In this case there are no identical operators in each monomial so the γ_i's and θ_i's are interchangeable.

[4]One can define displacement operator $D(\mu)$ in terms of Grassmann variables μ_i's [61]. However,the expectation value of observables in the displaced states would involve the product of Grassmann numbers, whose physical meanings are ambiguous to the author. Though an important completion of the theory, we do not consider it here.

The full notational conventions and some useful formula are in Appendix (A.1).

Eq. (2.16) is a more convenient definition of the Gaussian state, because the matrix G is always bounded by $G^T G \leq I$ according to Eqs. (**??**). The Majorana representation Eq. (2.11) looks singular in the zero temperature limit $\beta \to \infty$, while in the Grassmann representation, this limit corresponds to $\lambda_i \to \pm 1$. This reflects the physical situation that at zero temperature, negative energy modes are occupied and positive energy modes are empty.

2.1.2 Fermionic Gaussian Channels

A linear map $\mathcal{N} : \mathcal{C}_{2n} \to \mathcal{C}_{2n}$ is Gaussian if and only if it admits an integral representation

$$\mathcal{N}(X)(\theta) = C \int \exp[S(\theta, \eta) + i\eta^T \mu] X(\mu) D\eta D\mu, \tag{2.17}$$

where

$$S(\theta, \eta) = \frac{i}{2}(\theta^T, \eta^T) N \begin{pmatrix} \theta \\ \eta \end{pmatrix} \equiv \frac{i}{2}(\theta^T, \eta^T) \begin{pmatrix} A & B \\ -B^T & D \end{pmatrix} \begin{pmatrix} \theta \\ \eta \end{pmatrix} = \frac{i}{2}\theta^T A\theta + \frac{i}{2}\eta^T D\eta + i\theta^T B\eta. \tag{2.18}$$

Here A, B, D are $2n \times 2n$ complex matrices and A, D can be taken to be antisymmetric. C is a complex number.

To have the linear map be a valid quantum channel, the CPTP conditions should be satisfied. It turns out that the CP condition translates to $C \geq 0$ and requirement that the matrix N in Eq. (2.18) be real and satisfy $N^T N \leq I$. The TP condition is equivalent to $C = 1$ and the matrix $D = 0$. A map is unital if it preserves the identity, which means $\mathcal{N}(I) = I$. The unital condition is equivalent to $C = 1$ and $A = 0$.

One important ingredient is how to translate the description of quantum channels from the operator representation, e.g., a unitary time evolution written as $e^{iHt}\rho e^{-iHt}$, to the path integral representation defined in Eq. (2.17). [5] This is achieved by making use of the Choi-Jamiolkowski duality between linear maps and states. The duality says that for any linear map $\mathcal{E} : \mathcal{C}_{2n} \to \mathcal{C}_{2n}$, there is an isomorphism $\mathcal{J}$ such that $\mathcal{J}(\mathcal{E}) \in \mathcal{C}_{2n} \otimes \mathcal{C}_{2n}$ takes the form

$$\mathcal{J}(\mathcal{E}) = \sum_l \mathcal{E}(V_l) \otimes V_l^*, \tag{2.19}$$

where V_l's are a complete set of bases for the linear spaces $\mathcal{C}_{2n}$, which are the monomials of $\gamma_i \gamma_j ... \gamma_k$.

To get a compact formula, one uses the isomorphism $\mathcal{I} : \mathcal{C}_{2n} \otimes \mathcal{C}_{2n} \to \mathcal{C}_{4n}$ such that $\gamma_{p_1} .. \gamma_{p_i} \otimes \gamma'_{q_1} ... \gamma'_{q_j} \longmapsto \gamma_{p_1} ... \gamma_{p_i} \gamma_{q_1+2n} ... \gamma_{q_j+2n}$, where $1 \leq p_1 < ... < p_i \leq 2n$ and $1 \leq q_1 < ... < q_j \leq 2n$. This isomorphism induces a map $\mathcal{N}_1 \otimes_f \mathcal{N}_2 : \mathcal{C}_{4n} \to \mathcal{C}_{4n}$ such that for monomials

$$\mathcal{N}_1 \otimes_f \mathcal{N}_2 \left(\gamma_{p_1} ... \gamma_{p_i} \gamma_{q_1+2n} ... \gamma_{q_j+2n}\right) = \mathcal{N}_1 \left(\gamma_{p_1} ... \gamma_{p_i}\right) \mathcal{N}_2 \left(\gamma_{q_1+2n} ... \gamma_{q_j+2n}\right). \tag{2.20}$$

The definition can be extended to polynomials of $\mathcal{C}_{4n}$ by linearity.

Now let a linear map $\mathcal{E} : \mathcal{C}_{2n} \to \mathcal{C}_{2n}$ be parity preserving, which means it sends even(odd) order monomials to even(odd) order monomials, then the operator $\rho_{\mathcal{E}} \in \mathcal{C}_{4n}$ dual to $\mathcal{E}$ is defined as

$$\rho_{\mathcal{E}} = \left(\mathcal{E} \otimes_f \hat{I}\right)(\rho_I), \tag{2.21}$$

[5] We draw an analogy of this procedure to transforming from a Hamiltonian formalism to a Lagrangian formalism, as is suggested by the title of Ref. [54].

where

$$\rho_I = \frac{1}{2^{2n}} \prod_{i=1}^{2n} \left(\hat{I} + i\gamma_i \gamma_{2n+i} \right). \tag{2.22}$$

Intuitively, this is a maximally entangled state in the sense that each mode of γ_i is linked to γ_{2n+i}. One can work out the form of the density matrix explicitly to show it is the density matrix of a maximally entangled state up to some one-site local unitaries. One can now make use of Eq.(2.10) to write Eq. (2.21) in the Grassmann representation. The isomorphism is such that $\gamma_1, ..., \gamma_{2n} \mapsto \theta_1, ..., \theta_{2n}$ and $\gamma_{2n+1}, ..., \gamma_{4n} \mapsto \eta_1, ..., \eta_{2n}$. Given the integral representation of the map $\mathcal{E}$, a straightforward calculation of Eq. (2.18) will give

$$\rho_{\mathcal{E}}(\theta, \eta) = \frac{C}{2^{2n}} \exp\left(S(\theta, \eta)\right) \tag{2.23}$$

as the operator representation of a map. Conversely, if one knows the operator representation of the map $\mathcal{E}$, one can calculate Eq. (2.21) explicitly and perform the isomorphism Eq. (2.10) to achieve a form similar to Eq. (2.23), so that the integral representation can be read out.

We conclude this section by mentioning an important property of the composition of two Gaussian channels. If $\mathcal{E}_1$ and $\mathcal{E}_2$ are CP fermionic Gaussian maps, then the composite map $\mathcal{E}_2 \circ \mathcal{E}_1$ is still a CP Gaussian map. Similarly, the composition of two TP Gaussian maps is still a TP Gaussian map. The proof of the results listed in this section can be found in Ref. [54].

2.2 Construction of the Petz recovery map

In this section we give the explicit construction of the Petz recovery map, so that the result claimed in the introduction is obtained: the Petz recovery map of a Gaussian channel with a

Gaussian reference state is a Gaussian channel itself, and has its information specified in the Grassmann integral representation as in Eq. (1.5). Readers who are interested in the calculation details throughout this section can refer to Appendix A.2.

It is obvious from Eq. (1.3) that $\mathcal{P}_{\sigma,\mathcal{N}}$ is composed of three linear maps [17]: $\mathcal{P}_{\sigma,\mathcal{N}} = \mathcal{N}_3 \circ \mathcal{N}_2 \circ \mathcal{N}_1$, where

$$\begin{aligned} &\mathcal{N}_1 : X \mapsto \mathcal{N}(\sigma)^{-\frac{1}{2}} X \mathcal{N}(\sigma)^{-\frac{1}{2}}, \\ &\mathcal{N}_2 : X \mapsto \mathcal{N}^*(X), \\ &\mathcal{N}_3 : X \mapsto \sigma^{\frac{1}{2}} X \sigma^{\frac{1}{2}}. \end{aligned} \tag{2.24}$$

The approach to the construction of $\mathcal{P}_{\sigma,\mathcal{N}}$ is therefore straightforward. We first find the Grassmann representations of the three separate maps in Eq. (2.24). Since they each admit an integral representation as in Eq. (2.17), the three separate maps are Gaussian linear maps. So it follows that the Petz map is Gaussian. Then we find the formula to combine the three maps together, thus obtaining an explicit expression for the Petz recovery map.

2.2.1 Separate construction of three linear maps

The linear maps $\mathcal{N}_1$ and $\mathcal{N}_3$ are of similar form: they represent an operator sandwiched by a Hermitian Gaussian state. Their integral representations are obtained by the map-operator duality described in Section (2.1.2).

We present the construction of $\mathcal{N}_3$, since that for $\mathcal{N}_1$ follows in a similar way. The details of the calculation are collected in Appendix (A.2.2).

Consider $\mathcal{N}_3 : X \mapsto \sigma^{\frac{1}{2}} X \sigma^{\frac{1}{2}}$ where σ is a Gaussian state with covariance matrix $G^{(\sigma)}$.

Using Eq. (2.12), define $\tilde{\gamma}_i = \sum_j O_{ij}\gamma_j$ and $\tilde{\gamma}_{2n+i} = \sum_j O_{ij}\gamma_{2n+j}$ where i, j goes from 1 to $2n$. So the Gaussian state σ can be written as

$$\sigma = \frac{1}{2^n}\prod_{i=1}^{n}\left(\hat{I} - i\lambda_i^{(\sigma)}\tilde{\gamma}_{2i-1}\tilde{\gamma}_{2i}\right). \tag{2.25}$$

One can write $\sigma^{\frac{1}{2}}$ as:

$$\sigma^{\frac{1}{2}} = \frac{1}{2^{\frac{n}{2}}}\prod_{i=1}^{n}\frac{1}{\sqrt{1+\lambda_i^{(\sigma^{\frac{1}{2}})2}}}\left(\hat{I} - i\lambda_i^{(\sigma^{\frac{1}{2}})}\tilde{\gamma}_{2i-1}\tilde{\gamma}_{2i}\right), \tag{2.26}$$

where

$$\lambda_i^{(\sigma^{\frac{1}{2}})} = -\lambda_i^{(\sigma)-1}\left(\sqrt{1-\lambda_i^{(\sigma)2}} - 1\right). \tag{2.27}$$

The Choi-Jamiolkowski dual of $\mathcal{N}_3$ can be explicitly calculated via Eq. (2.21) after substitution $\gamma_i \to \theta_i$, $\gamma_{i+2n} \to \eta_i$. Comparing with Eqs. (2.18), (2.23) and making use of Eq. (A.16), one can read out that the linear map $\mathcal{N}_3 : X \mapsto \sigma^{\frac{1}{2}}X\sigma^{\frac{1}{2}}$ corresponds to the following Grassmann integral representation:

$$A_3 = G^{(\sigma)}, B_3 = \sqrt{I_{2n} + (G^{(\sigma)})^2}, C_3 = \frac{1}{2^n}, D_3 = -G^{(\sigma)}. \tag{2.28}$$

One can calculate $N_3^T N_3 = I$ together with $C_3 > 0$ to see that $\mathcal{N}_3$ is a CP map, where N_3 is defined as in Eq. (2.18).

A similar calculation gives the Grassmann integral representation for $\mathcal{N}_1 : X \mapsto \mathcal{N}(\sigma)^{-\frac{1}{2}}X\mathcal{N}(\sigma)^{-\frac{1}{2}}$,

$$A_1 = -G^{(\mathcal{N}(\sigma))}, B_1 = \sqrt{I_{2n} + (G^{(\mathcal{N}(\sigma))})^2}, C_1 = 2^n \det \left(I_{2n} + \left(G^{(\mathcal{N}(\sigma))} \right)^2 \right)^{-\frac{1}{2}}, D_1 = G^{(\mathcal{N}(\sigma))}. \tag{2.29}$$

We have $N_1^T N_1 = I$ and $C_1 > 0$ so that $\mathcal{N}_1$ is completely positive as well. Here we have assumed that $\lambda^{(\sigma)} \neq \pm 1$ so $\mathcal{N}(\sigma)^{-\frac{1}{2}}$ is invertible. We discuss this in detail in Appendix (A.3.1).

$\mathcal{N}_2$ is the adjoint map of a given Gaussian linear map $\mathcal{N}$. As stated in the introduction, $\mathcal{N}^*$ is defined via $\langle A, \mathcal{N}(B) \rangle \equiv \langle \mathcal{N}^*(A), B \rangle$, where $\langle A, B \rangle = \text{tr}(A^\dagger B)$. So

$$\text{tr}\left(X^\dagger \mathcal{N}(Y) \right) = \text{tr}\left(\mathcal{N}^*(X)^\dagger Y \right). \tag{2.30}$$

One can obatian the following Grassmann integral representation of the adjonit map $\mathcal{N}^*$ for a general Gaussian linear map $\mathcal{N}$:

$$A_{\mathcal{N}^*} = D^\dagger, B_{\mathcal{N}^*} = B^\dagger, C_{\mathcal{N}^*} = C^\dagger, D_{\mathcal{N}^*} = A^\dagger. \tag{2.31}$$

For the case that $\mathcal{N}$ is a quantum channel, i.e. A, B are real, $C = 1$ and $D = 0$, we get

$$A_2 = 0, B_2 = B^T, C_2 = 1, D_2 = -A \tag{2.32}$$

The adjoint map of a quantum channel is a completely positive and unital map. This can be explicitly verified by the integral representation of $\mathcal{N}^*$ in Eq.(2.32). The calculation for this part is in Appendix (A.2.3).

We summarize the integral representation of the three maps:

$$A_1 = -G^{(\mathcal{N}(\sigma))}, B_1 = \sqrt{I_{2n} + (G^{(\mathcal{N}(\sigma))})^2}, C_1 = 2^n \det\left(I_{2n} + \left(G^{(\mathcal{N}(\sigma))}\right)^2\right)^{-\frac{1}{2}}, D_1 = G^{(\mathcal{N}(\sigma))};$$
$$A_2 = 0, B_2 = B^T, C_2 = 1, D_2 = -A;$$
$$A_3 = G^{(\sigma)}, B_3 = \sqrt{I_{2n} + (G^{(\sigma)})^2}, C_3 = \frac{1}{2^n}, D_3 = -G^{(\sigma)}. \tag{2.33}$$

2.2.2 Composition of three linear maps

Consider two Gaussian linear maps which are specified by A_1, B_1, C_1, D_1 and A_2, B_2, C_2, D_2. The combination of the two Gaussian linear maps is still a Gaussian linear map. We can readily calculate the corresponding $A_{2\circ 1}, B_{2\circ 1}, C_{2\circ 1}, D_{2\circ 1}$, by performing the $D\theta, D\beta$ integral in the expression

$$\mathcal{N}_2 \circ \mathcal{N}_1(X)(\alpha) = \int D\beta D\theta D\eta D\mu \exp\left(S_2(\alpha,\beta) + i\beta^T\theta\right) \exp\left(S_1(\theta,\eta) + i\eta^T\mu\right) X(\mu). \tag{2.34}$$

Using Eq. (A.6c) twice to integrate first over θ then β, and comparing with the form in Eq.(2.18), one can find

$$A_{2\circ 1} = A_2 + B_2\left(D_2 + A_1^{-1}\right)^{-1} B_2^T,\ B_{2\circ 1} = B_2\left(D_2 + A_1^{-1}\right)^{-1} A_1^{-1} B_1,$$
$$C_{2\circ 1} = C_1 C_2 (-1)^n \mathrm{Pf}\left(A_1\right) \mathrm{Pf}\left(D_2 + A_1^{-1}\right),\ D_{2\circ 1} = D_1 + B_1^T D_2\left(D_2 + A_1^{-1}\right)^{-1} A_1^{-1} B_1. \tag{2.35}$$

Here we have assumed the invertibility of the matrices A_1 and $\left(D_2 + A_1^{-1}\right)$.

One can make use of Eq.(2.35) twice to obtain the Gaussian map for the combination of three Gaussian linear maps. We have to do the Grassmann integration four times so we assume the following matrices are invertible: $G^{(\mathcal{N}(\sigma))}$, $A + \left(G^{(\mathcal{N}(\sigma))}\right)^{-1}$, $B^T\left(A + \left(G^{(\mathcal{N}(\sigma))}\right)^{-1}\right)^{-1}B$ and $\left(B^T\left(A + \left(G^{(\mathcal{N}(\sigma))}\right)^{-1}\right)^{-1}B\right)^{-1} + G^{(\sigma)}$. (Label this set of assumptions as $1' - 4'$.) This is equivalent to assuming the invertibility of $G^{(\mathcal{N}(\sigma))}$, $A + \left(G^{(\mathcal{N}(\sigma))}\right)^{-1}$, B, and $I_{2n} + \left(G^{(\mathcal{N}(\sigma))}\right)^2$. (Label them as $1 - 4$.) We discuss these assumptions in Appendix (A.3.1). One can show that the independent assumptions are $1, 3, 4$. It turns out that $1, 3$ can be overcome by continuity arguments when these matrices are singular. Assumption 4 is related to the requirement that $\mathcal{N}(\sigma)$ be invertible. When it is not invertible, we can only determine the Petz recovery map on the support of $\mathcal{N}(\sigma)$.

After a fair amount of algebra, (collected in Appendix (A.2.4).) one can find that the composition of the three maps in Eq. (2.24) gives a Gaussian linear map whose integral representation is

$$B_{\mathcal{P}} = \sqrt{I_{2n} + (G^{(\sigma)})^2}B^T\left(\sqrt{I_{2n} + (G^{(\mathcal{N}(\sigma))})^2}\right)^{-1},\ A_{\mathcal{P}} = G^{(\sigma)} - B_{\mathcal{P}}G^{(\mathcal{N}(\sigma))}B_{\mathcal{P}}^T,\ C_{\mathcal{P}} = 1,\ D_{\mathcal{P}} = 0. \tag{2.36}$$

Note that the form of $A_{\mathcal{P}}$ guarantees that the reference state σ can always be recovered: $\mathcal{P}_{\sigma,\mathcal{N}} \circ \mathcal{N}(\sigma) = \sigma$. It is obvious that the Petz recovery map is trace preserving since $C_{\mathcal{P}} = 1, D_{\mathcal{P}} = 0$. Complete positivity follows from the complete positivity of the three separate maps. So the Petz recovery map is indeed a quantum channel. The form of Eq. (2.36) is quite analogous to that for bosonic Gaussian states obtained in [17].[6]

[6] It is plausible to argue that the differences between the formula of the Petz recovery map for bosons and fermions mainly arise from the fact that the covariance matrix for boson is block-diagonalized by $J \in SP(2n)$, while for

2.2.3 Rotated recovery map

The definition of the rotated recovery map in Eq.(1.4) explicitly shows that it is a composition of three maps. So we can make use of the techniques developed above to construct the rotated recovery map.

We first construct the isometry map $\mathcal{U}_{\sigma,t}$. It is the same method as the construction of $\mathcal{N}_1$ and $\mathcal{N}_3$. The first step is the Majorana representation of the operator σ^{it}. It is defined by exponential series:

$$\sigma^{it} = \sum_{k=0}^{\infty} \frac{(it)^k}{k!} (\log \sigma)^k \tag{2.37}$$

in which σ is written in the form as in Eq.(2.25). In this subsection, we assume that σ and $\mathcal{N}(\sigma)$ are strictly positive operators. This corresponds the constraints of the Williamson eigenvalues $|\lambda_i^{(\sigma)}| < 1$ and $|\lambda_i^{(\mathcal{N}(\sigma))}| < 1$, so that ambiguities such as 0^{is} or the points lying on the radius of convergence are not discussed here. We can further expand $\log \sigma$ since $||i\lambda_i^{(\sigma)}\tilde{\gamma}_{2i-1}\tilde{\gamma}_{2i}|| < 1$ with $|\lambda_i^{(\sigma)}| < 1$. After doing the contraction and the re-summation, the result is

$$\sigma^{it} = \frac{1}{2^{itn}} \prod_{i=1}^{n} \frac{1}{2} \left((1-\lambda_i^{(\sigma)})^{it} + (1+\lambda_i^{(\sigma)})^{it} \right) \hat{I} + \frac{1}{2} \left((1+\lambda_i^{(\sigma)})^{it} - (1-\lambda_i^{(\sigma)})^{it} \right) (-i\tilde{\gamma}_{2i-1}\tilde{\gamma}_{2i}). \tag{2.38}$$

This agrees with the result of naive analytic continuation from σ^k, $k \in \mathbb{Z}_+$.

The second step is to perform the calculation that is similar to Eq.(A.21) to read off the

fermion $O \in SO(2n)$ plays this role, see Eq. (2.12). In this work we do not further our discussion to deriving Eq. (2.36) based on above group theoretical arguments.

Grassmann representation of this isometry. It turns out that

$$A_{\sigma,t} = D_{\sigma,t} = 0, \quad C_{\sigma,t} = 1. \tag{2.39}$$

In the bases that $G^{(\sigma)}$ is block diagonalized, the matrix $B_{\sigma,t}$ is block diagonalized for each mode as well. In each block, the entries are

$$B_{\sigma,t}^{block,i} = \begin{pmatrix} \frac{1}{2}\left(\left(\frac{1-\lambda_i^{(\sigma)}}{1+\lambda_i^{(\sigma)}}\right)^{it} + \left(\frac{1-\lambda_i^{(\sigma)}}{1+\lambda_i^{(\sigma)}}\right)^{-it}\right) & \frac{i}{2}\left(\left(\frac{1-\lambda_i^{(\sigma)}}{1+\lambda_i^{(\sigma)}}\right)^{it} - \left(\frac{1-\lambda_i^{(\sigma)}}{1+\lambda_i^{(\sigma)}}\right)^{-it}\right) \\ -\frac{i}{2}\left(\left(\frac{1-\lambda_i^{(\sigma)}}{1+\lambda_i^{(\sigma)}}\right)^{it} - \left(\frac{1-\lambda_i^{(\sigma)}}{1+\lambda_i^{(\sigma)}}\right)^{-it}\right) & \frac{1}{2}\left(\left(\frac{1-\lambda_i^{(\sigma)}}{1+\lambda_i^{(\sigma)}}\right)^{it} + \left(\frac{1-\lambda_i^{(\sigma)}}{1+\lambda_i^{(\sigma)}}\right)^{-it}\right) \end{pmatrix} \tag{2.40}$$

Making use of the Eq.(A.16) and noticing that $\log\left(\frac{1-x}{1+x}\right) = -2\text{arctanh}x$ for $|x| < 1$, we can write $B_{\sigma,t}$ in a basis independent manner as $B_{\sigma,t} = e^{-2t\,\text{arctan}\,G^{(\sigma)}}$. One can show that $\mathcal{U}_{\sigma,t}$ is indeed a valid quantum channel.

The last step is to combine three quantum channels in Eq.(1.4) into one, using Eqs.(2.35) twice. The singular matrices we encounter can be treated by continuity argument as if they were invertible, as is discussed in Section (2.2.2) and (A.3.1). It is straightforward to get

$$A_{\mathcal{R},t} = B_{\sigma,t} A_{\mathcal{P}} B_{\sigma,t}^T, \quad B_{\mathcal{R},t} = B_{\sigma,t} B_{\mathcal{P}} B_{\mathcal{N}(\sigma),-t}, \quad C_{\mathcal{R},t} = 1, \quad D_{\mathcal{R},t} = 0. \tag{2.41}$$

2.3 Fidelity between two fermionic Gaussian states

In this section we give a formula for the fidelity of two fermionic Gaussian states in terms of their covariance matrices. This is an immediate application of the quantum map techniques developed above.

Fidelity is a measure of the similarity between two quantum states. We take the definition of the fidelity between ρ and σ to be

$$F(\rho,\sigma) = \mathrm{tr}\left(\sqrt{\sigma^{\frac{1}{2}}\rho\sigma^{\frac{1}{2}}}\right). \tag{2.42}$$

Fidelity is symmetric in the two argument, $F(\rho,\sigma) = F(\sigma,\rho)$, and it is bounded by $0 \leq F(\rho,\sigma) \leq 1$ [62]. Two states are identical if and only if $F(\rho,\sigma) = 1$ and are orthogonal to each other if and only if $F(\rho,\sigma) = 0$.

We can first make use of the map $\mathcal{N}_3 : X \mapsto \sigma^{\frac{1}{2}} X \sigma^{\frac{1}{2}}$. For the square root of a Gaussian operator, the construction is the same as that of $\sigma^{\frac{1}{2}}$ described in Eq. (A.18), and its covariance matrix is obtained by applying Eq. (A.16) to Eq. (2.27). After a straightforward calculation, we get

$$F(\rho,\sigma) = \frac{1}{2^{\frac{n}{2}}}\det(I_{2n} - G^{(\rho)}G^{(\sigma)})^{\frac{1}{4}}\det\left(I_{2n} + \sqrt{I_{2n} + \left(\tilde{G}^{(\sigma\rho)}\right)^2}\right)^{\frac{1}{4}} \tag{2.43}$$

where $\tilde{G}^{(\sigma\rho)} \equiv \left(G^{(\sigma)} + G^{(\rho)}\right)\left(I_{2n} - G^{(\sigma)}G^{(\rho)}\right)^{-1}$.

We present the calculation details in Appendix (A.2.5). A variation of the formula for the fidelity for fermionic Gaussian states can be found in [53].[7] A similar formula for the fidelity of bosonic Gaussian states can be found in Refs. [60],[63].

2.4 Summary

In Chapter (2), we constructed the Petz recovery map for Gaussian quantum channels with a Gaussian reference state in which the degrees of freedom are fermionic. Using the Lagrangian

[7]The authors do not derive the equivalence of Eq.(2.43) and the one in [53]. But a numerical test for the fidelity between random Gaussian states gives the same result for the two formula.

representation of Gaussian linear maps, we are able to express the Petz recovery map in terms of the covariance matrix of the reference state, and the matrices A, B that encode the information of the Gaussian quantum channel. The main result is collected in Eq. (2.36). The corresponding result for the rotated Petz channel is presented in Eq. (2.41). As an immediate application of the techniques, we derived a formula for the fidelity of two arbitrary fermionic Gaussian states in terms of their covariance matrices, which is shown in Eq. (2.43). The supplementary materials are collected in Appendix (A).

Chapter 3: Universal approximate recovery channel in quantum field theory

In this chapter we present the proof of the main theorems. We start by charifying the notations. Section (3.1) gives an introduction to the Tomita-Takesaki theory, as well as the inclusion of von Neumann algebras. The Theorems (3.1.1) and (3.1.2) are proven in Section (3.2). In Section (3.3) we present an alternative strategy of proving the main theorem (3.1.1). The chapter is concluded by two applications of the theorems in Section (3.4): (1) the case of type-I algebras and (2) the half-sided modular inclusion.

Notations and conventions: Calligraphic letters $\mathcal{A}, \mathcal{M}, \dots$ denote von Neumann algebras. Calligraphic letters $\mathscr{H}, \mathscr{K}, \dots$ denote more general linear spaces or subsets thereof. $\mathbb{S}_a = \{z \in \mathbb{C} \mid 0 < \Re(z) < a\}$ denotes an open strip, and we often write $\mathbb{S} = \mathbb{S}_1$. We typically use the physicist's "ket"-notation $|\psi\rangle$ for vectors in a Hilbert space. The scalar product is written

$$(|\psi\rangle, |\psi'\rangle)_{\mathscr{H}} = \langle\psi|\psi'\rangle \tag{3.1}$$

and is anti-linear in the first entry. The norm of a vector is sometimes written simply as $\||\psi\rangle\| =: \|\psi\|$. The action of a linear operator T on a ket is sometimes written as $T|\phi\rangle = |T\phi\rangle$. In this spirit, the norm of a bounded linear operator T on $\mathscr{H}$ is written as $\|T\| = \sup_{|\psi\rangle:\|\psi\|=1} \|T\psi\|$.

3.1 Basic definitions and main results

3.1.1 Tomita-Takesaki theory

Here we outline some elements of von Neumann algebra theory relevant for this work; for details, see [64, 65, 66]. A von Neumann algebra, $\mathcal{A}$, is a subspace of the set of all bounded operators $B(\mathscr{H})$ containing the unit operator 1 that is closed under: products, the star operation denoted a^* and limits in the ultra-weak operator topology. States on $\mathcal{A}$ are linear functionals that are positive, $\rho(a^*a) \geq 0$, normalized, $\rho(1) = 1$, and "normal" i.e., continuous in the ultra-weak operator topology. The set of normal states is contained in the "predual" $\mathcal{A}_\star$ of $\mathcal{A}$, i.e. the set of all ultra-weakly continuous linear functionals on $\mathcal{A}$. One defines the support projection $\pi^{\mathcal{A}}$ associated to a state ρ as the smallest projection $\pi = \pi^{\mathcal{A}}(\rho)$ in $\mathcal{A}$ that satisfies $\rho(\pi) = 1$. Faithful states by definition have unit support projection.

We will work with the von Neumann algebra in a so called standard form, $(\mathcal{A}, \mathscr{H}, J, \mathscr{P}^\natural)$, where $\mathcal{A}$ acts on the Hilbert space $\mathscr{H}$ and where there is an anti-linear, unitary involution J and a self-dual "natural" cone $\mathscr{P}^\natural$ left invariant by J. The existence and detailed properties of a normal form are proven in [67]; here we only mention: One has $J\mathcal{A}J = \mathcal{A}'$ where $\mathcal{A}' \subset B(\mathscr{H})$, the "commutant", is the von Neumann algebra of all bounded operators on $\mathscr{H}$ that commute with $\mathcal{A}$. The natural cone defines a set of vectors in the Hilbert space that canonically represent states on $\mathcal{A}$ via

$$\mathcal{A}_\star \ni \rho \mapsto |\xi_\rho\rangle \in \mathscr{P}^\natural\,, \qquad \rho(\cdot) = \omega_{\xi_\rho}(\cdot) \equiv \langle \xi_\rho| \cdot |\xi_\rho\rangle \tag{3.2}$$

and where we use the notation $\omega_\psi(\cdot) \equiv \langle\psi| \cdot |\psi\rangle \in \mathcal{A}_\star$ for the linear functional on $\mathcal{A}$ induced by a vector $\psi \in \mathscr{H}$. The vector in the natural cone representing ω_ψ will also be denoted by $|\xi_\psi\rangle$. It is known that it is related to $|\psi\rangle$ by a partial isometry $v'_\psi \in \mathcal{A}'$,

$$|\xi_\psi\rangle = v'_\psi |\psi\rangle. \tag{3.3}$$

Furthermore, it is known that[1] proximity of the state functionals implies that of the vector representatives in the natural cone and vice versa, in the sense that

$$\|\xi_\phi - \xi_\psi\| \, \|\xi_\phi + \xi_\psi\| \geq \|\omega_\phi - \omega_\psi\| \geq \|\xi_\phi - \xi_\psi\|^2 \tag{3.4}$$

holds.

We now introduce the modular operators that are central to our discussion of relative entropy [68, 69] and non-commutative L_p-spaces [70]. This is most straightforward if we a have cyclic and separating vector $|\eta\rangle$ for the algebra $\mathcal{A}$, meaning that $\{a|\eta\rangle : a \in \mathcal{A}\}$ is dense in $\mathscr{H}$ and that $a|\eta\rangle = 0$ implies that $a = 0$. Then Tomita-Takesaki theory establishes that one can define an anti-linear, unitary operator J and a positive, self-adjoint operator Δ_η by the relations

$$J \Delta_\eta^{1/2} a \, |\eta\rangle = a^* \, |\eta\rangle \ , \quad \forall a \in \mathcal{A} \tag{3.5}$$

Δ_η is in general unbounded. J can be used in this case to define a standard form, with $\mathscr{P}^\natural$ given by the closure of $\{aJaJ|\eta\rangle : a \in \mathcal{A}\}$, but we emphasize that a standard form exists generally even without a faithful state $|\eta\rangle$. From now on, we regard such a standard form, hence J, as fixed. We will continue to take $\eta \in \mathscr{P}^\natural$.

We will also need the concept of relative modular operator $\Delta_{\phi,\psi}$ [68]. In a slight gener-

[1]For the case of matrix algebras, the second inequality is known as the Powers-Störmer inequality.

alization of the above definitions, let $|\phi\rangle, |\psi\rangle \in \mathscr{P}^\natural$. Then there is a non-negative, self-adjoint operator $\Delta_{\phi,\psi}$ characterized by

$$J\Delta_{\phi,\psi}^{1/2}\left(a\,|\psi\rangle + |\chi\rangle\right) = \pi^{\mathcal{A}}(\psi)a^*\,|\phi\rangle\ , \quad \forall\ a\in\mathcal{A}\,,\ |\chi\rangle \in (1-\pi^{\mathcal{A}'}(\psi))\mathscr{H} \tag{3.6}$$

The non-zero support of $\Delta_{\phi,\psi}$ is $\pi^{\mathcal{A}}(\phi)\pi^{\mathcal{A}}(\psi)\mathscr{H}$, and the functions $\Delta^z_{\phi,\psi}$ are understood via the functional calculus on this support and are defined as 0 on $1-\pi^{\mathcal{A}}(\phi)\pi^{\mathcal{A}}(\psi)$. We can similarly define relative modular operators for vectors outside of the natural cone, for a detailed discussion of such matters see e.g., [70], Appendix C. For example, we may use the well known transformation property of the modular operators $\Delta_{u'\phi,v'\psi} = v'\Delta_{\phi,\psi}v'^*$ where $v', u' \in \mathcal{A}'$ is a partial isometry (with appropriate initial and final support), to define:

$$\Delta_{\phi,\psi} \equiv {v'_\psi}^*\Delta_{\xi_\phi,\xi_\psi}v'_\psi\,, \qquad |\psi\rangle, |\phi\rangle \in \mathscr{H}. \tag{3.7}$$

Similarly we can define the relative modular operators for the commutant in direct analogy. We will often denote it by $\Delta'_{\phi,\psi}$.

When $|\psi\rangle = |\phi\rangle$ we will denote these operators as $\Delta_{\phi,\phi} \equiv \Delta_\phi$. This is the non-relative modular operator already discussed from which we can define modular flow:

$$\varsigma^t_\phi(a) = \Delta^{it}_\phi a \Delta^{-it}_\phi \in \mathcal{A}\,, \tag{3.8}$$

where $a \in \mathcal{A}$ and we have taken ϕ to be cyclic and separating. The modular flow can also be extracted from the relative modular operators:

$$\Delta_{\phi,\psi}^{it} a \Delta_{\phi,\psi}^{-it} = \varsigma_{\phi}^{t}(a)\pi^{\mathcal{A}'}(\psi) \tag{3.9}$$

for any $\psi \in \mathscr{H}$.

The modular operators satisfy various relations that we need to draw on below and we simply quote these here (recall that $\eta \in \mathscr{P}^{\natural}$):

$$\Delta_{\psi,\eta}^{-z} = (\Delta'_{\eta,\psi})^{z}\,, \qquad J\Delta_{\xi_\psi,\eta}^{-z} = \Delta_{\eta,\xi_\psi}^{\bar{z}} J\,, \qquad \Delta_{\psi,\eta}^{-it} a \Delta_{\eta}^{it} \in \mathcal{A} \tag{3.10}$$

for $t \in \mathbb{R}$, $z \in \mathbb{C}$ and $a \in \mathcal{A}$ and where these equations make sense when acting on vectors in appropriate domains – we are more specific about this when we get to use these equations. The Connes cocycle $(D\psi : D\phi)_t$ is the partial isometry from $\mathcal{A}$ defined by $(t \in \mathbb{R})$

$$(\Delta_{\psi,\phi}^{-it}\Delta_{\phi}^{it}) = \Delta_{\psi,\eta}^{-it}\Delta_{\phi,\eta}^{it}\pi^{\mathcal{A}'}(\phi) \equiv (D\psi : D\phi)_{-t}\pi^{\mathcal{A}'}(\phi). \tag{3.11}$$

According to [68, 69], if $\pi^{\mathcal{A}}(\phi) \geq \pi^{\mathcal{A}}(\psi)$, the relative entropy may be defined as

$$S(\psi|\phi) = -\lim_{\alpha\to 0^+} \frac{\langle\psi|\Delta_{\phi,\psi}^{\alpha}\psi\rangle - 1}{\alpha}, \tag{3.12}$$

otherwise, it is by definition equal to $+\infty$. The relative entropy only depends on the functionals ω_ψ, ω_ϕ but not on the particular choice of vectors that define them.

3.1.2 Inclusions of von Neumann algebras and Petz map

Now consider a von Neumann subalgebra $\mathcal{B}$ of $\mathcal{A}$. It is convenient to take $\mathcal{B}$ to be in a standard form $(\mathcal{B}, \mathscr{K}, J_{\mathcal{B}}, \mathscr{P}^{\natural}_{\mathcal{B}})$. In this representation $\mathcal{B}$ acts on a (potentially) different Hilbert space $\mathscr{K}$ and to distinguish these representations we define the embedding $\iota : \mathcal{B} \to \mathcal{A}$ as a $*$-isomorphism of von Neumann algebras from $\mathcal{B}$ to the range $\iota(\mathcal{B}) \subset \mathcal{A}$.

Normal states ρ on $\mathcal{B}$ are induced from states on $\mathcal{A}$ in the obvious way: $\rho|_{\mathcal{B}} \equiv \rho \circ \iota \equiv \iota^{+}\rho$, so $\iota^{+}(\mathcal{A}_{\star}) \subset \mathcal{B}_{\star}$. We adopt the convention that the corresponding support projection will be labelled in the following manner:

$$\pi^{\mathcal{B}}(\rho) \equiv \pi^{\mathcal{B}}(\rho \circ \iota)\,, \quad \rho \in \mathcal{A}_{\star} \tag{3.13}$$

and we have

$$\pi^{\mathcal{A}}(\rho) \leq \iota(\pi^{\mathcal{B}}(\rho)), \tag{3.14}$$

where for two self-adjoint elements $a, b \in \mathcal{A}$ we say that $a \leq b$ if $a - b$ is a non-negative operator. Given $\rho, \sigma \in \mathcal{A}_{\star}$, we may define the relative entropy $S_{\mathcal{A}}(\rho|\sigma) \equiv S(\rho|\sigma)$ as above, and we put

$$S_{\mathcal{B}}(\rho|\sigma) \equiv S(\rho \circ \iota | \sigma \circ \iota). \tag{3.15}$$

By monotonicity of the relative entropy [21], we have $S_{\mathcal{A}}(\rho|\sigma) - S_{\mathcal{B}}(\rho|\sigma) \geq 0$.

Given a faithful state $\sigma \in \mathcal{A}_{\star}$, an isometry $V_{\sigma} : \mathscr{K} \to \mathscr{H}$ can be naturally defined as follows [71, 72, 73]:

$$V_{\sigma} b \big|\xi^{\mathcal{B}}_{\sigma}\big\rangle := \iota(b)\, \big|\xi^{\mathcal{A}}_{\sigma}\big\rangle\,, \qquad b \in \mathcal{B}\,, \tag{3.16}$$

where we use the notation $|\xi_\sigma^{\mathcal{B}}\rangle$ for the vector representative of the state $\sigma\circ\iota\in\mathcal{B}_\star$ in the natural cone of the algebra $\mathcal{B}$ and $|\xi_\sigma^{\mathcal{A}}\rangle$ for the vector representative of the state $\sigma\in\mathcal{A}_\star$ in the natural cone of the algebra $\mathcal{A}$. As reviewed in Appendix (B.1), this embedding V_σ commutes with the action of b,

$$V_\sigma\left(b\,|\chi\rangle\right)=\iota(b)V_\sigma\,|\chi\rangle\ ,\qquad \chi\in\mathscr{K}\ ,\qquad b\in\mathcal{B} \tag{3.17}$$

and satisfies $V_\sigma^*\iota(b)V_\sigma=b$ for all $b\in\mathcal{B}$ as well as $V_\sigma(\mathscr{K})=\pi_{\mathscr{K}}\mathscr{H}$ for some projector $V_\sigma V_\sigma^*\equiv\pi_{\mathscr{K}}\in\iota(\mathcal{B})'$.

We now recall the concept of approximate sufficiency. First, recall that a linear mapping $\alpha:\mathcal{A}\to\mathcal{B}$ is called a "channel" if it is completely positive, ultra-weakly continuous and $\alpha(1)=1$, see [73].

Definition 3.1.1. Following [12, 73] we say that the inclusion $\mathcal{B}\subset\mathcal{A}$ is *ϵ-approximately sufficient* for a set of states $\mathscr{S}\subset\mathcal{A}_\star$, if there exists a fixed channel

$$\alpha:\mathcal{A}\to\mathcal{B}, \tag{3.18}$$

called the "*recovery channel* ", for which the recovered state is close to the original state in the sense that

$$\|\rho-\rho\circ\iota\circ\alpha\|\equiv\sup_{a\in\mathcal{A}:\|a\|\le 1}|\rho(a)-\rho\circ\iota\circ\alpha(a)|\le\epsilon,\,,\quad\forall\ \rho\in\mathscr{S}. \tag{3.19}$$

Here we take all $\rho\in\mathscr{S}$ to be normalized $\rho(1)=1$.

Note that if $\mathcal{A}\subset\mathcal{B}$ is ϵ-sufficient for $\mathscr{S}$, then $\mathcal{A}\subset\mathcal{B}$ is ϵ-sufficient for the closed convex hull of states $\overline{\mathrm{conv}(\mathscr{S})}$.

We would now like to construct an α that works as a recovery map for a set of states that are close in relative entropy under restriction to the sub-algebra. We take the relative entropy to compare to a fixed state $\sigma \in \mathcal{A}_\star$. That is, we consider the set

$$\mathscr{R}_\delta^{(\sigma)} = \{\rho \in \mathcal{A}_\star : \rho(1) = 1\,,\ \rho \geq 0\,,\ S_{\mathcal{A}}(\rho|\sigma) - S_{\mathcal{B}}(\rho|\sigma) \leq \delta\} \tag{3.20}$$

The required recovery channel is related to the so-called Petz map, which is defined in the sub-algebra context (and faithful σ) as (see e.g., [73], sec. 8):

$$\alpha_\sigma(\cdot) = J_{\mathcal{B}} V_\sigma^* J_{\mathcal{A}}\,(\cdot)\,J_{\mathcal{A}} V_\sigma J_{\mathcal{B}} \tag{3.21}$$

It maps operators on $\mathscr{H}$ to operators on $\mathscr{K}$, and furthermore

$$\alpha_\sigma(\mathcal{A}) \subset \mathcal{B}. \tag{3.22}$$

As shown in [73], prop. 8.3 this map satisfies the defining properties of a recovery channel used in def. (3.1.1) – in fact, in the subalgebra context considered here it is equal to the generalized conditional expectation introduced even earlier by [74]. In the non-faithful case there is a slightly more complicated expression that we will discuss below in Lemma (3.1.1).

3.1.3 Main theorems

Given two states $\rho, \sigma \in \mathcal{A}_\star$, the fidelity is defined as [75]:

$$F(\sigma, \rho) \equiv \sup_{u' \in \mathcal{A}' : u'u'^* = 1} |\langle \xi_\sigma | u' \xi_\rho \rangle|. \tag{3.23}$$

Some of its properties in our setting are discussed in Lemma (3.2.1) below.

One of the two main theorems we would like to establish is:

Theorem 3.1.1 (Faithful case). Montonicity of relative entropy can be strengthened to

$$S_{\mathcal{A}}(\rho|\sigma) - S_{\mathcal{B}}(\rho|\sigma) \geq -2 \int_{-\infty}^{\infty} \ln F(\rho, \rho \circ \iota \circ \alpha_\sigma^t) p(t) \, \mathrm{d}t, \tag{3.24}$$

where we assume that ρ, σ are normal, σ is faithful and where $\alpha_\sigma^t : \mathcal{A} \to \mathcal{B}$ is the rotated Petz map, defined as

$$\alpha_\sigma^t(a) = \varsigma_{-t}^{\sigma,\mathcal{B}} \left(J_{\mathcal{B}} V_\sigma^* J_{\mathcal{A}} \varsigma_t^{\sigma,\mathcal{A}}(a) J_{\mathcal{A}} V_\sigma J_{\mathcal{B}} \right). \tag{3.25}$$

$p(t)$ is the normalized probability density defined by

$$p(t) = \frac{\pi}{\cosh(2\pi t) + 1}. \tag{3.26}$$

$\varsigma_t^{\sigma,\mathcal{A}}$ resp. $\varsigma_t^{\sigma,\mathcal{B}}$ are the modular flows of σ on $\mathcal{A}$ resp. of $\sigma \circ \iota$ on $\mathcal{B}$.

We may extend this theorem to the case where σ is non-faithful. The basic idea is contained in the following lemma:

Lemma 3.1.1. Consider a sub-algebra $\iota(\mathcal{B}) \subset \mathcal{A}$, of a general von Neumann algebra, and a normal state σ with support projectors $\pi^{\mathcal{A}}(\sigma),\ \pi^{\mathcal{B}}(\sigma)$ and $\pi^{\mathcal{A}'}(\sigma) \equiv J_{\mathcal{A}}\pi^{\mathcal{A}}(\sigma)J_{\mathcal{A}},\ \pi^{\mathcal{B}'}(\sigma) \equiv J_{\mathcal{B}}\pi^{\mathcal{B}}(\sigma)J_{\mathcal{B}}$. Then the following statements hold:

(i) The projected sub-algebras, are (σ-finite) von Neumann sub-algebras,

$$\iota_\pi(\mathcal{B}_\pi) \subset \mathcal{A}_\pi, \tag{3.27}$$

$$\mathcal{A}_\pi = \pi^{\mathcal{A}}(\sigma)\mathcal{A}\pi^{\mathcal{A}}(\sigma)\pi^{\mathcal{A}'}(\sigma)\,, \qquad \mathcal{B}_\pi = \pi^{\mathcal{B}}(\sigma)\mathcal{B}\pi^{\mathcal{B}}(\sigma)\pi^{\mathcal{B}'}(\sigma) \tag{3.28}$$

acting respectively on $\mathscr{H}_\pi = \pi^{\mathcal{A}}(\sigma)\pi^{\mathcal{A}'}(\sigma)\mathscr{H}$ and $\mathscr{K}_\pi = \pi^{\mathcal{B}}(\sigma)\pi^{\mathcal{B}'}(\sigma)\mathscr{K}$. The projected inclusion is defined as:

$$\iota_\pi(b) \equiv \Phi_{\mathcal{A}}^{-1} \circ \iota \circ \Phi_{\mathcal{B}}(b) \qquad b \in \mathcal{B}_\pi, \tag{3.29}$$

where we defined the (ultra weakly continuous) *-isomorphism of von Neumann algebras

$$\Phi_{\mathcal{B}} : \mathcal{B}_\pi \to \pi^{\mathcal{B}}(\sigma)\mathcal{B}\pi^{\mathcal{B}}(\sigma) \quad \text{via} \quad \Phi_{\mathcal{B}}(b\pi^{\mathcal{B}'}(\sigma)) = b \tag{3.30a}$$

$$\Phi_{\mathcal{A}} : \mathcal{A}_\pi \to \pi^{\mathcal{A}}(\sigma)\mathcal{A}\pi^{\mathcal{A}}(\sigma) \quad \text{via} \quad \Phi_{\mathcal{A}}(a\pi^{\mathcal{A}'}(\sigma)) = a. \tag{3.30b}$$

The projected algebras are in a standard form. For example the standard form of $\mathcal{A}_\pi$ is $(\mathcal{A}_\pi, \mathscr{H}_\pi, J_{\mathcal{A}}, \pi(\sigma)\pi'(\sigma)\mathscr{P}^\natural)$ where $J_{\mathcal{A}}$ maps the subspace $\mathscr{H}_\pi$ to itself.

(ii) The relative entropy satisfies

$$S(\rho|\sigma) = S(\rho \circ \Phi|\sigma \circ \Phi)\,, \qquad S(\rho \circ \iota|\sigma \circ \iota) = S(\rho \circ \Phi \circ \iota_\pi|\sigma \circ \Phi \circ \iota_\pi) \tag{3.31}$$

for all states such that $\pi^{\mathcal{A}}(\rho) \leq \pi^{\mathcal{A}}(\sigma)$, where $\Phi \equiv \Phi_{\mathcal{A}}$.

(iii) Consider a channel on the projected algebras:

$$\alpha_\pi \,:\, \mathcal{A}_\pi \to \mathcal{B}_\pi \tag{3.32}$$

We can construct a new cannel on the algebras of interest $\alpha \,:\, \mathcal{A} \to \mathcal{B}$ via:

$$\alpha(a) \equiv \Phi_{\mathcal{B}} \circ \alpha_\pi \circ \Phi_{\mathcal{A}}^{-1}(\pi^{\mathcal{A}}(\sigma) a \pi^{\mathcal{A}}(\sigma)) + \sigma(a)(1 - \pi^{\mathcal{B}}(\sigma)). \tag{3.33}$$

Then for all $\rho \in \mathcal{A}_\star$ with $\pi^{\mathcal{A}}(\rho) \leq \pi^{\mathcal{A}}(\sigma)$ we have:

$$\rho(a) = \rho(\pi^{\mathcal{A}}(\sigma) a \pi^{\mathcal{A}}(\sigma)) \quad \text{and} \quad \rho \circ \iota \circ \alpha(a) = \rho \circ \iota \circ \alpha(\pi^{\mathcal{A}}(\sigma) a \pi^{\mathcal{A}}(\sigma))\,, \qquad \forall a \in \mathcal{A} \tag{3.34}$$

and

$$F(\rho, \rho \circ \iota \circ \alpha) = F(\rho \circ \Phi, \rho \circ \iota \circ \alpha \circ \Phi) = F(\rho \circ \Phi, \rho \circ \Phi \circ \iota_\pi \circ \alpha_\pi) \tag{3.35}$$

Similarly:

$$\|\rho - \rho \circ \iota \circ \alpha\| = \|\rho \circ \Phi - \rho \circ \Phi \circ \iota_\pi \circ \alpha_\pi\|. \tag{3.36}$$

(iv) The explicit form of the resulting Petz map coming from the inclusion $\iota_\pi(\mathcal{B}_\pi) \subset \mathcal{A}_\pi$ is:

$$\alpha_\sigma^t(a) \equiv \Phi_{\mathcal{B}} \left(\varsigma_{-t}^{\sigma;\mathcal{B}} \left(J_{\mathcal{B}} (V_\sigma^{(\iota_\pi)})^* J_{\mathcal{A}} \varsigma_t^{\sigma,\mathcal{A}}(a) J_{\mathcal{A}} V_\sigma^{(\iota_\pi)} J_{\mathcal{B}} \right)\right) + \sigma(a)(1 - \pi^{\mathcal{B}}(\sigma)), \tag{3.37}$$

where the embedding $V_\sigma^{(\iota_\pi)}$ is defined for the projected inclusion as

$$V_\sigma^{(\iota_\pi)}\left(b\middle|\xi_\sigma^{\mathcal{B}}\right\rangle) = \iota_\pi(b)\left|\xi_\sigma^{\mathcal{A}}\right\rangle , \qquad b \in \mathcal{B}_\pi, \tag{3.38}$$

and where $|\xi_\sigma^{\mathcal{A}}\rangle$ and $|\xi_\sigma^{\mathcal{B}}\rangle$ are now cyclic and separating for $\mathcal{A}_\pi$ and $\mathcal{B}_\pi$ respectively.

Proof. The proof of this lemma uses standard properties of support projectors and is left to the reader. □

Note that the modular automorphism groups in (3.37) can be understood as being associated to the non-cyclic and separating vector $|\xi_\sigma^{\mathcal{A}}\rangle$ (resp. $|\xi_\sigma^{\mathcal{B}}\rangle$) for the original algebra $\mathcal{A}$ (resp. $\mathcal{B}$), which are however defined to project to zero away from the $\mathscr{H}_\pi$ (resp. $\mathscr{K}_\pi$) subspace. So, for example $\varsigma_{t=0}^\sigma(a) = \pi^{\mathcal{A}'}(\sigma)\pi^{\mathcal{A}}(\sigma)a\pi^{\mathcal{A}}(\sigma)$. Similarly $V_\sigma^{(\iota_\pi)}$ can be understood in this way, as being defined on the subspaces $\mathscr{K}_\pi$ and projecting to zero away from this subspace via:

$$V_\sigma^{(\iota_\pi)}\left(\pi^{\mathcal{B}}(\sigma)b\middle|\xi_\sigma^{\mathcal{B}}\right\rangle + |\zeta\rangle) = \iota(\pi^{\mathcal{B}}(\sigma))\iota(b)\left|\xi_\sigma^{\mathcal{A}}\right\rangle , \quad b \in \mathcal{B}\,, \quad |\zeta\rangle \in (1-\pi^{\mathcal{B}'}(\sigma)\pi^{\mathcal{B}}(\sigma))\mathscr{K} \tag{3.39}$$

An obvious corollary is:

Corollary 3.1.1.1 (Theorem 1 in the non-faithful case). Theorem (3.1.1) continues to hold when σ is non-faithful but still $\pi^{\mathcal{A}}(\rho) \leq \pi^{\mathcal{A}}(\sigma)$. The recovery map is now given by (3.37).

From this result one can characterize approximately sufficiency using relative entropy:

Theorem 3.1.2. Consider a set of normal states $\mathscr{S}$ on a general von Neumann algebra $\mathcal{A}$ with a subalgebra $\mathcal{B}$. If $\mathscr{S}$ contains a state σ such that for all $\rho \in \mathscr{S}$ the following condition holds:

$$S(\rho|\sigma) < \infty \quad \text{and} \quad S_{\mathcal{A}}(\rho|\sigma) - S_{\mathcal{B}}(\sigma|\rho) \leq \delta, \tag{3.40}$$

then there exists a universal recovery channel $\alpha_{\mathscr{S}}$ such that $\mathcal{A} \subset \mathcal{B}$ is ϵ-approximately sufficient for $\mathscr{S}$. (Here $\delta = -\ln(1 - \epsilon^2/4)$.)

The explicit form of the recovery map is:

$$\alpha_{\mathscr{S}} : \mathcal{A} \ni a \mapsto \int_{-\infty}^{\infty} \alpha_\sigma^t(a)\, p(t) \mathrm{d}t \in \mathcal{B}, \tag{3.41}$$

where α_σ^t was given in (3.37). We can make sense of the later integral as a Lebesgue integral of a weakly measurable function with values in $\mathcal{B}$, thought of as a Banach space.

Remark 1. Less powerful antecedents of Theorems. (3.1.1), (3.1.2) can be found in [13, 76, 77, 78, 79, 80].

An example of a set of states that satisfy the assumptions in Theorem (3.1.2) is simply $\mathscr{S} = \mathscr{R}_\delta^{(\sigma)}$ (3.20) for any state σ. If we were to additionally assume that $\mathcal{A}$ is σ-finite then we could also pick $\mathscr{S}$ to be any closed convex set of states such that

$$\rho_{1,2} \in \mathscr{S}\,, \quad \pi^{\mathcal{A}}(\rho_1) \leq \pi^{\mathcal{A}}(\rho_2) \implies S_{\mathcal{A}}(\rho_1|\rho_2) < \infty \quad \text{and} \quad S_{\mathcal{A}}(\rho_1|\rho_2) - S_{\mathcal{B}}(\rho_1|\rho_2) \leq \delta. \tag{3.42}$$

To see this, note that the σ-finite condition imposes that all families of mutual orthogonal projectors in $\mathcal{A}$ are at most countable. This is satisfied for von Neumann algebras that act on a separable Hilbert space, and is equivalent to the assumption that there is a faithful state in $\mathcal{A}_\star$. Then (3.42) is sufficient for finding a σ that works with Theorem (3.1.2) due to the following basic result:

Lemma 3.1.2. Given a closed convex subset of normal states $\mathscr{S} \subset \mathcal{A}_\star$ for a σ-finite von Neumann algebra $\mathcal{A}$ then we can always find a $\sigma \in \mathscr{S}$ such that:

$$\pi^{\mathcal{A}}(\rho) \leq \pi^{\mathcal{A}}(\sigma)\,, \qquad \forall \rho \in \mathscr{S} \tag{3.43}$$

Proof. We apply Zorn's lemma. Consider the following set of projectors:

$$\Pi_{\mathscr{S}} = \{\pi(\rho_i) - \pi(\rho_j) : \rho_{i,j} \in \mathscr{S}\,,\ \pi(\rho_j) \leq \pi(\rho_i)\} \tag{3.44}$$

where the later condition requires a proper subset. These differences are still projectors since $(\pi(\rho_i) - \pi(\rho_j))^2 = \pi(\rho_i) - \pi(\rho_j)$ by the inclusion condition which implies that $\pi(\rho_j)\pi(\rho_i) = \pi(\rho_i)$.

If $\Pi_{\mathscr{S}}$ is the empty set then it must be the case that $\pi(\rho_i) = \pi(\rho_j)$ for all $\rho_{i,j} \in \mathscr{S}$, since otherwise we could use convexity to show a contradiction:

$$\pi\left(\frac{\rho_i + \rho_j}{2}\right) - \pi(\rho_i) \in \Pi_{\mathscr{S}}. \tag{3.45}$$

So in this case (3.43) is trivial.

We may thus assume from now on that $\Pi_{\mathscr{S}}$ is non-empty. By Zorn's lemma we can pick a maximal family of mutually orthogonal projectors from $\Pi_{\mathscr{S}}$, where family means a subset of $\Pi_{\mathscr{S}}$, and maximal means that there are no other orthogonal families of projectors that are strictly larger under the order of inclusion. Call the maximal family $q_{\max}$. By the σ-finite condition, it is a countable family

$$q_{\max} = \{\pi(\rho_{i_n}) - \pi(\rho_{j_n}) :\ n = 1, 2 \ldots\}. \tag{3.46}$$

Given $q_{\max}$ we define:

$$\sigma = \sum_{n=1}^{\infty} 2^{-n} \rho_{i_n} \tag{3.47}$$

The infinite sum converges in the linear functional norm and so by convexity and closedness of $\mathscr{S}$ we find that $\sigma \in \mathscr{S}$. The support projector for this state satisfies:

$$\pi(\sigma)\mathscr{H} = \bigoplus_{n=1}^{\infty} \pi(\rho_{i_n})\mathscr{H} \tag{3.48}$$

(understood as a direct sum in the norm topology.) By the maximality condition we can show (3.43). To see this, suppose that this is not true for some ρ_k then:

$$\mathcal{B}_\sigma \subset \pi\left(\frac{\sigma + \rho_k}{2}\right) - \pi(\sigma) \in \Pi_{\mathscr{S}} \quad \text{and} \quad \left(\pi\left(\frac{\sigma + \rho_k}{2}\right) - \pi(\sigma)\right) \perp (\pi(\rho_{i_n}) - \pi(\rho_{j_n})) \tag{3.49}$$

for all n. This contradicts the maximality of $q_{\max}$, which is absurd. □

3.2 Proof of main theorems

Our eventual goal in this section is to prove our main results, Theorems (3.1.1) and (3.1.2). As discussed above, without loss of generality we can take σ to be faithful and so we will assume this from now on.

The proof is divided into several steps. In subsec. (3.2.1), we first fix some notation and recall basic facts about the vectors that we are dealing with. In subsec. (3.2.2), we introduce the non-commutative L_p-space by Araki and Masuda [70] and explain its – in principle well-known – relation to the fidelity. We make certain minor modifications to the standard setup and prove a simple but important intermediate result which we call a "first law", Theorem (3.2.1). In subsec.

(3.2.3), we motivate the definition of certain interpolating vectors that will be of main interest in the following subsections and in subsec. (3.2.4) we prove some of their basic properties. Subsec. (3.2.5) is the most technical section. It introduces certain regularized ("filtered") versions of our interpolating vectors and their properties. Our definition of filtered vectors involves a certain cutoff, P, that is defined in terms of relative modular operators. A quite general result of independent interest is that the relative entropy behaves continuously as this cutoff is removed, Theorem (3.2.3). Armed with this technology, we can then complete the proofs in subsec. (3.2.6) using an interpolation result for Araki-Masuda L_p spaces, Lemma (3.2.7).

3.2.1 Isometries V_ψ for general states, notation

Since the two states σ, ρ play a central role in Theorem (3.1.1) we will use a special notation for the vectors that represent these states in their respective natural cones:

$$|\eta_{\mathcal{A}}\rangle \equiv \left|\xi_\sigma^{\mathcal{A}}\right\rangle , \quad |\eta_{\mathcal{B}}\rangle \equiv \left|\xi_\sigma^{\mathcal{B}}\right\rangle , \qquad |\psi_{\mathcal{A}}\rangle \equiv \left|\xi_\rho^{\mathcal{A}}\right\rangle , \quad |\psi_{\mathcal{B}}\rangle \equiv \left|\xi_\rho^{\mathcal{B}}\right\rangle \tag{3.50}$$

where $|\eta_{\mathcal{A}}\rangle \in \mathscr{H}$ $(|\eta_{\mathcal{B}}\rangle \in \mathscr{K})$ are cyclic and separating for $\mathcal{A}$ $(\mathcal{B})$.

We will also choose to label various objects, such as support projectors, and the modular operators discussed below, for the most part with the vector rather than the linear functional as we did in Section (3.1). This will be convenient since we will occasionally have to work with vectors that do not necessarily live in the natural cone. For example, given a $|\chi\rangle \in \mathscr{H}$ we define:

$$\pi^{\mathcal{A}'}(\chi) \equiv \pi^{\mathcal{A}'}(\omega'_\chi) , \qquad \pi^{\mathcal{A}}(\chi) \equiv \pi^{\mathcal{A}}(\omega_\chi) \tag{3.51}$$

where $\omega'_\chi \in \mathcal{A}'_\star$ is the induced linear functional of $|\chi\rangle \in \mathscr{H}$ on the commutant. For vectors $|\xi\rangle$ in the natural cone we have a symmetry between the support projectors $\pi^{\mathcal{A}}(\xi) = J_{\mathcal{A}}\pi^{\mathcal{A}}(\xi)J_{\mathcal{A}}$. We use similar notation for objects associated to the algebras $\mathcal{B}$. When the only algebra in question is $\mathcal{A}$, we write

$$\pi(\chi) \equiv \pi^{\mathcal{A}}(\chi), \quad \pi'(\chi) \equiv \pi^{\mathcal{A}'}(\chi). \tag{3.52}$$

We have already recalled that a general vector $|\chi\rangle \in \mathscr{H}$ is related to a unique vector in the natural cone inducing the same linear functional on $\mathcal{A}$. More precisely, there is a partial isometry in $v'_\chi \in \mathcal{A}'$ such that

$$|\chi\rangle = {v'_\chi}^* |\xi_\chi\rangle \ , \qquad v'_\chi {v'_\chi}^* = \pi^{\mathcal{A}'}(\chi) \, , \qquad {v'_\chi}^* v'_\chi = \pi^{\mathcal{A}'}(\chi) \tag{3.53}$$

Now consider a vector $|\psi_{\mathcal{A}}\rangle = |\xi^{\mathcal{A}}_\psi\rangle \in \mathscr{P}^\natural_{\mathcal{A}}$ and define a corresponding vector in $\mathscr{K}$ using $|\psi_{\mathcal{B}}\rangle \equiv \xi^{\mathcal{B}}_\psi \in \mathscr{P}^\natural_{\mathcal{B}}$. The vector $V_\eta |\psi_{\mathcal{B}}\rangle \in \mathscr{H}$ induces the same linear functional on $\iota(\mathcal{B})$ as $|\psi_{\mathcal{A}}\rangle$, where we use exchangeably the notation $V_\eta = V_\sigma$ for the embedding (3.16). Thus there exists a partial isometry $u'_{\psi;\eta}$in $\iota(\mathcal{B})'$, with implied initial and final support, relating the two vectors

$$V_\eta |\psi_{\mathcal{B}}\rangle = {u'_{\psi,\eta}}^* |\psi_{\mathcal{A}}\rangle \, . \tag{3.54}$$

Combining this with (3.17) we have for $b \in \mathcal{B}$

$$V_\eta b |\psi_{\mathcal{B}}\rangle = \iota(b) {u'_{\psi,\eta}}^* |\psi_{\mathcal{A}}\rangle \, . \tag{3.55}$$

Since this notation is cumbersome we will simply define a new isometry $V_\psi : \mathscr{K} \to \mathscr{H}$ that is defined with reference to $|\psi\rangle$

$$V_\psi \equiv u'_{\psi,\eta} V_\eta\,. \tag{3.56}$$

It will also be convenient to have V_χ defined for states $|\chi\rangle \in \mathscr{H}$ that are not necessarily in the natural cone. In that case, we extend this definition further:

$$V_\chi \equiv {v'_\chi}^* u'_{\xi_\chi;\xi_\eta} V_\eta\,. \tag{3.57}$$

These satisfy

$$V_\chi b \left|\xi_\chi^{\mathcal{B}}\right\rangle = \iota(b)\,|\chi\rangle\,. \tag{3.58}$$

3.2.2 L_p spaces, fidelity and relative entropy

In this part we introduce various quantum information measures that will be useful to characterize sufficiency. We have already seen the importance of relative entropy and the fidelity. What we need are quantities interpolating between them. These will be provided by the non-commutative L_p norm associated with a von Neumann algebra, with reference to a state/vector. There exist different definitions of such norms/spaces in the literature; here we basically follow the version by Araki and Masuda [70], suitably generalized to non-faithful states. Such a generalization was considered up to a certain extent by [81], see also [82] for related work.

Definition 3.2.1. [70] Let $\mathcal{M}$ be a von Neumann algebra in standard form acting on a Hilbert space $\mathscr{H}$. For $1 \le p \le 2$ the Araki-Masuda $L_p(\mathcal{M}, \psi)$ norms, with reference to a fixed vector

$|\psi\rangle \in \mathscr{H}$, are defined by[2]:

$$\|\zeta\|^{\mathcal{M}}_{p,\psi} = \inf_{\chi \in \mathscr{H}: \|\chi\|=1, \pi^{\mathcal{M}}(\chi) \geq \pi^{\mathcal{M}}(\zeta)} \|\Delta^{1/2-1/p}_{\chi,\psi} \zeta\| \tag{3.59}$$

where the definition above only depends on the functional ω_ψ but not the choice of vector representative, $|\psi\rangle$.

Remark 2. 1) The norm is always finite for this range of p. We will use the L_p norms mostly for the commutant algebra $\mathcal{A}'$ of $\mathcal{A}$. Then,

$$\|\zeta\|^{\mathcal{A}'}_{p,\psi} = \left\|\pi^{\mathcal{A}}(\psi)\zeta\right\|^{\mathcal{A}'}_{p,\psi}, \tag{3.60}$$

due to the (possibily) restricted support of the relative modular operator.

2) For $1 \geq \alpha \geq 1/2$, the quantity $\frac{1}{\alpha-1} \ln \|\eta\|^{2\alpha}_{2\alpha,\psi}$ is sometimes called the "sandwiched Renyi entropy" (between $|\eta\rangle, |\psi\rangle$). It is in general different from the "usual" Renyi-Petz entropy, $\frac{1}{\alpha-1} \ln\langle\psi|\Delta^{1-\alpha}_{\psi,\eta}\psi\rangle$. Both quantities, as well as the L_p norms, can be defined or more general values of the parameters but are not needed here.

When $p = 2$, the L_p norm becomes the projected Hilbert space norm:

$$\|\zeta\|^{\mathcal{A}'}_{2,\psi} = \left\|\pi^{\mathcal{A}}(\psi)\zeta\right\|. \tag{3.61}$$

Taking a derivative at $p = 2$ will give the relative entropy comparing ζ with ψ as linear functionals

[2]The Araki-Masuda norms were originally defined assuming a faithful normal reference state. For the most part we will only ever need the definition of the norm (3.59) for vectors in the Hilbert space, along with some simple consequences of this variational formula. Thus we will not need the full machinery developed by [70], except at some crucial steps in the interpolation argument below that we will highlight. When this is the case we will apply their results for a *faithful state* and prove that one can extrapolate to the case at hand.

on $\mathcal{A}$, see below.

At $p = 1$ we have the following lemma:

Lemma 3.2.1. 1. At $p = 1$ the Araki-Masuda norm (3.59) relative to $\mathcal{A}'$ becomes the fidelity

$$\|\phi\|_{1,\psi} = F(\omega_\psi, \omega_\phi) \equiv \sup_{u' \in \mathcal{A}' : (u')^* u' = 1} |\langle\psi| u' |\phi\rangle|, \tag{3.62}$$

where $\omega_\phi, \omega_\psi \in \mathcal{A}$ are the induced linear functionals for $|\phi\rangle, |\psi\rangle$, respectively.

2. The fidelity may also be written as

$$F(\omega_\psi, \omega_\phi) = \sup_{x' \in \mathcal{A}' : \|x'\| \le 1} |\langle\psi| x' |\phi\rangle|. \tag{3.63}$$

3. It is related to the linear functional norm (Fuchs-van-der-Graff inequalities) by

$$1 - F(\omega_\psi, \omega_\phi) \le \frac{1}{2}\|\omega_\psi - \omega_\phi\| \le \sqrt{1 - F(\omega_\psi, \omega_\phi)^2}. \tag{3.64}$$

Proof. While these results are standard, we include the proof in the Appendix (B.2.1) because we also treat the non-faithful case for the generalized Araki-Masuda norm in (3.59) which has not explicitly appeared elsewhere as far as we are aware. Note that an argument conditional on other – unproven in the non-faithful case – properties of Araki-Masuda norms was given in [81]. □

We will also need the following result that is potentially of independent interest.

Theorem 3.2.1 (First Law for Renyi Relative Entropy). Consider a one parameter family of vectors $|\zeta_\lambda\rangle \in \mathscr{H}$ for $\lambda \geq 0$, which are normalized $\|\zeta_\lambda\| = 1$ and satisfy

$$\lim_{\lambda \to 0^+} \frac{\|\zeta_\lambda - \psi\|^2}{\lambda} = 0, \tag{3.65}$$

where $|\psi\rangle = |\zeta_0\rangle$. Then:

1) The Petz-Renyi relative entropy satisfies:

$$\lim_{\lambda \to 0^+} \frac{1}{\lambda} \ln \langle\zeta_\lambda| \Delta_{\psi,\zeta_\lambda}^{x(\lambda)} |\zeta_\lambda\rangle = 0\,, \qquad 0 \leq x(\lambda) \leq 1-\epsilon, \tag{3.66}$$

where $\epsilon > 0$ and there is no other constraint on $x(\lambda)$.

2) The sandwiched Renyi relative entropy satisfies:

$$\lim_{\lambda \to 0^+} \frac{1}{\lambda} \ln \|\zeta_\lambda\|_{p(\lambda),\psi}^{\mathcal{A}'} = 0\,, \qquad 1 \leq p(\lambda) \leq 2, \tag{3.67}$$

with no other constraint on how the function $p(\lambda)$ behaves under the limit.

In order to prove this, we first prove the following lemma:

Lemma 3.2.2. Given two normalized vectors $|\psi\rangle, |\zeta\rangle \in \mathscr{H}$, we have:

1) For compact subsets K of the complex strip $\{0 \leq \mathrm{Re} z < 1\}$, there exists a constant C_K such that:

$$0 \leq \mathrm{Re}\left(1 - \langle\zeta| \Delta_{\psi,\zeta}^{z} |\zeta\rangle\right) \leq C_K \|\zeta - \psi\|^2 \tag{3.68}$$

for all $z \in K$. C_K is independent of $|\psi\rangle, |\zeta\rangle$.

2) We also have for $1 \leq p \leq 2$:

$$0 \leq 1 - \langle\zeta| \Delta_{\psi,\zeta}^{2/p-1} |\zeta\rangle \leq 1 - \left(\|\zeta\|_{p,\psi}^{\mathcal{A}'}\right)^2 \leq 1 - \left(\langle\zeta| \Delta_{\psi,\zeta}^{1-p/2} |\zeta\rangle\right)^{2/p}, \tag{3.69}$$

and we have the elementary bound:

$$1 - \left(\langle\zeta| \Delta_{\psi,\zeta}^{1-p/2} |\zeta\rangle\right)^{2/p} \leq \frac{2}{p}\left(1 - \langle\zeta| \Delta_{\psi,\zeta}^{1-p/2} |\zeta\rangle\right). \tag{3.70}$$

Proof. (1) This is demonstrated by an application of Harnack's inequality (see e.g. [83], sec. 2, Theorem 11) which applies to any $h(z)$ that is harmonic and non negative in some connected open set O: for all compact subsets $K \subset O$ there exists a constant $1 \leq C(K,O) < \infty$ such that:

$$h(z) \leq C(K,O)h(w), \qquad \forall z, w \in K, \tag{3.71}$$

where notably this constant is independent of the particular h satisfying the assumptions.

We work with the real part of two holomorphic functions in two strips:

$$h_1(z) = \mathrm{Re}(1 - \langle\psi| \Delta_{\psi,\zeta}^{z} |\zeta\rangle), \qquad O_1 = \{z \in \mathbb{C} : -1/2 < \mathrm{Re}(z) < 1/2\} \tag{3.72a}$$

$$h_2(z) = \mathrm{Re}(1 - \langle\zeta| \Delta_{\psi,\zeta}^{z} |\zeta\rangle), \qquad O_2 = \{z \in \mathbb{C} : 0 < \mathrm{Re}(z) < 1\}. \tag{3.72b}$$

These functions are continuous on the closure of the above strips and they are non-negative since for normalized vectors $|\langle\psi| \Delta_{\psi,\zeta}^{z} |\zeta\rangle|, |\langle\zeta| \Delta_{\psi,\zeta}^{z} |\zeta\rangle| \leq 1$ by an easy application of the Hadamard three lines theorem – these facts are standard results of Tomita-Takesaki theory for the relative modular operators. There is no need for any of the vectors to be in the natural cone.

We can thus apply Harnack's inequality. Using the fact that:

$$h_1(0) = \frac{1}{2}\|\psi - \zeta\|^2, \tag{3.73}$$

and picking the compact subset $K_1 \subset O_1$ with $0 \in K_1$ we have:

$$0 \leq h_1(z) \leq \frac{1}{2}C(K_1, O_1)\|\psi - \zeta\|^2 \qquad \forall\ z \in K_1. \tag{3.74}$$

We have to relate this to $h_2(z)$ which is what we are most concerned with. We can relate the two functions using the Cauchy-Schwarz inequality where the two defining strips overlap, $0 \leq \mathrm{Re}z \leq 1/2$:

$$\begin{aligned}\mathrm{Re}\left(- \langle\zeta| \Delta^{z}_{\psi,\zeta} |\zeta\rangle + \langle\psi| \Delta^{z}_{\psi,\zeta} |\zeta\rangle + \langle\zeta| \psi\rangle - 1\right) &\leq \left|\left(|\zeta\rangle - |\psi\rangle , \Delta^{z}_{\psi,\zeta} |\zeta\rangle - |\psi\rangle\right)\right| \\ &\leq \|\zeta - \psi\| \left(\mathrm{Re}\left(1 + \langle\zeta| \Delta^{z+\bar{z}}_{\psi,\zeta} |\zeta\rangle - 2 \langle\psi| \Delta^{z}_{\psi,\zeta} |\zeta\rangle\right)\right)^{1/2} \\ &\leq \|\zeta - \psi\| \left(\mathrm{Re}\left(2 - 2 \langle\psi| \Delta^{z}_{\psi,\zeta} |\zeta\rangle\right)\right)^{1/2},\end{aligned} \tag{3.75}$$

which translates to:

$$h_2(z) \leq \frac{1}{2}\left(\|\zeta - \psi\| + \sqrt{2h_1(z)}\right)^2, \tag{3.76}$$

so that

$$0 \leq h_2(z) \leq \frac{1}{2}\left(1 + \sqrt{C(K_1, O_1)}\right)^2 \|\psi - \zeta\|^2 \qquad \forall\ z \in K_1 \cap \overline{O}_2. \tag{3.77}$$

We can split the compact set K in the statement of the lemma into two compact pieces $K_1 = K \cap \{z \in \mathbb{C} : 0 \leq \mathrm{Re}z \leq 1/4\}$ and $K_2 = K \cap \{z \in \mathbb{C} : 1/4 \leq \mathrm{Re}z \leq 1\}$. These satisfy

$K_i \subset O_i \ : \ i = 1, 2$. Repeatedly applying Harnack's inequality as above gives the following upper bound for C_K:

$$\frac{1}{2}\max\left\{\left(1+\sqrt{C(\{0\}\cup K_1, O_1)}\right)^2,\ C(\{\tfrac{1}{4}\}\cup K_2, O_2)\left(1+\sqrt{C(\{0,\tfrac{1}{4}\}, O_1)}\right)^2\right\}, \quad (3.78)$$

where it was necessary to add the points $\{0, 1/4\}$ since they may not have been in the original K.

(2) This result is basically the well-known Araki-Lieb-Thirring inequality [84], for a proof in the von Neumann algebra setting see [81], Theorem 12, for L_p norms based on a not necessarily cyclic and separating vector $|\psi\rangle$. □

Proof of Theorem (3.2.1). (1) is a consequence of Lemma (3.2.2) (1): We can take $K = [0, 1-\epsilon]$ which satisfies the assumptions of this lemma so:

$$0 \leq \lim_{\lambda\to 0^+} \frac{\left(1 - \langle\zeta_\lambda|\, \Delta^{x(\lambda)}_{\psi,\zeta_\lambda}\, |\zeta_\lambda\rangle\right)}{\lambda} \leq \lim_{\lambda\to 0^+} C_K \frac{\|\zeta_\lambda - \psi\|^2}{\lambda} = 0. \quad (3.79)$$

Then using differentiability of $\ln(x)$ at $x = 1$ and the chain rule we show (3.66).

(2) Here we need Lemma (3.2.2) (1) with $K = [0, 1/2]$. Applying Lemma (3.2.2) (2):

$$\begin{aligned} 0 \leq \lim_{\lambda\to 0^+} \frac{\left(1 - \|\zeta_\lambda\|^{\mathcal{A}'}_{p(\lambda),\psi}\right)}{\lambda} &\leq \lim_{\lambda\to 0^+} \frac{2}{p(\lambda)}\left(1 - \langle\zeta_\lambda|\, \Delta^{1-p(\lambda)/2}_{\psi,\zeta_\lambda}\, |\zeta_\lambda\rangle\right) \\ &\leq \lim_{\lambda\to 0^+} 2C_K \frac{\|\zeta_\lambda - \psi\|^2}{\lambda} = 0. \end{aligned} \quad (3.80)$$

Again differentiability of $\ln(x)$ at $x = 1$ and the chain rule gives (3.67). □

3.2.3 Exact recoverability/sufficiency

This section is meant as an informal summary of some of the results given in [71, 72], defining the exact notion of recoverability or sufficiency. We will focus only on the properties associated to sufficiency that we make contact with in this paper, and we will also treat only the case of faithful linear functionals and drop all support projectors here.

By definition, the quantum channel $\iota : \mathcal{B} \to \mathcal{A}$ is exactly reversible for at least two fixed states ρ, σ if there exists a recovery channel $\alpha : \mathcal{A} \to \mathcal{B}$ such that:

$$\rho \circ \iota \circ \alpha(a) = \rho(a)\,, \qquad \forall a \in \mathcal{A}, \tag{3.81}$$

and similarly for σ. Since the relative entropy is monotonous [21] under both α, ι, we must have $S_{\mathcal{A}}(\rho, \sigma) = S_{\mathcal{B}}(\rho, \sigma)$, see (3.15) for our notation. Representing σ, ρ by vectors in the natural cone as in (3.50) and using a standard integral representation of the relative entropy based on the spectral theorem and the elementary identity $(x, y > 0)$

$$\ln y - \ln x = \int_0^\infty \left(\frac{1}{x+\beta} - \frac{1}{y+\beta} \right) \mathrm{d}\beta\,, \tag{3.82}$$

we get that

$$S_{\mathcal{A}}(\rho|\sigma) - S_{\mathcal{B}}(\rho|\sigma) = \int_0^\infty \langle \psi_{\mathcal{B}}| \left(V_\psi^* \frac{1}{\beta + \Delta_{\eta_{\mathcal{A}}, \psi_{\mathcal{A}}}} V_\psi - \frac{1}{\beta + \Delta_{\eta_{\mathcal{B}}, \psi_{\mathcal{B}}}} \right) |\psi_{\mathcal{B}}\rangle \, \mathrm{d}\beta \tag{3.83}$$

vanishes. Known properties of the modular operators imply that the integrand is positive [71, 72, 73]. Therefore,

$$V_\psi^* \frac{1}{\beta + \Delta_{\eta_\mathcal{A},\psi_\mathcal{A}}} |\psi_\mathcal{A}\rangle = \frac{1}{\beta + \Delta_{\eta_\mathcal{B},\psi_\mathcal{B}}} |\psi_\mathcal{B}\rangle \tag{3.84}$$

for all $\beta > 0$, which can be integrated against a specific kernel that we will not write to arrive at a statement about the relative modular flow:

$$V_\psi^* \Delta^{it}_{\eta_\mathcal{A},\psi_\mathcal{A}} |\psi_\mathcal{A}\rangle = \Delta^{it}_{\eta_\mathcal{B},\psi_\mathcal{B}} |\psi_\mathcal{B}\rangle \quad \Longrightarrow \quad |\psi_\mathcal{A}\rangle = \Delta^{-it}_{\eta_\mathcal{A},\psi_\mathcal{A}} V_\psi \Delta^{it}_{\eta_\mathcal{B},\psi_\mathcal{B}} |\psi_\mathcal{B}\rangle \,. \tag{3.85}$$

Further manipulations give a derivation that the Petz map is a perfect recovery channel, although we will not go through this. Here we simply note that it is a reasonable guess at this point that for the approximate version of recoverability, one must require that $|\psi_\mathcal{A}\rangle$ must be close to $\Delta^{-it}_{\eta_\mathcal{A},\psi_\mathcal{A}} V_\psi \Delta^{it}_{\eta_\mathcal{B},\psi_\mathcal{B}} |\psi_\mathcal{B}\rangle$ in some metric. We will use the non-commutative Araki-Masuda L_p norms to provide such a metric.

3.2.4 Interpolating vector

Motivated by the above discussion we consider the following vector in $\mathscr{H}$:

$$|\Gamma_\psi(z)\rangle = \Delta^{z}_{\eta_\mathcal{A},\psi_\mathcal{A}} V_\psi \Delta^{-z}_{\eta_\mathcal{B},\psi_\mathcal{B}} |\psi_\mathcal{B}\rangle \,, \tag{3.86}$$

defined at first for purely imaginary z, and assuming at first that $|\psi\rangle, |\eta\rangle$ are in the natural cone (of $\mathcal{A}$), see (3.50) for our notation.

Remark 3. The vector defined here is similar in spirit but does not quite coincide with the interpolating vector considered by [2]. It seems possible to consider other vectors instead, and we briefly comment on this in Appendix (3.3).

Our first result will be an analytic continuation of the vector (3.86) into a strip:

Theorem 3.2.2. 1. There is a vector-valued function $|\Gamma_\psi(z)\rangle$ that is holomorphic in the strip $\mathbb{S}_{1/2} = \{0 < \mathrm{Re}(z) < 1/2\}$, weakly continuous in the closure of the strip and has the following explicit form at the top and bottom edges:

$$|\Gamma_\psi(1/2+it)\rangle = \Delta^{it}_{\eta_\mathcal{A},\psi_\mathcal{A}} J_\mathcal{A} V_\eta J_\mathcal{B} \Delta^{-it}_{\eta_\mathcal{B},\psi_\mathcal{B}} |\psi_\mathcal{B}\rangle \tag{3.87a}$$

$$|\Gamma_\psi(it)\rangle = \Delta^{it}_{\eta_\mathcal{A},\psi_\mathcal{A}} V_\psi \Delta^{-it}_{\eta_\mathcal{B},\psi_\mathcal{B}} |\psi_\mathcal{B}\rangle \, . \tag{3.87b}$$

The norm of the vector $|\Gamma_\psi(z)\rangle$ is bounded by 1 everywhere in the closure of $\mathbb{S}_{1/2}$, and $\big|\Gamma_\psi(0)\big\rangle = |\psi_\mathcal{A}\rangle$.

2. On the top edge of the strip $\mathbb{S}_{1/2}$ this vector induces the the following state on $\mathcal{A}$:

$$(|\Gamma_\psi(1/2+it)\rangle\, , a_+ \,|\Gamma_\psi(1/2+it)\rangle) \le \langle\psi|\, \iota(\alpha^t_\eta(a_+))\, |\psi\rangle = \omega_\psi \circ \iota \circ \alpha^t_\eta(a_+), \tag{3.88}$$

where a_+ is any non-negative self-adjoint element in $\mathcal{A}$, and where α^t_η is the rotated Petz map (3.25) for the state σ induced by $|\eta\rangle$.

Remark 4. 1) A variant of this theorem holds when $|\psi\rangle$ is replaced by a unit vector $|\chi\rangle$ that is not necessarily in the natural cone. In this case, we should define

$$|\Gamma_\chi(z)\rangle = v'_\chi \left|\Gamma_{\xi_\chi}(z)\right\rangle \tag{3.89}$$

with v'_χ as in (3.53). The limiting values (3.87b), (3.87a) at the boundaries of the strip are then readily computed using (3.54). In particular, (3.87b) takes the same form as before as seen using

(3.57), (3.58), which also implies $\left|\Gamma_\chi(0)\right\rangle = |\chi\rangle$. (3.88) follows from (3.7).

2) The proof shows that we would have equality in (2) if $\pi^{\mathcal{A}'}(\psi) = 1$, i.e. if $|\psi\rangle$ is cyclic for $\mathcal{A}$.

Proof. Let us use in this proof the shorthands $\Delta_{\eta_\mathcal{B},\psi_\mathcal{B}} = \Delta_{\eta,\psi;\mathcal{B}}$ and $\Delta_{\eta_\mathcal{A},\psi_\mathcal{A}} = \Delta_{\eta,\psi;\mathcal{A}}$.

(1) Given an $a' \in \mathcal{A}'$, consider the function:

$$g(z) = \left(\Delta^{\bar{z}-1/2}_{\eta,\psi;\mathcal{A}} a' \left|\eta_\mathcal{A}\right\rangle, J_\mathcal{A} V_\eta J_\mathcal{B} \Delta^{-z+1/2}_{\eta,\psi;\mathcal{B}} \left|\psi_\mathcal{B}\right\rangle\right), \tag{3.90}$$

which using Tomita-Takesaki theory is analytic in the strip $\mathbb{S}_{1/2}$, continuous in the closure, and bounded by:

$$|g(z)| \leq \max_{0\leq\theta\leq 1/2} \|(\Delta'_{\eta,\psi;\mathcal{A}})^\theta a'\eta_\mathcal{A}\| \, \|(\Delta_{\eta,\psi;\mathcal{B}})^\theta \psi_\mathcal{B}\|, \tag{3.91}$$

where $\theta = \mathrm{Re}(1/2 - z)$. The maximum is achieved by continuity and compactness of the interval. This bound is however not uniform over vectors $a' \left|\eta_\mathcal{A}\right\rangle \in \mathscr{H}$ with norm 1. For this, we need to use the Phragmén-Lindelöf theorem. Our function has the following form at the edges of the strip ($t \in \mathbb{R}$):

$$g(1/2 + it) = \left(a' \left|\eta_\mathcal{A}\right\rangle, \left|\Gamma_\psi(1/2 + it)\right\rangle\right) \tag{3.92a}$$

$$g(it) = \left(a' \left|\eta_\mathcal{A}\right\rangle, \left|\Gamma_\psi(it)\right\rangle\right), \tag{3.92b}$$

where we made use of the expressions/definitions in (3.87a) and (3.87b) respectively. The first equation above is rather trivial but the second equation requires some lines of algebra:

$$\begin{aligned} g(it) &= \left(\Delta_{\eta,\psi;\mathcal{A}}^{-it-1/2} a' \left|\eta_{\mathcal{A}}\right\rangle , J_{\mathcal{A}} V_\eta \Delta_{\psi,\eta;\mathcal{B}}^{-it} \pi^{\mathcal{B}}(\psi) \left|\eta_{\mathcal{B}}\right\rangle\right) \\ &= \left(\Delta_{\eta,\psi;\mathcal{A}}^{-it-1/2} a' \left|\eta_{\mathcal{A}}\right\rangle , J_{\mathcal{A}} V_\eta b \left|\eta_{\mathcal{B}}\right\rangle\right) , \qquad b = \Delta_{\psi,\eta;\mathcal{B}}^{-it} \pi^{\mathcal{B}}(\psi) \Delta_{\eta;\mathcal{B}}^{it} \in \mathcal{B} \\ &= \left(\Delta_{\eta,\psi;\mathcal{A}}^{-it-1/2} a' \left|\eta_{\mathcal{A}}\right\rangle , J_{\mathcal{A}} \iota(b) \left|\eta_{\mathcal{A}}\right\rangle\right) = \left(\Delta_{\eta,\psi;\mathcal{A}}^{-it} a' \left|\eta_{\mathcal{A}}\right\rangle , \iota(b)^* \left|\psi_{\mathcal{A}}\right\rangle\right) \\ &= \left(\Delta_{\eta,\psi;\mathcal{A}}^{-it} a' \left|\eta_{\mathcal{A}}\right\rangle , V_\psi b^* \left|\psi_{\mathcal{B}}\right\rangle\right) = \left(\Delta_{\eta,\psi;\mathcal{A}}^{-it} a' \left|\eta_{\mathcal{A}}\right\rangle , V_\psi \Delta_{\eta,\psi;\mathcal{B}}^{-it} \left|\psi_{\mathcal{B}}\right\rangle\right) , \end{aligned} \tag{3.93}$$

where in the first line we used (3.6), in the second we inserted $\Delta_{\eta;\mathcal{B}}^{it}$ for free giving rise to b which is in $\mathcal{A}$ from the last equation in (3.10), we used (3.16) in the third line after which we passed $\Delta_{\eta,\psi;\mathcal{A}}^{-1/2}$ to the right which is allowed since this vector is now in the domain of this operator. We used (3.58) in line four and finally b can be rewritten as:

$$\pi^{\mathcal{B}'}(\psi) b = \Delta_{\psi;\mathcal{B}}^{-it} \pi^{\mathcal{B}}(\psi) \Delta_{\eta,\psi;\mathcal{B}}^{it} \tag{3.94}$$

using (3.11). This finally leads to (3.92b). Since both expressions in (3.87a) and (3.87b) involve products of partial isometries we have the following bound on the edges of the strip:

$$|g(it)|, |g(1/2+it)| \leq \|a' \eta_{\mathcal{A}}\|, \tag{3.95}$$

which then extends inside the strip via the Phragmén-Lindelöf theorem. That theorem also requires the (weaker) bound we derived in (3.91) and it applies inside the closure of the strip. Since $\mathcal{A}' \left|\eta_{\mathcal{A}}\right\rangle$ is dense in the Hilbert space we can extend the definition of $g(z)$ to the full Hilbert space, at which point it is a continuous anti-linear functional on all vectors, weakly (hence strongly) holomorphic in $\mathbb{S}_{1/2}$. This then defines a vector in $\mathscr{H}$ which is then our definition of (3.86) on the strip $\mathbb{S}_{1/2}$. The bound on the norm of this vector follows also from Phragmén-Lindelöf theorem. For the continuity statements we further need the limit of $g(z)$, as $a' |\eta\rangle$ approaches an arbitrary vector, to be uniform in z. This follows easily from the uniform boundedness of $g(z)$ and the Banach-Steinhaus principle.

(2) The final property (3.88) follows from a short calculation:

$$
\begin{aligned}
&\left(J_{\mathcal{A}} V_\eta J_{\mathcal{B}} \Delta^{-it}_{\eta,\psi;\mathcal{B}} |\psi_{\mathcal{B}}\rangle , \Delta^{-it}_{\eta,\chi;\mathcal{A}} a_+ \Delta^{it}_{\eta,\chi;\mathcal{A}} J_{\mathcal{A}} V_\eta J_{\mathcal{B}} \Delta^{-it}_{\eta,\psi;\mathcal{B}} |\chi_{\mathcal{B}}\rangle\right) \\
&\quad = \Big(J_{\mathcal{A}} V_\eta J_{\mathcal{B}} \Delta^{-it}_{\eta,\psi;\mathcal{B}} |\psi_{\mathcal{B}}\rangle , \varsigma^t_\eta(a_+) \pi^{\mathcal{A}'}(\psi) J_{\mathcal{A}} V_\eta J_{\mathcal{B}} \Delta^{-it}_{\eta,\psi;\mathcal{B}} |\chi_{\mathcal{B}}\rangle\Big) \\
&\quad = \Big(J_{\mathcal{A}} V_\eta J_{\mathcal{B}} \Delta^{-it}_{\eta,\psi;\mathcal{B}} |\psi_{\mathcal{B}}\rangle , \varsigma^t_{\eta;\mathcal{A}}(a_+)^{1/2} \pi^{\mathcal{A}'}(\psi) \varsigma^t_{\eta;\mathcal{A}}(a_+)^{1/2} J_{\mathcal{A}} V_\eta J_{\mathcal{B}} \Delta^{-it}_{\eta,\psi;\mathcal{B}} |\psi_{\mathcal{B}}\rangle\Big) \\
&\quad \le \left(|\psi_{\mathcal{B}}\rangle , \Delta^{it}_{\eta,\psi;\mathcal{B}} J_{\mathcal{B}} \left(V^*_\eta J_{\mathcal{A}} \varsigma^t_{\eta,\mathcal{A}}(a^+) J_{\mathcal{A}} V_\eta\right) J_{\mathcal{B}} \Delta^{-it}_{\eta,\psi;\mathcal{B}} |\psi_{\mathcal{B}}\rangle\right) \\
&\quad = \left(|\psi_{\mathcal{B}}\rangle , \alpha^t_{\eta;\mathcal{A}}(a_+) |\psi_{\mathcal{B}}\rangle\right) = \omega_\psi \circ \iota \circ \alpha^t_\eta(a_+),
\end{aligned}
\tag{3.96}
$$

where we used (3.9) in the second line, the positivity of $\varsigma^t_\eta(a_+)$ in the third line, the bound $\pi^{\mathcal{A}'}(\psi) \le 1$ in the fourth line, the fact that $V^*_\eta \mathcal{A}' V_\eta \subset \mathcal{B}'$ (see (B.7)) and again (3.9) for the $\mathcal{B}$ algebra in the fifth line. □

3.2.5 Strengthened monotonicity

3.2.5.1 Basic strategy

We will apply interpolation theory to the vector $\left|\Gamma_\psi(z)\right\rangle$, following the basic strategy of [2]. By Theorem (3.2.2) (2) we get the rotated Petz recovered state on the top of the strip at $z = 1/2 + it$, so we need to interpolate to the $L_1(\mathcal{A}', \psi)$ norm there where it becomes the fidelity by Lemma (3.2.1) (1). Close to $z = 0$ we will need to approach the $p = 2$ norm (the $\pi(\psi)$ projected Hilbert space norm) by (3.61) where we will show that we can extract the difference in relative entropy. A generalized sum rule, using sub-harmonic analysis, relates the $z = 0$ limit to an integral over the fidelities of the $z = 1/2 + it$ vector.

Extracting the relative entropy difference is the most difficult part of the proof and requires some modifications to the basic strategy. We proceed by extending the domain of holomorphy to a larger strip so that we can take derivatives at $z = 0$ easily. This requires defining a class of states with filtered spectrum for the relative modular operator. We then approach the original state as a limit. After a continuity argument, we show that this is sufficient to prove a strengthened monotonicity statement for all states with finite $\mathcal{B}$ relative entropy.

3.2.5.2 Filtering and continuity

Our first task will be to extend $|\Gamma_\psi(z)\rangle$ holomorphically into the larger strip $\{-1/2 < \mathrm{Re} z \leq 1/2\}$. This might not be possible for general $|\psi\rangle$, so to make progress we work with vectors that have approximately bounded spectral support for the relative modular operator $\Delta_{\eta,\psi}$. Thus we now introduce a *filtering* procedure that produces from $|\psi\rangle$ a vector $|\psi_P\rangle$ with approximately bounded spectral support.

For convenience, we work with $|\eta\rangle, |\psi\rangle \in \mathscr{H}$ in the natural cone, and consider a related vector $|\psi_P\rangle$ (which is not in the natural cone of $\mathcal{A}$), defined by:

$$|\psi_P\rangle = \int_{-\infty}^{\infty} f_P(t) \Delta_{\eta,\psi}^{it} |\psi\rangle \, \mathrm{d}t = \tilde{f}_P(\ln \Delta_{\eta,\psi}) |\psi\rangle \,, \tag{3.97}$$

where $\tilde{f}_P$ is the Fourier transform of a certain function f_P and provides a kind of damping.

All modular operators and support projections in this subsection refer to $\mathcal{A}$, and since we only consider one algebra in this subsection, we drop the subscripts to lighten the notation. Note that $\ln \Delta_{\eta,\psi}$ is defined on $\pi'(\psi)\pi(\psi)\mathscr{H}$ since $\Delta_{\eta,\psi}$ is only invertible there. Away from this subspace the operator acts as 0.

We take f_P to have the following properties, motivated by the desire to prove nice continuity statements as $P \to \infty$. Since we want to think of P as a cutoff, we take f_P to be a scaling function:

$$f_P(t) = Pf(tP), \tag{3.98}$$

and now specify properties of $f(t)$. (Note that the Fourier transform satisfies $\tilde{f}_P(p) = \tilde{f}(p/P)$.)

Definition 3.2.2. We call the function f in (3.98) a *smooth filtering function* if it satisfies the following properties.

(A) The Fourier transform of f

$$\tilde{f}(p) = \int_{-\infty}^{\infty} e^{-itp} f(t)\mathrm{d}t \tag{3.99}$$

exists as a real and non-negative Schwarz-space function. This implies that the original function f is Schwarz and has finite $L_1(\mathbb{R})$ norm, $\|f\|_1 < \infty$.

(B) $f(t)$ has an analytic continuation to the upper complex half plane such that the $L_1(\mathbb{R})$ norm of the shifted function has $\|f(\cdot + i\theta)\|_1 < \infty$ for $0 < \theta < \infty$.

Note that the Fourier transform of the shifted function satisfies:

$$\widetilde{f(\cdot + i\theta)}(p) = \tilde{f}(p)e^{-\theta p}. \tag{3.100}$$

Examples of such smooth filtering functions include Gaussians as well as the Fourier transform of smooth functions $\tilde{f}$ with compact support. The norms satisfy:

$$\|\tilde{f}_P\|_\infty = \|\tilde{f}\|_\infty \geq \tilde{f}(0)\,, \qquad \|f_P\|_1 = \|f\|_1 \geq \|\tilde{f}\|_\infty, \tag{3.101}$$

where the later inequality is well-known as the Hausdorff-Young inequality.

We now establish some properties of the resulting vector $|\psi_P\rangle$:

Lemma 3.2.3. The filtered vector $|\psi_P\rangle$ defined in (3.97) based on a smooth filtering function f, has the following properties:

1. $\lim_{P\to\infty} |\psi_P\rangle = \tilde{f}(0)\,|\psi\rangle$ strongly.

2. There exists $a_P \in \mathcal{A}$ such that $|\psi_P\rangle = a_P\,|\psi\rangle$, and

$$\|a_P\| \leq \|f\|_1, \tag{3.102}$$

   such that $a_P\pi(\psi) = a_P$.

3. The induced linear functional on $\mathcal{A}'$ is dominated by

$$\omega'_{\psi_P} \leq \|f\|_1^2\,\omega'_\psi, \tag{3.103}$$

   and $\pi'(\psi_P) \leq \pi'(\psi)$.

4. There exists $a'_P \in \mathcal{A}'$ such that $|\psi_P\rangle = a'_P\,|\eta\rangle$, and $\|a'_P\| \leq \|f(\cdot + iP/2)\|_1$.

5. The induced linear functional on the algebra $\mathcal{A}$ is dominated by

$$\omega_{\psi_P} \leq \|f(\cdot + iP/2)\|_1^2 \, \omega_\eta. \tag{3.104}$$

We need property (A) of def. (3.2.2) for (1-3) and property (B) for (4-5).

Proof. (1) Letting $E_{\eta,\psi}(\mathrm{d}\lambda)$ be the spectral resolution of $\ln \Delta_{\eta,\psi}$, we have

$$\|\psi_P - \tilde{f}(0)\psi\|^2 = \int_{\mathbb{R}} \left(\tilde{f}(\lambda/P) - \tilde{f}(0)\right)^2 \langle \psi | E_{\eta,\psi}(\mathrm{d}\lambda)\psi \rangle \, . \tag{3.105}$$

We can take the pointwise limit $P \to \infty$ using dominated convergence (since $\tilde{f}$ is a bounded function); this immediately gives the statement.

(2) We insert $\Delta_\psi^{-it}\pi'(\psi)$ next to $|\psi\rangle$ in the first expression of (3.97) and find

$$a_P = \int_{\mathbb{R}} f_P(t) \Delta_\eta^{it} \Delta_{\psi,\eta}^{-it} \mathrm{d}t. \tag{3.106}$$

This is an integral over Connes-cocycles, hence defines an element of $\mathcal{A}$. The operator norm is bounded by

$$\|a_P\| \leq \int_{\mathbb{R}} |f_P(t)| \|\Delta_\eta^{it} \Delta_{\psi,\eta}^{-it}\| \, \mathrm{d}t \leq \int_{\mathbb{R}} |f_P(t)| \, \mathrm{d}t = \|f_P\|_1 = \|f\|_1, \tag{3.107}$$

since $\Delta_\eta^{it}\Delta_{\psi,\eta}^{-it}$ are isometries.

(3) We establish this via

$$\langle \psi_P | \, a'_+ \, |\psi_P\rangle = \langle \psi | \, {a'_+}^{1/2} a_P^* a_P {a'_+}^{1/2} \, |\psi\rangle \leq \|a_P\|^2 \, \langle \psi | \, a'_+ \, |\psi\rangle \ , \qquad a'_+ \in \mathcal{A}' \, , a'_+ \geq 0, \tag{3.108}$$

which gives (3.103) after using the bound (3.102). The bound on the support projectors follows since $\pi'(\psi_P)$ is the smallest projector $\pi' \in \mathcal{A}'$ that satisfies $\omega'_{\psi_P}(1-\pi') = 0$. But $\pi' = \pi'(\psi)$ satisfies this since $0 \leq \omega'_{\psi_P}(1-\pi'(\psi)) \leq \|f\|_1^2 \omega'_\psi(1-\pi'(\psi)) = 0$.

(4) Note that $\Delta_{\psi,\eta}^{1/2} |\eta\rangle = J|\psi\rangle = |\psi\rangle$ since $|\psi\rangle$ is in the natural cone. Then, shifting the integration contour as is legal by def. (3.2.2) (A),

$$|\psi_P\rangle = \int_{-\infty}^{\infty} f_P(t) \Delta_{\eta,\psi}^{it} \Delta_{\psi,\eta}^{1/2} |\eta\rangle \, \mathrm{d}t = \int_{-\infty}^{\infty} f_P(t+i/2) \Delta_{\eta,\psi}^{it} \Delta_{\eta}^{-it} |\eta\rangle \, \mathrm{d}t. \tag{3.109}$$

Note that $\Delta_{\eta,\psi}^{it} \Delta_\eta^{-it}$ is a Connes-cocycle for $\mathcal{A}'$, and hence an element of $\mathcal{A}'$. Now define

$$a'_P = \int_{-\infty}^{\infty} f_P(t+i/2) \Delta_{\eta,\psi}^{it} \Delta_\eta^{-it} \, \mathrm{d}t \in \mathcal{A}'. \tag{3.110}$$

Since the Connes-cocycle is isometric, the norm of a'_P may be bounded by

$$\|a'_P\| \leq \int_{-\infty}^{\infty} |f_P(t+i/2)| \, \|\Delta_{\eta,\psi}^{it} \Delta_\eta^{-it}\| \, \mathrm{d}t = \int_{-\infty}^{\infty} |f(t+iP/2)| \, \mathrm{d}t = \|f(\cdot + iP/2)\|_1. \tag{3.111}$$

(5) We have $\langle \psi_P | a_+ |\psi_P\rangle = \langle \eta | a_+^{1/2} {a'_P}^* a'_P a_+^{1/2} |\eta\rangle \leq \|a'_P\|^2 \langle \eta | a_+ |\eta\rangle$, which gives the statement in view of (4). □

We would now like to see how the relative entropy between $|\eta\rangle, |\psi_P\rangle$ behaves in the limit $P \to \infty$. We will find the conditions on f for which the relative entropy converges to that between $|\eta\rangle, |\psi\rangle$ as $P \to \infty$.

Theorem 3.2.3. Suppose $|\psi\rangle, |\eta\rangle$ are states on a von Neumann algebra $\mathcal{A}$, assumed to be in the natural cone, and suppose $|\psi_P\rangle$ is given by (3.97) with scaling function (3.98) satisfying property

(A) of def. (3.2.2) and $\tilde{f}(0) = 1$. Then:

1. $S(\psi_P|\eta) < \infty$.

2. We have

$$-2\ln(\|f\|_1) + \limsup_{P\to\infty} S(\psi_P|\eta) \leq S(\psi|\eta) \leq \liminf_{P\to\infty} S(\psi_P|\eta). \tag{3.112}$$

3. The relative entropy behaves continuously for $P \to \infty$,

$$\lim_{P\to\infty} S(\psi_P|\eta) = S(\psi|\eta), \tag{3.113}$$

iff the Fourier transform of the scaling function, $\tilde{f}(t)$, is a Gaussian centered at the origin.

Remark 5. The above statements hold even if $S(\psi|\eta) = \infty$ with limits understood as living on the compactified real line. So for example in this case (3.112) or (3.113) implies that $\lim_{P\to\infty} S(\psi_P|\eta) = \infty$.

Proof. (1) In view of (3.103), [69], Theorem 3.6, Eq. (3.7), applied to the algebra $\mathcal{A}'$, gives:

$$\frac{1}{\Delta'_{\psi_P,\eta} + \beta} \geq \frac{1}{\|f\|_1^2 \Delta'_{\psi,\eta} + \beta} \tag{3.114}$$

for all $\beta > 0$.[3] The following type of integral representation for the relative entropy is well-

[3]When applying [69], Theorem 3.6, Eq. (3.7) to the commutant $\mathcal{A}'$ using (3.6), where one switches $\mathcal{A} \leftrightarrow \mathcal{A}'$ as well as any support projectors $\pi \leftrightarrow \pi'$. Note further that [69], Theorem 3.6 refers to the natural cone but the specific representative of the linear functional does not affect the modular operators above since $\Delta'_{\xi'_{\psi_P},\eta} = \Delta'_{\psi_P,\eta}$ using the notation (3.53) (now for the commutant).

known, see e.g. [73]:

$$S(\psi_P|\eta) = \int_0^\infty \langle\psi_P| \left(-\frac{1}{\Delta^{-1}_{\eta,\psi_P} + \beta} + \frac{1}{\beta+1} \right) |\psi_P\rangle \, \mathrm{d}\beta, \tag{3.115}$$

and integral converges iff the relative entropy is finite. The bound in (3.114) can be used to bound (3.115) from above due to the first equation in (3.10) and this gives:

$$\begin{aligned} S(\psi_P|\eta) &\leq 2\ln(\|f\|_1) \langle\psi_P|\, \psi_P\rangle + \int_0^\infty \langle\psi_P| \left(-\frac{1}{\Delta^{-1}_{\eta,\psi} + \beta} + \frac{1}{\beta+1} \right) |\psi_P\rangle \, \mathrm{d}\beta \\ &= 2\ln(\|f\|_1) \langle\psi_P|\, \psi_P\rangle - \langle\psi| \ln\Delta_{\eta,\psi} \left(\tilde{f}_P(\ln\Delta_{\eta,\psi})\right)^2 |\psi\rangle \,. \end{aligned} \tag{3.116}$$

Using the spectral decomposition of $\ln\Delta_{\eta,\psi}$, we can write

$$\langle\psi| \ln\Delta_{\eta,\psi} \left(\tilde{f}_P(\ln\Delta_{\eta,\psi})\right)^2 |\psi\rangle = -\int_{-\infty}^\infty p \left(\tilde{f}(p/P)\right)^2 \langle\psi|\, E_{\eta,\psi}(\mathrm{d}p)\, |\psi\rangle \,. \tag{3.117}$$

This integral converges because $p\tilde{f}(p/P)^2$ is uniformly bounded, by the Schwartz condition in def. (3.2.2) (A). Thus the right hand side of (3.116) is finite and so we have shown (1).

(2) Let us continue by first assuming that $S(\psi|\eta) < \infty$. Strong convergence of ψ_P, Lemma (3.2.3) (1), guarantees that $\lim_P \langle\psi_P|\, \psi_P\rangle = 1$ since $\tilde{f}(0) = 1$. Now the integral on the right hand side of (3.117) can be split into two parts:

$$\lim_{P\to\infty} \int_0^{\pm\infty} |p| \left(\tilde{f}(p/P)\right)^2 \langle\psi|\, E_{\eta,\psi}(\mathrm{d}p)\, |\psi\rangle = \int_0^{\pm\infty} |p| \, \langle\psi|\, E_{\eta,\psi}(\mathrm{d}p)\, |\psi\rangle \,, \tag{3.118}$$

where we have applied the dominated convergence theorem to each term using the facts that $\tilde{f}_P(p)$ is bounded and that the relative entropy is finite. Taking the lim sup on both sides of

(3.116) gives the first inequality in (3.112). Lower semi-continuity of relative entropy [69] gives the second inequality.

If instead $S(\psi|\eta) = \infty$, then we find from lower semi-continuity:

$$\limsup_{P\to\infty} S(\psi_P|\eta) \geq \liminf_{P\to\infty} S(\psi_P|\eta) = \infty, \tag{3.119}$$

thus the limit must exist on the extended positive real line where it is infinite. This shows (2).

(3) Note that $\|f\|_1 \geq \|\tilde{f}\|_\infty \geq \tilde{f}(0) = 1$ so we get the continuity in (3.113) iff the Hausdorff-Young inequality is saturated and $\tilde{f}(0) = \|\tilde{f}\|_\infty$. It was shown by Lieb [85] that the only functions that saturate the Hausdorff-Young bound are in fact Gaussians. The condition $\tilde{f}(0) = \|\tilde{f}\|_\infty$ then simply means the Gaussian $\tilde{f}$ must be centered at the origin. □

3.2.5.3 Updated interpolating vector

We now consider again our interpolating vector (3.86). With the intention to extend the domain of holomorphy, we consider the filtered states $|\psi_P\rangle$ instead of $|\psi\rangle$. Although $|\psi_P\rangle$ is not in the natural cone, we can still define $\left|\Gamma_{\psi_P}(z)\right\rangle$ in view of Remark (4) (1). This will however by itself not be sufficient: It turns out that we also have to apply a projector Π_Λ to our vectors, so we consider

$$\Pi_\Lambda \left|\Gamma_{\psi_P}(z)\right\rangle, \qquad \Pi_\Lambda \equiv \int_{-\Lambda}^{\Lambda} E_{\psi_P}(\mathrm{d}\lambda), \tag{3.120}$$

where $E_{\psi_P}(\mathrm{d}\lambda)$ is the spectral decomposition of $\ln \Delta_{\psi_P}$, so that $\lim_{\Lambda\to\infty} \Pi_\Lambda = \pi(\psi_P)\pi'(\psi_P)$ in the strong sense. We intend to send the regulators $\Lambda, P \to \infty$, and in that process we will tune $\tilde{f}(0)$ to maintain $\|\,|\psi_P\rangle\,\| = 1$, and require (A) and (B) of def. (3.2.2). With those changes in place, we claim the following updated version of Theorem (3.2.2).

Lemma 3.2.4. 1. The vector valued function $z \mapsto \Pi_\Lambda \big|\Gamma_{\psi_P}(z)\big\rangle$ can be continued analytically to the extended strip $-1/2 < \mathrm{Re}z < 1/2$. It is bounded and weakly continuous in the closure.

2. Its norm is bounded above by 1 in the closed upper half strip $\{0 \leq \mathrm{Re}z \leq 1/2\}$ and we have the following estimate in the lower half strip $\{-1/2 \leq \mathrm{Re}z \leq 0\}$:

$$\big\|\Pi_\Lambda \Gamma_{\psi_P}(z)\big\| \leq \left(\|f(\cdot + iP/2)\|_1 e^{\Lambda/2}\right)^{-2\mathrm{Re}z} . \tag{3.121}$$

3. We have

$$\frac{\mathrm{d}}{\mathrm{d}z}\left(\Pi_\Lambda\big|\Gamma_{\psi_P}(\bar{z})\big\rangle, \Pi_\Lambda\big|\Gamma_{\psi_P}(z)\big\rangle\right)\bigg|_{z=0} = 2\frac{\mathrm{d}}{\mathrm{d}z}\big\langle\psi_P\big|\Gamma_{\psi_P}(z)\big\rangle\bigg|_{z=0} \tag{3.122a}$$

$$= -2\left(S_{\mathcal{A}}(\psi_P|\eta) - S_{\mathcal{B}}(\psi_P|\eta)\right). \tag{3.122b}$$

Proof. In order for the proof to run in parallel with that of Theorem (3.2.2), we consider instead of $|\psi_P\rangle$ the corresponding vector $|\xi_{\psi_P}\rangle$ in the natural cone of $\mathcal{A}$. By Remark (4) (1), and transformation formulas such as $\Delta^z_{\psi_P} = {v'_{\psi_P}}^* \Delta^z_{\xi_{\psi_P}} v'_{\psi_P}$ (which give corresponding transformation formulas for Π_Λ), we find that $\Pi_{\Lambda,\psi_P}\big|\Gamma_{\psi_P}(z)\big\rangle = v'_{\psi_P}\Pi_{\Lambda,\xi_{\psi_P}}\big|\Gamma_{\xi_{\psi_P}}(z)\big\rangle$. The partial isometry v'_{ψ_P} is evidently of no consequence for the claims made in this lemma. By abuse of notation, we can assume without loss of generality for the rest of this proof that $|\psi_P\rangle$ is in the natural cone.

(1) Then, as in the proof of Theorem (3.2.2), we also use the shorthand $\Delta_{\eta_\mathcal{B},\psi_{P\,\mathcal{B}}} = \Delta_{\eta,\psi_P;\mathcal{B}}$

etc. With these notations understood, let us write out

$$\Pi_\Lambda \big|\Gamma_{\psi_P}(z)\big\rangle = \left(\Pi_\Lambda \Delta^{z}_{\psi_P\,\mathcal{A}}\right)\left(\Delta^{-z}_{\psi_P\,\mathcal{A}}\Delta^{z}_{\eta,\psi_P;\mathcal{A}}\right) V_{\psi_P}\Delta^{-z}_{\eta,\psi_P;\mathcal{B}}\big|\psi_{P\,\mathcal{B}}\big\rangle, \tag{3.123}$$

which is initially defined only for purely imaginary z. We now consider the bracketed operator above: $\Delta^{-z}_{\psi_P}\Delta^{z}_{\eta,\psi_P}$. It is well known that the majorization condition (3.104) ensures that this operator has an analytic continuation to the strip $-1/2 < \mathrm{Re}z < 0$. For completeness we give this argument here using a similar approach as in the proof of Theorem (3.2.2).

Thus, we define, dropping temporarily the subscript $\mathcal{A}$ as all quantities refer to this algebra:

$$G(z) = \left(c^*\big|\psi_P\big\rangle + |\zeta\rangle\,, \Delta^{-z}_{\psi_P}\Delta^{z}_{\eta,\psi_P} d'\big|\eta\big\rangle\right) = \left(\Delta^{-\bar{z}}_{\psi_P} c^*\big|\psi_P\big\rangle, \Delta^{z}_{\eta,\psi_P} d'\,|\eta\rangle\right), \tag{3.124}$$

where: $c \in \mathcal{A},\ d' \in \mathcal{A}'$ and $|\zeta\rangle \in (1 - \pi'(\psi_P))\mathscr{H}$. This function is holomorphic in the lower strip $\{-1/2 < \mathrm{Re}z < 0\}$ and is continuous in the closure due to Tomita-Takesaki theory. As in the proof of Theorem (3.2.2) we can easily derive an upper bound on $|G(z)|$ that is not uniform with c, d'. We can then improve this to a uniform bound using the Phragmén-Lindelöf theorem by checking the top and bottom edges of the strip. At the top we have:

$$|G(it)| \le \left\|c^*\big|\psi_P\big\rangle\right\| \left\|d'\,|\eta\rangle\right\|, \tag{3.125}$$

and at the bottom we need the following calculation:

$$
\begin{aligned}
G(-1/2+it) &= \left(\Delta_{\psi_P}^{it}\Delta_{\psi_P}^{1/2}c^*\big|\psi_P\big\rangle, \Delta_{\eta,\psi_P}^{it}\Delta_{\eta,\psi_P}^{-1/2}d'\,|\eta\rangle\right) \\
&= \left(\Delta_{\psi_P}^{it}\Delta_{\psi_P}^{1/2}c^*\big|\psi_P\big\rangle, \Delta_{\eta,\psi_P}^{it}Jd'^*J\Delta_{\psi_P}^{-it}\big|\psi_P\big\rangle\right) \\
&= \left(\Delta_{\psi_P}^{it}\Delta_{\psi_P}^{1/2}c^*\big|\psi_P\big\rangle, \Delta_{\eta}^{it}Jd'^*J\Delta_{\psi_P,\eta}^{-it}\big|\psi_P\big\rangle\right) \\
&= \left(\Delta_{\psi_P}^{it}c^*\big|\psi_P\big\rangle, J\left(\Delta_{\eta}^{it}Jd'^*J\Delta_{\psi_P,\eta}^{-it}\right)^*J\big|\psi_P\big\rangle\right) \\
&= \left(\Delta_{\psi_P}^{it}c^*\big|\psi_P\big\rangle, \Delta_{\eta,\psi_P}^{it}d'\Delta_{\eta}^{it}\big|\psi_P\big\rangle\right).
\end{aligned} \tag{3.126}
$$

Consequently,

$$
\begin{aligned}
|G(-1/2+it)| &\leq \left\|\pi(\psi_P)c^*\big|\psi_P\big\rangle\right\|\left\|\pi'(\psi_P)d'\Delta_\eta^{it}\big|\psi_P\big\rangle\right\| \leq \left\|c^*\big|\psi_P\big\rangle\right\|\left\|\varsigma'^{t}_{\eta}(d')\big|\psi_P\big\rangle\right\| \\
&\leq \|f(\cdot+iP)\|_1\left\|c^*\big|\psi_P\big\rangle\right\|\left\|\varsigma'^{t}_{\eta}(d')\big|\eta\big\rangle\right\| = \|f(\cdot+iP)\|_1\left\|c^*\big|\psi_P\big\rangle\right\|\left\|d'\big|\eta\big\rangle\right\|
\end{aligned} \tag{3.127}
$$

where in the first line we dropped the support projectors and defined modular flow on $\mathcal{A}'$, $\varsigma'^{t}_{\eta}(d') = \Delta_\eta^{-it}d'\Delta_\eta^{it}$. In the second line we finally used the majorization condition (3.104) that is true for these filtered states. These bounds at the edges of the strip, and the weaker bound derived earlier, can be extended into the full strip such that $G(z)\|f(\cdot+iP)\|_1^{2z}$ is holomorphic and bounded by 1 everywhere for $-1/2 \leq \mathrm{Re}(z) \leq 0$. Since $c^*\big|\psi_P\big\rangle + |\zeta\rangle$ and $d'\big|\eta\big\rangle$ for all $c \in \mathcal{A}$ and $d' \in \mathcal{A}'$ are dense, we can extend the definition of the operator $\Delta_{\psi_P}^{-z}\Delta_{\eta,\psi_P}^{z}$ to the entire Hilbert space where it remains bounded,

$$
\|\Delta_{\psi_P}^{-z}\Delta_{\eta,\psi_P}^{z}\| \leq \|f(\cdot+iP)\|_1^{-2\mathrm{Re}z}. \tag{3.128}
$$

Since the limit on $G(z)$ as $c^*\big|\psi_P\big\rangle$ and $d'\big|\eta\big\rangle$ approaches two general vectors in the Hilbert space and is uniform in z, we get the same continuity statement for $\Delta_{\psi_P}^{-z}\Delta_{\eta,\psi_P}^{z}$ in the weak operator topology. We also get holomorphy for this operator in the interior of the strip. Note that since $\Delta_{\psi_P}^{-z}\Delta_{\eta,\psi_P}^{z} = (D\psi_P : D\eta)_{-iz}\pi'(\psi_P)$ for the Connes-cocycle $(D\psi_P : D\eta)_{-iz} \in \mathcal{A}$ holds along $z = it$ for real t, it continues to take this form in the lower strip.

Now let us turn to the first bracketed operator in (3.123), $\Pi_\Lambda \Delta_{\psi_P}^{z}$, which is a holomorphic operator (and thus continuous in the strong operator topology) in the entire strip due to the projection on a bounded support of the spectrum of $\ln \Delta_{\psi_P}$. In fact, the operator norm satisfies $\|\Pi_\Lambda \Delta_{\psi_P}^{z}\| \leq e^{-\Lambda \mathrm{Re} z}$ for $\mathrm{Re} z \leq 0$. Finally we analyze the following vector appearing in (3.123), $\Delta_{\eta,\psi_P;\mathcal{B}}^{-z}\big|\psi_{P\,\mathcal{B}}\big\rangle$ which is holomorphic in $\{-1/2 < \mathrm{Re} z < 0\}$ and strongly continuous in the closure of this region due to Tomita-Takesaki theory. This vector is also norm bounded by 1.

At this stage, we can combine the above holomorphy statements in (3.123) showing that this vector is analytic in the lower strip $\{-1/2 < \mathrm{Re} z < 0\}$. For the continuity statement in z, note that an operator that is uniformly bounded and continuous in the weak operator topology such as $\Delta_{\psi_P,\eta}^{-z}\Delta_{\eta}^{z}$, acting on a strongly continuous vector $\Delta_{\eta,\psi_P;\mathcal{B}}^{-z}\big|\psi_{P\,\mathcal{B}}\big\rangle$ gives a weakly continuous vector. Similarly, an operator that is continuous in the strong operator topology $\Pi_\Lambda \Delta_{\psi_P}^{z}$ acting on a weakly continuous vector – the output of the last statement – gives a weakly continuous vector.

Now we use the vector-valued edge of the wedge theorem (see e.g. [86], Appendix A), in conjunction with Theorem (3.2.2), which already establishes an analytic extension to the upper strip $0 < \mathrm{Re} z < 1/2$. We thereby extend $\Pi_\Lambda\big|\Gamma_{\psi_P}(z)\big\rangle$ holomorphically to the full strip $-1/2 < \mathrm{Re} z < 1/2$.

(2) The bound (3.121) follows by combining the operator norm bounds above.

(3) Holomorphy at $z = 0$ allows us to take the derivative in (3.122a) on the bra and ket separately and it is easy to see that they give the same contribution. The equality in (3.122a) also

relies on $\Pi_\Lambda \big|\psi_P\big\rangle = \big|\psi_P\big\rangle$. The second line (3.122b) follows by working with the right hand side of in (3.122a) and taking the derivative as a limit along $z = it$ for $t \to 0$. This gives:

$$
\begin{aligned}
&\lim_{t\to 0} \left(\big\langle \psi_{P\,\mathcal{A}} \big| \Delta^{it}_{\eta,\psi_P;\mathcal{A}} V_{\psi_P} \Delta^{-it}_{\eta,\psi_P;\mathcal{B}} \big| \psi_{P\,\mathcal{B}} \big\rangle - 1 \right) / (it) \\
=&\lim_{t\to 0} \left(\big\langle \psi_{P\,\mathcal{A}} \big| \Delta^{it}_{\eta,\psi_P;\mathcal{A}} \big| \psi_{P\,\mathcal{A}} \big\rangle - 1 \right) / (it) + \lim_{t\to 0} \left(\big\langle \psi_{P\,\mathcal{B}} \big| \Delta^{-it}_{\eta,\psi_P;\mathcal{B}} \big| \psi_{P\,\mathcal{B}} \big\rangle - 1 \right) / (it) \\
=& - S_{\mathcal{A}}(\psi_P|\eta) + S_{\mathcal{B}}(\psi_P|\eta),
\end{aligned}
\tag{3.129}
$$

where the later limits can be shown to exist when the ψ_P relative entropies are finite, as is indeed the case by Theorem (3.2.3) (1), see [73], Theorem 5.7. The first equality in (3.129) can be shown more explicitly by subtracting the two sides and observing that this is an inner product on two vectors. After applying the Cauchy-Schwarz inequality, one again uses the finiteness of ψ_P relative entropy, by Theorem (3.2.3) (1), to show that this difference vanishes in the limit:

$$
\begin{aligned}
&\lim_{t\to 0} \frac{\left| \left(\Delta^{-it}_{\eta,\psi_P;\mathcal{A}} \big| \psi_{P\,\mathcal{A}} \big\rangle - \big| \psi_{P\,\mathcal{A}} \big\rangle ,\ V_{\psi_P} \Delta^{-it}_{\eta,\psi_P;\mathcal{B}} \big| \psi_{P\,\mathcal{B}} \big\rangle - \big| \psi_{P\,\mathcal{A}} \big\rangle \right) \right|^2}{t^2} \\
\leq& \lim_{t\to 0} \frac{2\mathrm{Re}\left(1 - \big\langle \psi_{P\,\mathcal{A}} \big| \Delta^{it}_{\eta,\psi_P;\mathcal{A}} \big| \psi_{P\,\mathcal{A}} \big\rangle \right)}{t} \frac{2\mathrm{Re}\left(1 - \big\langle (\psi_{P\mathcal{B}} \big| \Delta^{-it}_{\eta,\psi_P;\mathcal{B}} \big| \psi_{P\,\mathcal{B}} \big\rangle \right)}{t} = 0.
\end{aligned}
\tag{3.130}
$$

□

3.2.5.4 L_p norms of updated interpolating vector

We now study L_p norms of the updated interpolating vector (3.120) and its limits as $P, \Lambda \to \infty$, $z \to 0$ and $p \to 1$ or $p \to 2$. First we consider $p = 1$.

Lemma 3.2.5. 1. The $L_1(\mathcal{A}', \psi_P)$-norm of (3.120) for $z = 1/2 + it$ satisfsfies:

$$\lim_{\Lambda\to\infty} \|\Pi_\Lambda \Gamma_{\psi_P}(1/2+it)\|^{\mathcal{A}'}_{1,\psi_P} = \|\Gamma_{\psi_P}(1/2+it)\|^{\mathcal{A}'}_{1,\psi_P} \leq F(\omega_{\psi_P}, \omega_{\psi_P}\circ\iota\circ\alpha^t_\eta) \quad (3.131)$$

where α^t_η is the rotated Petz map defined in (3.25).

2. We have

$$\lim_{P\to\infty} F(\omega_{\psi_P}, \omega_{\psi_P}\circ\iota\circ\alpha^t_\eta) = F(\omega_\psi, \omega_\psi\circ\iota\circ\alpha^t_\eta) \quad (3.132)$$

Proof. (1) For the first equality, we need an appropriate continuity property of the L_1-norm which is provided in Lemma (B.2.1), Appendix (B.2.2). It shows that strong convergence of the vectors implies the convergence of the L_1 norm. For the limit $\Lambda \to \infty$, this follows from the strong convergence of Π_Λ to $\pi'(\psi_P)\pi(\psi_P)$. In fact, we can drop these support projectors because by definition $\pi'(\psi_P)\big|\Gamma_{\psi_P}(z)\big\rangle = \big|\Gamma_{\psi_P}(z)\big\rangle$ and also because the L_p norms satisfy (3.60).

Next, Lemma (3.2.1) (1) gives $\|\Gamma_{\psi_P}(1/2+it)\|^{\mathcal{A}'}_{1,\psi_P} = F(\omega_{\psi_P}, \omega_{\Gamma_t})$, where we use the shorthand $|\Gamma_t\rangle \equiv |\Gamma_{\psi_P}(1/2+it)\rangle$. Now we use the majorization condition on ω_{Γ_t} (3.88), in conjunction with the concavity of the fidelity [75]:

$$\begin{aligned} F(\omega_{\psi_P}, \omega_{\psi_P}\circ\iota\circ\alpha^t_\eta) &= F(\omega_{\psi_P}, \omega_{\Gamma_t} + (\omega_{\psi_P}\circ\iota\circ\alpha^t_\eta - \omega_{\Gamma_t})) \\ &\geq F(\omega_{\psi_P}, \omega_{\Gamma_t}) + F(\omega_{\psi_P}, (\omega_{\psi_P}\circ\iota\circ\alpha^t_\eta - \omega_{\Gamma_t})) \\ &\geq F(\omega_{\psi_P}, \omega_{\Gamma_t}) \end{aligned} \quad (3.133)$$

This completes the proof of (1).

(2) We use the fact that, where the fidelity $F(\omega_{\psi_P}, \omega_{\psi_P}\circ\iota\circ\alpha^t_\eta)$ is concerned, we can pick

another vector that gives the same linear functional. We can replace:

$$F(\omega_{\psi_P}, \omega_{\psi_P} \circ \iota \circ \alpha_\eta^t) = \left\| \Delta_{\eta;\mathcal{A}}^{it} J_{\mathcal{A}} V_\eta J_{\mathcal{B}} \Delta_{\eta;\mathcal{B}}^{-it} \psi_{P\mathcal{B}} \right\|_{1,\psi_P}^{\mathcal{A}'}. \tag{3.134}$$

Then, in view of Lemma (B.2.1), Appendix (B.2.2), we only need establish the strong convergence of $\left|\psi_{P\,\mathcal{B}}\right\rangle$ and of $\left|\psi_{P\,\mathcal{A}}\right\rangle$ as $P \to \infty$, and this follows by combining Lemma (3.2.3) (1) and Eq. (3.4) [remembering the notations (3.50)]. □

Next, we consider simultaneously approaching $p = 2$ and $z = 0$.

Lemma 3.2.6. We have

$$\begin{aligned}
\lim_{\theta\to 0} \frac{1}{\theta} \ln \|\Pi_\Lambda \Gamma_{\psi_P}(\theta)\|_{p_\theta,\psi_P}^{\mathcal{A}'} &= \lim_{\theta\to 0} \frac{1}{2\theta} \ln \left(\Pi_\Lambda \left|\Gamma_{\psi_P}(\theta)\right\rangle, \Pi_\Lambda \left|\Gamma_{\psi_P}(\theta)\right\rangle\right) \\
&= -\left(S_{\mathcal{A}}(\psi_P|\eta) - S_{\mathcal{B}}(\psi_P|\eta)\right)
\end{aligned} \tag{3.135}$$

with $p_\theta = 2/(1+2\theta)$.

Proof. Define the normalized vector

$$|\zeta_\theta\rangle \equiv \frac{\Pi_\Lambda \big|\Gamma_{\psi_P}(\theta)\big\rangle}{\|\Pi_\Lambda \Gamma_{\psi_P}(\theta)\|}. \tag{3.136}$$

We can then use Lemma (3.2.4), (3.122a) to show that:

$$\lim_{\theta\to 0^+} \frac{\|\zeta_\theta - \psi_P\|^2}{\theta} = 0. \tag{3.137}$$

So we can apply the "first law" (3.67) for the L_p norms in Lemma (3.2.1) to $|\zeta_\theta\rangle$, to conclude

$$\lim_{\theta\to 0^+}\frac{1}{\theta}\ln\|\zeta_\theta\|^{\mathcal{A}'}_{p_\theta,\psi_P}=0, \tag{3.138}$$

since $p_\theta = 2/(1+2\theta)$ satisfies the assumptions of Lemma (3.2.1). The L_p norms are homogenous so we can pull out the normalization:

$$\lim_{\theta\to 0^+}\frac{1}{\theta}\ln\|\Pi_\Lambda\Gamma_{\psi_P}(\theta)\|^{\mathcal{A}'}_{p_\theta,\psi_P}=\lim_{\theta\to 0^+}\frac{1}{\theta}\ln\|\Pi_\Lambda\Gamma_{\psi_P}(\theta)\|, \tag{3.139}$$

and this gives the desired answer after applying (3.122a) again. □

The last ingredient that we will need is an interpolation theorem for the Araki-Masuda L_p norms on a von Neumann algebra:

Lemma 3.2.7. Let $|G(z)\rangle$ be a $\mathscr{H}$-valued holomorphic function on the strip $\mathbb{S}_{1/2}=\{0<\mathrm{Re}z<1/2\}$ that is uniformly bounded in the closure, $|\psi\rangle\in\mathscr{H}$ a possibly non-faithful state of a sigma-finite von Neumann algebra $\mathcal{M}$ in standard form acting on $\mathscr{H}$. Then, for $0<\theta<1/2$,

$$\frac{1}{p_\theta}=\frac{1-2\theta}{p_0}+\frac{2\theta}{p_1} \tag{3.140}$$

with $p_0, p_1\in[1,2]$, we have

$$\begin{aligned}&\ln\|G(\theta)\|^{\mathcal{M}}_{p_\theta,\psi} \\ &\leq\int_{-\infty}^{\infty}\mathrm{d}t\left((1-2\theta)\alpha_\theta(t)\ln\|G(it)\|^{\mathcal{M}}_{p_0,\psi}+(2\theta)\beta_\theta(t)\ln\|G(1/2+it)\|^{\mathcal{M}}_{p_1,\psi}\right),\end{aligned} \tag{3.141}$$

where

$$\alpha_\theta(t) = \frac{\sin(2\pi\theta)}{(1-2\theta)(\cosh(2\pi t) - \cos(2\pi\theta))}, \qquad \beta_\theta(t) = \frac{\sin(2\pi\theta)}{2\theta(\cosh(2\pi t) + \cos(2\pi\theta))}. \tag{3.142}$$

Proof. See Appendix (B.3). In the commutative setting this is closely related to the Stein interpolation theorem [87]. In the non-commutative setting, a proof appears for type I factors and the usual non-commutative Schatten L_p norms in [2]. We will make sure that it works in the setting of the Araki-Masuda L_p norms defined in (3.59) with reference to a possibly non-faithful state. □

3.2.6 Proof of Theorems 3.1.1 and 3.1.2

We close out this long section by combining the above auxiliary results into proofs of the main theorems.

Proof of Theorem (3.1.1). Given the two normal states ρ, σ we consider as above representers $|\psi\rangle, |\eta\rangle$ in the natural cone. From this we construct the filtered vector $|\psi_P\rangle$ as in (3.97). We then apply Lemma (3.2.7) with $p_1 = 2, p_0 = 1$, $\mathcal{M} = \mathcal{A}'$, $|G(z)\rangle = \Pi_\Lambda \big|\Gamma_{\psi_P}(z)\big\rangle$ and use that the L_2 norm is actually the (projected) Hilbert space norm, see Eq. (3.61), so

$$\|\Pi_\Lambda \Gamma_{\psi_P}(it)\|^{\mathcal{A}'}_{2,\psi_P} = \|\Pi_\Lambda \Gamma_{\psi_P}(it)\| \leq 1. \tag{3.143}$$

Taking the limit $\theta \to 0^+$ with the aid of Lemma (3.2.6) we have:

$$\begin{aligned} S_{\mathcal{A}}(\psi_P|\eta) - S_{\mathcal{B}}(\psi_P|\eta) &\geq -2 \lim_{\Lambda\to\infty} \int_{-\infty}^{\infty} \beta_0(t) \ln \|\Pi_\Lambda \Gamma_{\psi_P}(1/2+it)\|^{\mathcal{A}'}_{1,\psi_P} \,\mathrm{d}t \\ &= -2 \int_{-\infty}^{\infty} \beta_0(t) \ln \|\Gamma_{\psi_P}(1/2+it)\|^{\mathcal{A}'}_{1,\psi_P} \,\mathrm{d}t \\ &\geq -2 \int_{-\infty}^{\infty} \beta_0(t) \ln F\left(\omega_{\psi_P}, \omega_{\psi_P} \circ \iota \circ \alpha^t_\eta\right) \mathrm{d}t, \end{aligned} \tag{3.144}$$

where the limit exits due to Lemma (3.2.5) (1) and where we have used the monotonicity of $\ln$. Taking the limit $P \to \infty$ we get in view of Lemma (3.2.5) (2), Theorem (3.2.3) (3) for a Gaussian filtering function satisfying (A) and (B) of def. (3.2.2) and lower semi-continuity of the $\mathcal{B}$ relative entropy that

$$S_{\mathcal{A}}(\psi|\eta) - S_{\mathcal{B}}(\psi|\eta) \geq -2 \int_{-\infty}^{\infty} \beta_0(t) \ln F\left(\omega_\psi, \omega_\psi \circ \iota \circ \alpha^t_\eta\right) \mathrm{d}t. \tag{3.145}$$

We can then re-write the answer in terms of the original states ρ, σ and we arrive at (3.24). (Recall that we are using $\alpha^t_\eta = \alpha^t_\sigma$ interchangeably.) □

Theorem (3.1.1) forms the basis of the next proof:

Proof of Theorem (3.1.2). Since all states $\rho_i \in \mathscr{S}$ have finite relative entropy with respect to $\sigma \in \mathscr{S}$ we learn that $\pi(\rho_i) \leq \pi(\sigma)$. This implies, via Lemma (3.1.1), (in particular (3.36)) that if $\iota_\pi(\mathcal{B}_\pi) \subset \mathcal{A}_\pi$ is ϵ-approximately sufficient for $\mathscr{S}_\pi$ then $\iota(\mathcal{B}) \subset \mathcal{A}$ is ϵ-approximately sufficient for $\mathscr{S}$. Here

$$\mathscr{S}_\pi = \{\rho \circ \Phi \in (\mathcal{A}_\pi)_\star : \rho \in \mathscr{S}\}, \tag{3.146}$$

and we have used (3.30b). The recovery channel $\alpha_{\mathscr{S}}$ is derived from the recovery channel for

$\iota_\pi(\mathcal{B}_\pi) \subset \mathcal{A}_\pi$. This later recovery channel $\alpha_{\mathscr{S}_\pi}$ then pertains to the "faithful" version of this theorem, and is derived from Theorem (3.1.1), as we will show below. In this way we can proceed by simply assuming that σ is faithful for $\mathcal{A}$, now without loss of generality. In particular we may take (3.41) to be determined by the faithful Petz map in (3.25).

In the faithful case we first check that the map (3.41) is indeed a recovery channel. This follows since α_σ^t are recovery channels for each $t \in \mathbb{R}$ (generalizing the results in [11] to non-zero t) and so the weighted t integral is also clearly unital and completely positive.

We now check the continuity property of (3.41). The integral is rigorously defined as follows. For all $a \in \mathcal{A}$ the function $t \mapsto \alpha_\sigma^t(a)$ is continuous in t in the ultra-weak topology (thus Lebesgue measurable) and bounded on $\mathbb{R}$. So

$$\mathcal{B}_\star \ni \rho \mapsto \int_{\mathbb{R}} p(t)\rho(\alpha_\sigma^t(a))\mathrm{d}t \in \mathbb{C} \tag{3.147}$$

gives a continuous linear functional and thus defines an element in $\mathcal{B}$ (the continuous dual of the predual) that we call $\alpha_{\mathscr{S}}(a)$. Continuity in the linear functional norm follows from the convergence of the following integral:

$$\int_{\mathbb{R}} p(t)\|\alpha_\sigma^t(a)\| \,\mathrm{d}t \leq \|a\|. \tag{3.148}$$

This also guarantees that the resulting operator $\alpha_{\mathscr{S}}(a) = \int_{\mathbb{R}} p(t)\alpha_\sigma^t(a)\mathrm{d}t$ is a bounded operator:

$$\|\alpha_{\mathscr{S}}(a)\| = \sup_{\rho \in \mathcal{A}_\star} \frac{|\int_{\mathbb{R}} p(t)\rho(\alpha_\sigma^t(a))\mathrm{d}t|}{\|\rho\|} \leq \int_{\mathbb{R}} p(t)\|\alpha_\sigma^t(a)\|\mathrm{d}t \leq \|a\|. \tag{3.149}$$

We need to check the ultraweak continuity of $a \mapsto \alpha_{\mathscr{S}}(a)$. For all $\rho \in \mathcal{B}_\star$ we define the integral

$$\int_{\mathbb{R}} p(t)\rho \circ \alpha_\sigma^t \, \mathrm{d}t \tag{3.150}$$

in much the same way as above, as a Lebesgue integral on continuous functions valued in $\mathcal{A}_\star$. That is, the evaluation of this expression on $a \in \mathcal{A}$ defines an ultraweakly continuous functional on $\mathcal{A}$. This follows since the sequence

$$\int_{\mathbb{R}} p(t)\rho \circ \alpha_\sigma^t(a_n)\mathrm{d}t \tag{3.151}$$

converges to the integral of the pointwise limit by the dominated convergence theorem, as $p(t)|\rho \circ \alpha_\sigma^t(a)| \leq p(t)\|\rho\|\|a\|$ is integrable. Putting all the pieces together we find that

$$a \mapsto \alpha_{\mathscr{S}}(a) = \int_{-\infty}^{\infty} p(t)\alpha_\eta^t(a) \, \mathrm{d}t \tag{3.152}$$

is ultraweakly continuous, since for all $\rho \in \mathcal{B}_\star$,

$$\rho\left(\int_{\mathbb{R}} p(t)\alpha_\sigma^t(a_n - a)\right) \mathrm{d}t \equiv \int_{\mathbb{R}} p(t)\rho(\alpha_\sigma^t(a_n - a))\mathrm{d}t = \int_{\mathbb{R}} p(t)\rho \circ \alpha_\sigma^t(a_n - a)\mathrm{d}t \tag{3.153}$$

converges to zero whenever $a_n \to a$ ultraweakly.

The proof is then completed by rewriting Theorem (3.1.1) using the concavity of fidelity. For this, we require a version of Jensen's inequality for the convex functional $\sigma \mapsto F(\rho, \sigma)$ on normal states on $\mathcal{A}$ with respect to the measure $p(t)\mathrm{d}t$. This would give us

$$\int_{\mathbb{R}} F(\rho, \rho \circ \iota \circ \alpha_\sigma^t) p(t) \mathrm{d}t \leq F\left(\rho, \int_{\mathbb{R}} \rho \circ \iota \circ \alpha_\sigma^t \, p(t) \mathrm{d}t\right) \tag{3.154}$$

where ρ is a state in $\mathcal{A}_\star$. Then Theorem (3.1.1) becomes:

$$-2 \ln F(\rho, \rho \circ \iota \circ \alpha_{\mathscr{S}}) \leq S_{\mathcal{A}}(\rho|\sigma) - S_{\mathcal{B}}(\rho|\sigma), \tag{3.155}$$

which implies that $\mathcal{B}$ is ϵ-approximately sufficient as claimed by the theorem.

We are not aware of a proof for Jensen's inequality for convex functionals of a Banach space valued random variable that would apply straight away to the case considered here. In particular, it is not evident that the integrals in question can be approximated by Riemann sums in the general case, as was done in [2]. So we now demonstrate (3.154) by a more explicit argument using the detailed structure of the fidelity.

Consider the Hilbert space $\mathscr{Y} = L_2(\mathbb{R}; \mathscr{H}; p(t)\mathrm{d}t) \cong \mathscr{H} \bar{\otimes} L_2(\mathbb{R}; p(t)\mathrm{d}t)$ of strongly measurable square integrable functions valued in $\mathscr{H}$. Vectors $|\Upsilon\rangle$ in this space are (equivalence classes of) functions $t \mapsto |\Upsilon_t\rangle$. $\mathscr{Y}$ is evidently a module for $\mathcal{A}$. We denote this von Neumann algebra by $\mathcal{A} \otimes 1$ since it acts trivially in the second L_2 tensor factor of $\mathscr{Y}$. Now define the fidelity as:

$$F_{\mathcal{A}\otimes 1}(\Psi, \Upsilon) = \sup_{Y' \in (\mathcal{A}\otimes 1)', \, \|Y'\| \leq 1} |\langle \Psi | \, Y' \, | \Upsilon \rangle| \, . \tag{3.156}$$

We next formulate a lemma that will allow us to complete the proof.

Lemma 3.2.8. Let $|\Upsilon\rangle, |\Psi\rangle \in \mathscr{Y}$ induce linear functionals on $\mathcal{A} \otimes 1$ such that

$$\langle\Upsilon|\, a_+ \otimes 1 \,|\Upsilon\rangle \leq \sigma(a_+), \qquad \langle\Psi|\, a_+ \otimes 1 \,|\Psi\rangle \leq \rho(a_+). \tag{3.157}$$

where a_+ is an arbitrary non-negative element in $\mathcal{A}$ and σ, ρ states on $\mathcal{A}$. Then if $|\Upsilon_t\rangle, |\Psi_t\rangle$ are strongly continuous then $F(\Upsilon_t, \Psi_t)$ is continuous, and we have

$$F(\sigma, \rho) \geq \int_{\mathbb{R}} F(\Upsilon_t, \Psi_t) p(t) \mathrm{d}t. \tag{3.158}$$

Proof. If $|\Upsilon_t\rangle, |\Psi_t\rangle$ are strongly continuous then $F(\Upsilon_t, \Psi_t)$ is continuous in t by (B.45), and since the fidelity is the L^1 norm, see Appendix C.

The idea is now to construct a suitable family of elements $y_t' \in \mathcal{A}'$. This family should be chosen at the same time so as to satisfy: (i) $\|y_t'\| \leq 1$, (ii) $t \mapsto y_t'$ is strongly continuous, (iii) in the sup definition of the fidelity, (3.63) we are suitably close to saturating the supremum in the sense that $F(\Upsilon_t, \Psi_t)$ is approximately $|\langle\Upsilon_t|y_t'\Psi_t\rangle|$. Then (ii) implies that $y_t'|\Psi_t\rangle$ is weakly measurable and thus strongly measurable by the Pettis measurability theorem, see e.g. [88], Theorem 3.1.1.[4] By (i) we then see that the map $y_t'|\Psi_t\rangle$ is in the Hilbert space $\mathscr{Y}$ because boundedness y_t' clearly implies that it is square integrable. (ii) holds for instance if the function y_t' is continuous in the norm topology, and we will attempt to choose it in this way. Then y_t', as a function, will define an element Y in $(\mathcal{A} \otimes 1)'$ that can be used in the variational principle (3.156). We must therefore

[4]This theorem applies even without assuming $\mathscr{H}$ to be separable since the image $\{y_t'|\Psi_t\rangle : t \in \mathbb{R}\}$ is a separable open subset of $\mathscr{H}$, in the norm topology, by strong continuity.

have, using concavity of the fidelity in the same manner as in (3.133),

$$F(\sigma, \rho) \geq F_{\mathcal{A} \otimes 1}(\Psi, \Upsilon) \geq \left| \int_{\mathbb{R}} \langle \Upsilon_t | y'_t | \Psi_t \rangle p(t) \mathrm{d}t \right|, \tag{3.159}$$

using the variational principle (3.156) to obtain the last inequality, and using that the fidelity only depends on functionals in the first. The evident strategy is now to make our choice (iii) of of the function y'_t in such a way that the right side is close to the right side of (3.158), while being continuous in the operator norm topology and while satisfying $\|y'_t\| < 1$, so that (i) and (ii) hold as discussed.

To this end, consider the open unit ball in $\mathcal{A}'$ in the norm topology, $\mathcal{A}'_1 \equiv \{x' \in \mathcal{A}' : \|x'\| < 1\}$. For all t we define next a subset $\mathcal{X}'_t \subset \mathcal{A}'_1$ by

$$\mathcal{X}'_t \equiv \mathcal{A}'_1 \cap \{x' \in \mathcal{A}' : |\langle \Psi_t | \, x' \, | \Upsilon_t \rangle - F(\Psi_t, \Upsilon_t)| < \epsilon\}. \tag{3.160}$$

This set is open in the norm topology because the second set on the right hand side of (3.160) is open in the weak operator topology and so it is open in the norm topology, too. It is non empty since we know that in the sup definition of fidelity it is sufficient to take $\|x'\| < 1$ and still achieve $F(\Psi_t, \Upsilon_t)$.

We will be interested in the norm closures $\overline{\mathcal{X}'_t}$. What we then need to do is select a function from this set $y'_t \in \overline{\mathcal{X}'_t}$ that varies continuously in the operator norm. This problem can be solved by the Michael selection theorem [89]. Indeed, we can consider the mapping $t \in \mathbb{R} \to \overline{\mathcal{X}'_t} \in 2^{\mathcal{A}'}$ as a map from the paracompact space $\mathbb{R}$ to subsets of $\mathcal{A}'$ thought of as a the Banach space (with the operator norm). If it can be shown that the sets $\overline{\mathcal{X}'_t}$ are nonempty closed and convex and that this map is "lower hemicontinuous", then by the Micheal selection theorem, there is a continuous selection $y'_t \in \mathcal{X}'_t$ as we require.

We have seen that the sets are closed and nonempty. Convexity follows from

$$|\langle\Psi|\, p_1 x'_1 + p_2 x'_2 \,|\Upsilon\rangle - F(p_1+p_2)| \le p_1 \,|\langle\Psi|\, x'_1 \,|\Upsilon\rangle - F| + p_2 \,|\langle\Psi|\, x'_2 \,|\Upsilon\rangle - F|$$
$$\|p_1 x'_1 + p_2 x'_2\| \le p_1 \|x'_1\| + p_2 \|x'_2\| \tag{3.161}$$

where the first equation is schematic but is hopefully clear, and where $p_1, p_2 \ge 0, p_1 + p_2 = 1$. This implies that $\mathcal{X}'_t$ is convex and hence its closure is also convex.

Lower hemicontinuity at some point t is the property that for any open set $\mathcal{V} \subset \mathcal{A}'$ that intersects $\overline{\mathcal{X}'_t}$ there exists a δ such that $\overline{\mathcal{X}'_{t'}} \cap \mathcal{V} \neq \emptyset$ for all $|t - t'| < \delta$. We see this for the case at hand as follows. Take $\mathcal{V}$ satisfying the assumption, and note that $\mathcal{V} \cap \mathcal{X}'_t$ is also non empty. Pick a $y' \in \mathcal{V} \cap \mathcal{X}'_t$. There exists an $\epsilon' < \epsilon$ such that:

$$|\langle\Psi_t|\, y' \,|\Upsilon_t\rangle - F(\Psi_t, \Upsilon_t)| < \epsilon' < \epsilon. \tag{3.162}$$

Then, by the strong continuity of $|\Upsilon_t\rangle$ resp. $|\Psi_t\rangle$ and continuity of $F(\Psi_t, \Upsilon_t)$, we see that this condition is stable: Given $\epsilon - \epsilon' > 0$ there does indeed exist a δ such that

$$|\langle\Psi_{t'}|\, y' \,|\Upsilon_{t'}\rangle - F(\Psi_{t'}, \Upsilon_{t'})| < \epsilon\,, \qquad \forall |t - t'| < \delta \tag{3.163}$$

which implies that $y' \in \mathcal{V} \cap \mathcal{X}'_{t'} \subset \mathcal{V} \cap \overline{\mathcal{X}'_{t'}}$ as required.

From Michael's theorem we therefore get the desired norm continuous y'_t satisfying

$$|\langle \Psi_t | y'_t | \Upsilon_t \rangle - F(\Psi_t, \Upsilon_t)| \leq \epsilon \tag{3.164}$$

for all t. Using that the fidelity is real and (3.159) and that ϵ can be made arbitrarily small then readily implies the lemma. $\square$

We now use this lemma with $|\Upsilon_t\rangle := |\Gamma_\psi(i/2+t)\rangle$, which is weakly continuous by Theorem (3.2.2) (1). Actually, it is even strongly continuous since it is given by the product of bounded operators and $\Delta^{it}_{\eta;\mathcal{A}}, \Delta^{it}_{\eta;\mathcal{B}}$, which are strongly continuous as they are 1-parameter groups of unitaries generated by a self-adjoint operator by Stone's theorem, see e.g. [90], sec. 5.3. We also take $|\Psi_t\rangle = |\psi\rangle$, which is obviously strongly continuous as it is just constant. Then $|\Upsilon\rangle$ induces a state dominated by $\rho \circ \iota \circ \alpha_{\mathscr{S}}$, by Theorem (3.2.2) (2), and $|\Psi\rangle$ induces ρ by definition, and $|\Upsilon_t\rangle$ induces $\rho \circ \iota \circ \alpha^t_\sigma$. We thereby arrive at the concavity result (3.154), and this concludes the proof of Theorem (3.1.2). $\square$

3.3 An alternative strategy for proving Theorem 3.1.1

It is conceivable that our approach based on the vector (3.86) can be modified by choosing other interpolating vectors, and this may lead to new insights relating the argument to somewhat different entropic quantities. Here we sketch an approach which seems to avoid the use of L_p-norms, thus leading potentially to a substantial simplification. To this end, we consider now a vector

$$|\Xi_\psi(z,\phi)\rangle = \Delta^{z}_{\psi,\xi;\mathcal{B}} \Delta^{-z}_{\eta,\xi;\mathcal{B}} \Delta^{z}_{\eta,\phi;\mathcal{A}} |\psi\rangle, \tag{3.165}$$

similar to vectors considered in [91]. Here, $|\xi\rangle$ is some vector such that $\pi^{\mathcal{B}'}(\xi) \supset \pi^{\mathcal{B}'}(\psi)$, and where in this section we find it more convenient to think of $\mathcal{B}$ as defined on the same Hilbert space as $\mathcal{A}$. The vector (3.165) does not depend on the precise choice of $|\xi\rangle$ (but on the vector $|\eta\rangle$ in the natural cone of $\mathcal{A}$, although we suppress this).

(3.165) is defined a priori only for imaginary z. But if we consider the set of states majorizing $|\psi\rangle$, defined as $\mathscr{C}(\psi, \mathcal{A}') = \{|\phi\rangle \in \mathscr{H} : \|a'\psi\| \leq c_\phi \|a'\phi\| \quad \forall a' \in \mathcal{A}'\}$, then for $|\phi\rangle$ in this dense linear subspace of $\mathscr{H}$, it has an analytic continuation to the half strip $\mathbb{S}_{1/2} = \{0 < \mathrm{Re} z < 1/2\}$ that is weakly continuous on the boundary. This can be demonstrated by the same type of argument as in [91], prop. 2.5, making repeated use of the following lemma by [91], Lemma 2.1:

Lemma 3.3.1. Suppose $|G(z)\rangle$ is a vector valued analytic function for $z \in \mathbb{S}_{1/2}$, and A is a self-adjoint positive operator. Then $A^z|G(z)\rangle$ is an analytic function of $z \in \mathbb{S}_{1/2}$ if $\|A^z G(z)\|$ is bounded on the boundary of $\mathbb{S}_{1/2}$.

For example, we may write $\Delta^z_{\eta,\phi;\mathcal{A}}|\psi\rangle = \Delta^z_{\eta,\phi;\mathcal{A}}\Delta^{-z}_{\psi,\phi;\mathcal{A}}\Delta^z_{\psi,\phi;\mathcal{A}}\Delta^{-z}_{\psi;\mathcal{A}}|\psi\rangle$, at first for imaginary $z = it$. Using the relations (3.10), (3.11), $u'(z) = \Delta^z_{\psi,\phi;\mathcal{A}}\Delta^{-z}_{\psi;\mathcal{A}} = (D\psi : D\psi)^*_{-i\bar{z};\mathcal{A}'}$ is a Connes-cocycle for $\mathcal{A}'$. The condition $|\phi\rangle \in \mathscr{C}(\psi, \mathcal{A}')$ ensures that it has an analytic continuation from $z = it$ to $\mathbb{S}_{1/2}$, as an element of $\mathcal{A}'$ that is strongly continuous on the boundary of $\mathbb{S}_{1/2}$ – this is standard and a proof proceeds as that of Lemma 3.2.4, (1). Similarly, $v(z) = \Delta^z_{\eta,\phi;\mathcal{A}}\Delta^{-z}_{\psi,\phi;\mathcal{A}} = (D\eta : D\psi)_{-iz,\mathcal{A}}$ is a Connes-cocycle for $\mathcal{A}$.

Then, for imaginary $z = it$ we get $\Delta^z_{\eta,\phi;\mathcal{A}}|\psi\rangle = u'(z)v(z)|\psi\rangle$, which has an analytic continuation to $\mathbb{S}_{1/2}$ as $v(z)|\psi\rangle$ is analytic there by Tomita-Takesaki theory. One next applies the lemma with $|G(z)\rangle = \Delta^z_{\eta,\phi;\mathcal{A}}|\psi\rangle$ and $A^z = \Delta^{-z}_{\eta,\psi;\mathcal{B}}$ (chosing $|\xi\rangle = |\psi\rangle$ here). The conditions are verified using standard relations of relative Tomita-Takesaki theory as given e.g. in [70], Appendix C, such as (3.10), (3.11): At the upper boundary, $z = 1/2 + it$, one finds $|G(1/2 + it)\rangle = u'(1/2 + it)J_{\mathcal{A}}v(it)^* J_{\mathcal{A}}|\eta\rangle$ which is of the form $b'|\eta\rangle$ for $b' \in \mathcal{A}' \subset \mathcal{B}'$, and one finds $A^{1/2+it} = \Delta^{it}_{\psi,\eta;\mathcal{B}'} J_{\mathcal{B}'} S_{\psi,\eta;\mathcal{B}'}$. Together, this gives,

$$A^{1/2+it}|G(1/2 + it)\rangle = \Delta^{it}_{\psi,\eta;\mathcal{B}'} J_{\mathcal{B}'}[u'(1/2 + it)J_{\mathcal{A}}v(it)^* J_{\mathcal{A}}]^*|\psi\rangle, \tag{3.166}$$

which is bounded for real t. On the other hand, at the lower boundary $A^{it}|G(it)\rangle$ is bounded by definition. Continuing this type of argument gives the following lemma.

Lemma 3.3.2. For $|\phi\rangle \in \mathscr{C}(\mathcal{A}', \psi)$, $|\Xi_\psi(z, \phi)\rangle$ is analytic in the interior of the strip $\mathbb{S}_{1/2}$ and weakly continuous on the boundary.

The relationship with other approaches can be seen through the quantity

$$g(z) = \inf_{|\phi\rangle \in \mathscr{C}(\mathcal{A}',\psi), \|\phi\|=1} \|\Xi_\psi(z, \phi)\|. \tag{3.167}$$

In the setup of finite-dimensional v. Neumann subfactors described in sec. 3.4.1, we can write

$$|\Xi_\psi(z, \phi)\rangle = (\rho^z_{\mathcal{B}}\sigma^{-z}_{\mathcal{B}} \otimes 1_{\mathcal{C}})\sigma^z_{\mathcal{A}}\rho^{1/2}_{\mathcal{A}}\tau^{-z}_{\mathcal{A}} \tag{3.168}$$

If we take $z = \theta$ real then the infimum over $\tau_{\mathcal{A}}$ (the density matrix representing $|\phi\rangle$) readily yields an L_p-norm for $p_\theta = 2/(2\theta + 1)$,

$$g(z) = \left(\mathrm{tr}\left|(\rho^z_{\mathcal{B}}\sigma^{-z}_{\mathcal{B}} \otimes 1_{\mathcal{C}})\sigma^z_{\mathcal{A}}\rho^{1/2}_{\mathcal{A}}\right|^{p_\theta}\right)^{1/p_\theta}. \tag{3.169}$$

We recognize this again as (3.183) corresponding to an expression also studied by [2].

The strategy is now the following. First, Lemma B.3.1 also applies to the holomorphic Hilbert-space valued function $|\Xi_\psi(z,\phi)\rangle$ (because $z \mapsto \ln \|\Xi_\psi(z,\phi)\|$ is subharmonic). So we have for $0 < \theta < 1/2$ that

$$\ln \|\Xi_\psi(\theta,\phi)\| \leq \int_{-\infty}^{\infty} \left(\alpha_\theta(t) \ln \|\Xi_\psi(it,\phi)\|^{1-2\theta} + \beta_\theta(t) \ln \|\Xi_\psi(1/2+it,\phi)\|^{2\theta}\right) \mathrm{d}t. \tag{3.170}$$

Since $\forall t \in \mathbb{R},\ \|\Xi_\psi(it,\phi)\| \leq 1,\ \alpha_\theta(t) > 0$, we can drop the first term under the integral. Then, we want to divide by θ and take the infimum over $|\phi\rangle \in \mathscr{C}(\mathcal{A}',\psi), \|\phi\| = 1$. The next lemma will allow us to deal with the second term under the integral. Since $|\phi\rangle \in \mathscr{C}(\mathcal{A}',\psi)$, we can write $|\psi\rangle = a|\phi\rangle$, where $a \in \mathcal{A}$ is self-adjoint, see [66], 5.21. Then:

Lemma 3.3.3. We have

$$\|\Xi_\psi(1/2+it,\phi)\|^2 = \omega_\psi \circ \iota \circ \alpha_\eta^t(a^2) \tag{3.171}$$

for all $|\phi\rangle \in \mathscr{C}(\mathcal{A}',\psi)$.

Proof. On the left hand side of (3.171), we may choose $|\xi\rangle = |\eta\rangle$. It is most convenient to work with state vectors in the natural cones, for notations see (3.50). Define $b = \Delta^{1/2}_{\psi,\eta;\mathcal{B}} \Delta^{-1/2}_{\eta;\mathcal{B}}$, which is affiliated to the algebra $\mathcal{B}$ and extend the definition (3.173) to affiliated operators. Then we can write

$$
\begin{aligned}
&\|\Xi_\psi(1/2+it,\phi)\|^2\\
=&\|\Delta^{1/2}_{\psi,\xi;\mathcal{B}}\Delta^{-\frac{1}{2}-it}_{\eta,\xi;\mathcal{B}}\Delta^{\frac{1}{2}+it}_{\eta,\phi;\mathcal{A}}a\phi_{\mathcal{A}}\|^2\\
=&\|J_{\mathcal{B}}\varsigma^{-t}_{\eta;\mathcal{A}}\left(\varsigma^{t}_{\eta;\mathcal{B}}\left(b\right)\right)J_{\mathcal{A}}a\eta_{\mathcal{A}}\|^2\\
=&\langle\eta_{\mathcal{A}}|\varsigma^{t}_{\eta;\mathcal{B}}(b^*b)J_{\mathcal{A}}\varsigma^{t}_{\eta;\mathcal{A}}\left(a^2\right)|\eta_{\mathcal{A}}\rangle\\
=&\langle\eta_{\mathcal{B}}|\varsigma^{t}_{\eta;\mathcal{B}}(b^*b)J_{\mathcal{B}}\alpha_\eta(\varsigma^{t}_{\eta;\mathcal{A}}\left(a^2\right))|\eta_{\mathcal{B}}\rangle\\
=&\langle\eta_{\mathcal{B}}|b^*bJ_{\mathcal{B}}\varsigma^{-t}_{\eta;\mathcal{B}}\left(\alpha_\eta\left(\varsigma^{t}_{\eta;\mathcal{A}}\left(a^2\right)\right)\right)|\eta_{\mathcal{B}}\rangle\\
=&\langle\eta_{\mathcal{B}}|b^*J_{\mathcal{B}}\varsigma^{-t}_{\eta;\mathcal{B}}\left(\alpha_\eta\left(\varsigma^{t}_{\eta;\mathcal{A}}\left(a^2\right)\right)\right)b|\eta_{\mathcal{B}}\rangle\\
=&\langle\psi_{\mathcal{B}}|\alpha^t_\eta(a^2)|\psi_{\mathcal{B}}\rangle=\omega_\psi\circ\iota\circ\alpha^t_\eta(a^2).
\end{aligned}
\tag{3.172}
$$

(The choice $\pi^{\mathcal{A}'}(\psi)=J^2_{\mathcal{A}}\leq\pi^{\mathcal{A}'}(\phi)\leq\pi^{\mathcal{A}'}(\eta)=1$ guarantees the supports of vectors on $\mathcal{A}'$ are multiplied in the correct way, so we keep the $\pi^{\mathcal{A}'}$'s implicit in the derivation – everything should be understood to happen on $\pi^{A'}(\psi)$.) In the derivation we used the definition of the Petz recovery map, see e.g. [73] proof of prop. 8.4, such that $\forall\ a\in\mathcal{A}, b\in\mathcal{B}$,

$$
\langle\eta_{\mathcal{A}}|bJ_{\mathcal{A}}a|\eta_{\mathcal{A}}\rangle=\langle\eta_{\mathcal{B}}|bJ_{\mathcal{B}}\alpha_\eta(a)|\eta_{\mathcal{B}}\rangle.
\tag{3.173}
$$

Thus, we have (3.171). We obtain the claim in the lemma by taking the infimum in the set $\mathscr{C}(\mathcal{A}',\psi)$ on both sides of (3.171) and using (3.62). □

The lemma and concavity of $\ln$ allows us to conclude from (3.170) that

$$
\lim_{\theta\to 0^+}\frac{1}{\theta}\ln\|\Xi_\psi(\theta,\phi)\|\leq\ln\|a\zeta_{\mathscr{S}}\|^2=\ln\|\Delta^{1/2}_{\zeta_{\mathscr{S}},\phi}\psi\|^2,
\tag{3.174}
$$

where $|\zeta_{\mathscr{S}}\rangle$ is a vector representative of $\omega_\psi \circ \iota \circ \alpha_{\mathscr{S}} \in \mathcal{A}_\star$ and $\alpha_{\mathscr{S}}$ the recovery channel (3.41). Note that taking the infimum over $|\phi\rangle \in \mathscr{C}(\psi, \mathcal{A}')$ on the right side yields $2\ln F(\omega_\psi, \omega_\psi \circ \iota \circ \alpha_{\mathscr{S}})$ On the other hand, it is plausible to expect that for the term on the left side of (3.170), we obtain

$$\inf_{\phi \in \mathscr{C}(\mathcal{A}', \psi)} \lim_{\theta \to 0^+} \frac{1}{\theta} \ln \|\Xi_\psi(\theta, \phi)\| = -S_{\mathcal{A}}(\psi|\eta) + S_{\mathcal{B}}(\psi|\eta). \tag{3.175}$$

If this latter equation could be demonstrated – which is possible at a formal level[5] – then it is clear that we would obtain an alternative proof of thm. 3.1.2 (though not of thm. 3.1.1).

When attempting to demonstrate (3.175) (or equivalently (3.176)), one is facing similar technical difficulties as in the proof strategy described in the previous sections. There, we were forced to introduced suitably regularized versions $|\psi_P\rangle$ of the vector in question. Thus, while the strategy discussed here nicely avoids the use of L_p-spaces up to a certain point, it is not clear whether their use can be altogether avoided. We think that this would be an interesting research project.

3.4 Examples and applications

Here we illustrate our method and results in two representative examples.

[5] It is relatively straightforward to see that this equation would follow from the equation

$$\lim_{\theta \to 0^+} \frac{1}{2\theta} \left(1 - \|\Xi_\psi(\theta, \phi)\|^2\right) = \langle\psi| \ln \Delta_{\eta,\psi;\mathcal{B}} |\psi\rangle - \langle\psi| \ln \Delta_{\eta,\phi;\mathcal{A}} |\psi\rangle. \tag{3.176}$$

which is easier to check as it does not contain an infimum.

3.4.1 Example: finite type-I algebras

To compare our method to that of [2] in the subalgebra case, we work out our interpolating vector (3.86) in the matrix algebra case. Thus let $\mathcal{A} = M_n(\mathbb{C})$ and $\mathcal{B} = M_m(\mathbb{C})$, $\mathcal{C} = \mathcal{B}' \cap \mathcal{A}$, embedded as the subalgebra $b \mapsto \iota(b) = b \otimes 1_{\mathcal{C}}$ where $n = m \times k$ and these integers label the size of the matrices. We will work in the standard Hilbert space ($\mathscr{H} \simeq M_n(\mathbb{C}) \simeq \mathbb{C}^{n*} \otimes \mathbb{C}^n$) and identify state functionals such as σ with density matrices. So for example $\sigma_{\mathcal{A}} \in M_n(\mathbb{C})$, and we assume for simplicity that this has full rank (faithful state).

$\mathscr{H} \simeq M_n(\mathbb{C})$ is both a left and right module for $\mathcal{A}$,

$$l(m_1)\,|m_2\rangle = |m_1 m_2\rangle \qquad r(m_1)\,|m_2\rangle = |m_2 m_1\rangle\,, \tag{3.177}$$

and the inner product on $\mathscr{H}$ is the Hilbert-Schmidt inner product. The natural cone of $\mathcal{A}$ is defined to be the subset of positive semi-definite matrices in $\mathscr{H}$. The modular conjugation and relative modular operators (of $\mathcal{A}$) associated with this natural cone are:

$$J\big|m\big\rangle = \big|m^*\big\rangle \qquad \Delta_{\eta,\psi} = l(\sigma_{\mathcal{A}})r(\rho_{\mathcal{A}}^{-1}), \tag{3.178}$$

where we invert the density matrix $\rho_{\mathcal{A}}$ on its support. The natural cone vectors correspond to the unique positive square root of the corresponding density matrix, now thought of as pure states in the standard Hilbert space. So $|\psi_{\mathcal{A}}\rangle = \big|\rho_{\mathcal{A}}^{1/2}\big\rangle$ and $|\psi_{\mathcal{B}}\rangle = \big|\rho_{\mathcal{B}}^{1/2}\big\rangle$. The embedding is:

$$V_\eta = r(\sigma_{\mathcal{A}}^{1/2})T^* r(\sigma_{\mathcal{B}}^{-1/2})\,, \qquad T^*(m_{\mathcal{B}}) = m_{\mathcal{B}} \otimes 1_{\mathcal{C}} \tag{3.179}$$

Using these replacements it is easy to compute our interpolating vector (3.86) $|\Gamma_\psi(z)\rangle$ by starting with the expression in (3.87a)

$$|\Gamma_\psi(z)\rangle = \left|\sigma_{\mathcal{A}}^{z}(\sigma_{\mathcal{B}}^{-z}\rho_{\mathcal{B}}^{z} \otimes 1_{\mathcal{C}})\rho_{\mathcal{A}}^{1/2-z}\right\rangle \tag{3.180}$$

and

$$\Delta_\psi^{1/2-z}\,|\Gamma_\psi(z)\rangle = \left|\rho_{\mathcal{A}}^{1/2-z}\sigma_{\mathcal{A}}^{z}(\sigma_{\mathcal{B}}^{-z}\rho_{\mathcal{B}}^{z} \otimes 1_{\mathcal{C}})\right\rangle . \tag{3.181}$$

The $L_p(\mathcal{A}', \psi)$ norms can be computed using the well known correspondence between these norms and the sandwiched relative entropy discussed in [81]. This gives:

$$\||\Gamma_\psi(\theta)\rangle\|_{p,\psi}^{\mathcal{A}'} = \left(\mathrm{tr}\left|\rho_{\mathcal{A}}^{1/p-1/2}\Gamma_\psi(\theta)\right|^{p}\right)^{1/p} = \left(\mathrm{tr}\left|\rho_{\mathcal{A}}^{\theta}\sigma_{\mathcal{A}}^{\theta}(\sigma_{\mathcal{B}}^{-\theta}\rho_{\mathcal{B}}^{\theta} \otimes 1_{\mathcal{C}})\rho_{\mathcal{A}}^{1/2-\theta}\right|^{p_\theta}\right)^{1/p_\theta} , \tag{3.182}$$

where in the last equation we set $p = p_\theta$ and used $1/p_\theta - 1/2 = \theta$, and where $|\psi\rangle = |\ \rho_{\mathcal{A}}^{1/2}\ \rangle$. Similarly, we have

$$\left\|\Delta_\psi^{1/2-\theta}\,|\Gamma_\psi(\theta)\rangle\right\|_{p_\theta,\psi}^{\mathcal{A}'} = \left(\mathrm{tr}\left|\rho_{\mathcal{A}}^{1/2}\sigma_{\mathcal{A}}^{\theta}(\sigma_{\mathcal{B}}^{-\theta}\rho_{\mathcal{B}}^{\theta} \otimes 1_{\mathcal{C}})\right|^{p_\theta}\right)^{1/p_\theta} \tag{3.183}$$

and we recognize this later expression as [2], Eq. (25) with α there given by $p_\theta/2$.

3.4.2 Example: half-sided modular inclusions

Half-sided modular inclusions were introduced in [92, 93] and consist of the following data: An inclusion $\mathcal{B} \subset \mathcal{A}$ of von Neumann algebras acting on a common Hilbert space $\mathscr{H}$, containing a common cyclic and separating vector $|\eta\rangle$. Furthermore, for $t \geq 0$, it is required that

$\Delta_{\eta,\mathcal{A}}^{it}\mathcal{B}\Delta_{\eta,\mathcal{A}}^{-it} \subset \mathcal{B}$, hence the terminology "half-sided." This situation is common for light ray algebras in chiral CFTs, where $|\eta\rangle$ is the vacuum.

Wiesbrock's theorem [92, 93] is the result that for any half-sided modular inclusion, there exists a 1-parameter unitary group $U(s), s \in \mathbb{R}$ with self-adjoint, non-negative generator which can be normalized so that

$$\Delta_{\eta,\mathcal{A}}^{-it}\Delta_{\eta,\mathcal{B}}^{it} = U(e^{2\pi t} - 1) \tag{3.184}$$

for $t \in \mathbb{R}$. Furthermore, the unitaries $\Delta_{\eta,\mathcal{A}}^{it}, U(s)$ fulfill the Borchers commutation relations [94] and in particular $\mathcal{B} = U(1)\mathcal{A}U(1)^*$, $J_{\mathcal{A}}U(s)J_{\mathcal{A}} = U(-s)$. For any $a > 0$, the inclusion $\mathcal{A}_a = U(a)\mathcal{A}U(a)^* \subset \mathcal{A}$ is then also half sided modular.

For a half-sided modular inclusion, the embedding is trivial, $V_\eta = 1$. Using this information, one can easily show that in the case of the half-sided modular inclusions $\mathcal{A}_a = U(a)\mathcal{A}U(a)^* \subset \mathcal{A}$, the rotated Petz recovery channel, denoted here as $\alpha_a^t : \mathcal{B} \to \mathcal{A}$ to emphasize the dependence on a, is:

$$\alpha_\eta^t(x) \equiv U(a(1+e^{-2\pi t}))^* x U(a(1+e^{-2\pi t})). \tag{3.185}$$

Theorem (3.1.1) therefore gives the following corollary, conjectured in [14], after a change of integration variable.

Corollary 3.4.0.1. Let $\mathcal{B} \subset \mathcal{A}$ be a half-sided modular inclusion with respect to the reference vector $|\eta\rangle$, so $\mathcal{B} = \mathcal{A}_a = U(a)\mathcal{A}U(a)^*$. Then we have

$$\frac{1}{a}[S_{\mathcal{A}}(\omega_\psi|\omega_\eta) - S_{\mathcal{A}_a}(\omega_\psi|\omega_\eta)] \geq \int_a^\infty \ln F(\omega_\psi, U(y)\omega_\psi U(y)^*)^2 \, \frac{\mathrm{d}y}{y^2}. \tag{3.186}$$

For a half-sided modular inclusion, $V_\psi = u'_{\psi;\eta} \in \mathcal{B}'$ [from (3.57)] is the partial isometry that takes $|\psi_\mathcal{A}\rangle$ in the natural cone $\mathscr{P}^\natural_\mathcal{A}$ (defined w.r.t. $|\eta\rangle$) to the state representer in $\mathscr{P}^\natural_\mathcal{B}$ (also defined w.r.t. $|\eta\rangle$). The interpolation vector (3.86) thereby becomes in the case of half sided modular inclusions

$$|\Gamma_\psi(z)\rangle = \Delta^z_{\eta_\mathcal{A},\psi_\mathcal{A}} \Delta^{-z}_{\eta_\mathcal{B},\psi_\mathcal{B}} |\psi\rangle \, . \tag{3.187}$$

The vector (3.187) is similar to a vector studied in [14] in order to prove the quantum null energy condition (QNEC). Based on this and some preliminary calculations we speculate here that the QNEC can be understood in terms of the strengthened monotonicity result in Theorem (3.1.1).

Conjecture 3.4.1. The limit $a \to 0$ of Theorem (3.1.1) in the case of a half-sided modular inclusion $\mathcal{A}_a = U(a)\mathcal{A}U(a)^* \subset \mathcal{A}$ leads to a saturation of the bound:

$$\lim_{a\to 0} \frac{2}{a} \int_{-\infty}^{\infty} \ln F(\rho, \rho \circ \alpha^t_a) p(t) \mathrm{d}t = \frac{\mathrm{d}}{\mathrm{d}a} S_{\mathcal{A}_a}(\rho|\sigma)\bigg|_{a=0} . \tag{3.188}$$

This is a more refined version of a conjecture appearing in [14]. A corollary to this conjecture, if proven, would be a new proof of the QNEC since the recovery channel is translationally invariant so applying the same result to a further translated null cut one can use monotonicity of the fidelity to prove that $\frac{\mathrm{d}}{\mathrm{d}a} S_{\mathcal{A}_a}(\rho|\sigma)$ is monotonic in a as required by the QNEC.

Chapter 4: Approximate quantum error correction model of AdS/CFT

This chapter presents the analysis of quantum error correction models for AdS/CFT. We provide some basic definitions in Section (4.1). In Section (4.2), we discuss the constraints necessary for the HMERA to exhibit non-trivial correlation functions. We state a no-go theorem which requires that an HMERA with non-trivial correlators must necessarily contain more than one type of tensor. In Section (4.3), we, therefore, turn to the construction of models with multiple types of tensors, giving both general guidelines for constructions and an explicit realization (with additional details in Appendix (C)). Finally, in Section (4.4) we finish with a summary of this chapter.

4.1 Definitions

Typically, a MERA in the literature often refers to a multi-scale tensor network consisting of two types of tensors, the disentangler and isometry. However, the broader definition of MERA can extend to more general tensor networks such as the HaPPY code[31], the hyper-invariant tensor network[50], and other similar network geometries. To avoid this potential ambiguity, here we define MERA networks that are consistent with some hyperbolic tiling *hyper-invariant MERAs*, or HMERAs. We use MERA to specifically refer to the constructions described in [38].

Definition 4.1.1. A *hyper-invariant MERA (HMERA)* is a tensor network built on the dual graph

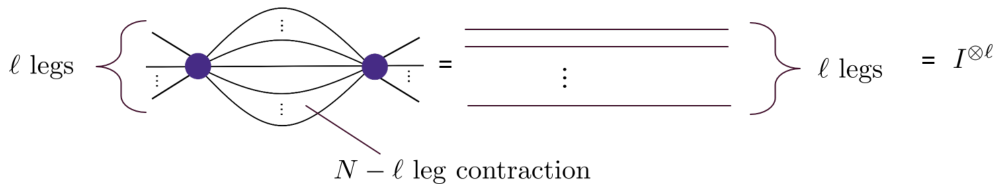

Figure 4.1: An example of a tensor where $N-\ell$ legs are contracted. Straight lines denote identity operators.

on a uniform hyperbolic tessellation such that the tensor layouts are consistent with the discrete symmetries of the tessellation.

Examples of such HMERAs include the HaPPY code and hyper-invariant tensor networks. In these constructions, all tensors associated with the tiles, vertices and edges are chosen to be the same. However, one can, in general, place different tensors in various locations as long as they have the right degrees, i.e., the number of dangling edges; see e.g. Figure (4.5) below for an example. The usual MERA (see for example figure 7 of [49]), on the other hand, is *not* an HMERA because the underlying tiling is not uniform.

Definition 4.1.2. A tensor of degree N with constant bond dimension on each leg is *ℓ-isometric* if contracting $N-\ell$ legs of the tensors with its conjugate transpose yields $I^{\otimes \ell}$. In addition, it is *permutation-invariant* if it is ℓ-isometric for any such $(N-\ell)$-leg contractions.

Graphically, this property is shown in Figure (4.1).

One can use such isometries as encoding isometries of quantum error correction codes. Here we call something a code when it encodes at least one logical degree of freedom (more generally, k of them). This, for example, rules out the $k=0$ codes which simply encode a state. The encoded logical degree of freedom is often referred to as the *bulk* degree of freedom in holographic tensor networks. We use these terms interchangeably in this work.

Isometric properties can also be translated into error correction properties. If a degree N

tensor is permutation invariant $\ell-$isometric, then it can also serve as an encoding isometry for an $[[n,k,d]]$ code where $n = N - k$, $k \geq 1$, and $d \geq \ell - k + 1$ [37]. This is because when *any* $\ell - k$ leg subsystem is maximally mixed, the map onto a subsystem is also a code that corrects at least that many erasures. Therefore any operation that alters the logical information must have support over at least $\ell - k + 1$ sites. Here we use this notation to denote a code over n qudits each with size given by the bond dimension of the tensor. If the tensor is not permutation invariant, then the resulting code can still correct such erasure on the *specific* $\ell - k$ legs required by the isometry. However, in this case no conclusive statement can be made about code distances in general.

Conversely, it is also straightforward to find examples of tensors with such isometric properties. For instance, any non-degenerate code with $d = \ell + 1$ satisfies the property that the reduced density matrix on ℓ qubits is maximally mixed. This yields a permutation invariant ℓ-isometry. The tensor that corresponds to this code is at least a $k + \ell$-isometry.

Definition 4.1.3. An HMERA is *regular* if it is built from a regular hyperbolic tessellation. If the tensors over different tiles in this network are identical and permutation-invariant, then we say it is *completely regular*.

Note that a (1-)uniform tiling can be regular or semi-regular. For example, the semi-regular pentagon-hexagon code (Figure 17a of [31]) and the hybrid holographic Bacon-Shor code[33] are completely semi-regular HMERAs. Here we focus on regular tilings where all polygonal tiles are identical. A completely regular tensor network will have individual tensors that obey the symmetries of the tiling. A completely regular HMERA is then a tensor network constructed by gluing together tensors that are also manifestly erasure correction codes. The HaPPY pentagon code and the holographic Steane code[35] are such completely regular HMERAs.

Definition 4.1.4. An HMERA is *locally contractible* if each tensor contracts to an isometry.

There are cases in which groups of tensors together contract to an isometry while each tensor as its own fundamental unit does not; see, for example, [50]. If the (groups of) tensors in the network do not contract to isometries, then it becomes more difficult to contract the network exactly when one computes quantities such as expectation values. This often leads to a much more costly algorithm, although there are instances where approximate contractions can also be performed in polynomial time[95, 96].

Lemma 4.1.1. A completely regular HMERA is locally contractible only if it has tensors that are least 2-isometric.

Proof. For a given layer of the hyperbolic tiling, there is at least one tile which has two edges facing inwards whereas all others have one edge facing inwards. As a result, the dual network contains loops. A tensor on this tile will have at least two legs facing inwards. If there are only 1-isometries, then it is impossible to contract this tensor from the outside, thus breaking local contractibility. □

Note that it is possible to generate completely regular tree tensor networks where all tensors are identical 1-isometries that are locally contractible. This lemma also ensures that a 5 qubit code is the simplest tensor that can be used as a building block for a locally contractible and completely regular HMERA that is also a non-trivial QECC. This is because the quantum Singleton bound requires that $n-k \geq 2(d-1)$. Complete regularity along with 2-isometry now ensure that each tensor block has $d \geq 3$. To encode a non-trivial amount of logical information, we also need $k \geq 1$. Hence this puts $n \geq 4+k \geq 5$. Hence the simplest building block for such a HMERA is indeed the $[[5,1,3]]$ code.

4.2 General Constraints and no-go theorem

When considering the holographic code, a "good" non-degenerate QECC that corrects two or more erasure errors necessarily has a trivial connected 2-point function on the boundary. This is because in order for the erasures to be correctable, they must contain none of the encoded logical information. Therefore, for non-degenerate codes, the state ρ_{AB} on the erased systems A, B on the boundary must be maximally mixed. Such states have zero mutual information between the two erasures. Hence, for unit norm operators O_A, O_B acting on A, B respectively,

$$\frac{1}{2}(\langle O_A O_B\rangle - \langle O_A\rangle\langle O_B\rangle)^2 \leq I(A:B) = 0. \tag{4.1}$$

This is, for example, the case for most two-site combinations in the HaPPY code. Therefore, to produce non-trivial correlation functions, one would have to consider a "bad" code with properties that are usually undesirable for quantum error correction. Additionally, it is difficult for it to properly capture the correct behaviour of subregion duality in holography.

This is not to say that it is impossible to produce a useful holographic code with non-trivial correlations. For example, degenerate codes may still sustain non-trivial two point functions while having the same code distance as a non-degenerate code. That is, let $\{|\bar{i}\rangle\}$ be an orthonormal basis for the code subspace; treating O_A, O_B as two single-site errors, the Knill-Laflamme condition is still satisfied,

$$\langle\bar{i}|O_A O_B|\bar{j}\rangle = C_{AB}\delta_{ij}, \tag{4.2}$$

as long as C_{AB} has off-diagonal elements while terms like $\langle\bar{i}|O_A|\bar{i}\rangle$ can vanish. Such is the case for the Shor code[97] but not for the $[[5,1,3]]$ code.

Another option is to consider approximate quantum error correction codes (AQECC), where the Knill-Laflamme condition is only satisfied approximately. This is a more natural approach because AdS/CFT should be described by an AQECC when the gravitational coupling is finite[98, 99]. In this case, it is possible to have a code that has "bad" erasure correction properties in general, but is nevertheless sufficiently close to a "good" code, such that it reproduces the desired behaviours like entanglement wedge reconstruction to leading order while also supporting correlation functions which become nontrivial as a result of $1/N$ corrections.

It might seem straightforward to construct such (A)QECCs using the same techniques of [33], where one replaces a code by its "noisy" counterparts. However, it is more difficult to maintain both non-trivial correlation functions and exact contractibility at the same time. On the one hand, exact contractibility requires (Lemma (4.1.1)) that the tensor be at least 2-isometric, meaning that certain two-site subsystems need to be maximally mixed. Heuristically, this very property makes it harder for the tensor network to sustain non-trivial two-point functions. On the other hand, adding "noisy" terms to the tensor network tends to spoil said isometric properties, making it easier to support non-trivial correlations but harder to contract exactly. Therefore, the challenge to building an exactly contractible (A)QECC model with non-trivial correlations is in balancing these two opposing forces such that each tensor is just good enough an error correction code, or, more generally, isometry, to give exact contractibility, but not so good as to require trivial correlation functions on the boundary.

The tension between contractibility and non-trivial correlation function in these holographic codes can be summarized in the following theorem. The simplest efficiently contractible construction which captures the discrete symmetries of the hyperbolic space is a locally contractible regular HMERA.

Theorem 4.2.1. A locally contractible and completely regular HMERA always contains a trivial connected boundary two-point function.

Proof. Consider a regular tiling of the Poincare disk with Schlafli symbol $\{p, q\}$, which tiles the plane with polygons of p edges with each vertex of the polygon adjacent to q p-gons.

Let us tile the space as follows. We start by having the central tile (top layer) then gradually add more tiles layer by layer by radiating outwards. The first layer consists of the p polygons whose edges are immediately adjacent to the central tile. Of the polygon in a layer, those that have edges facing toward the center we call *edge polygons* (EPs). We then repeat the process by adding more EPs for the polygons in the outer layers. Finally, we finish by adding polygons that have a vertex facing the center which fills the gap between EPs, which we call the *vertex polygons* (VPs). They have two edges facing inwards. If the tiles in an outer layer are immediately adjacent to a tile in the inner layer, then outer tiles are the"descendants" of the inner tile, which is the "ancestor."

To construct a completely regular HMERA, for each tile we now place the same tensor with p in-plane legs on the centroid of each polygon such that its legs are perpendicular to the p polygon edges. For two polygons that share a common edge, the two tensor legs that cross this edge are contracted. By lemma 4.1.1, the tensors are also at least 2-isometric for the network to be locally contractible.

Case 1 ($q > 3$) : For $q > 3$, no two adjacent polygons in the same layer can have the same ancestor. Thus for $q > 3$, all tiles can be divided into the above two categories[1].

[1]For $q > 3$ but odd, there are edges of VPs that are neither inward nor outward facing. However, we can take such legs to be outward facing choosing some sequence of adding tiles. For instance, when two adjacent tensors are connected on the same layer (two nearby polygons share a common edge that is neither inward nor outward facing), we can take one of them to be EP which has one inward facing edge and the other to be VP which has two.

Each EP has one inward facing leg that connects to the direct ancestor, and each VP has two. Note that a VP cannot have direct ancestors that are only VPs. This is by construction, where we always add VP after growing EPs. Therefore, for a VP, at least one of its direct ancestor/descendent is an EP.

Note that we will only focus on operator insertions where the operator is not proportional to the identity. This is because the connected two-point function for identity operators always vanishes. Then, for a single operator insertion on the boundary, it is either inserted on a tensor on EP or a VP. If the former, then the coarse-graining ascending super-operator can be reduced to contracting the 1-isometry with one operator insertion (Figure 4.2a). Because the tensor corrects at least two located errors $d \geq 3$, this contraction is zero. One can see this by first tracing the other $p-2$ legs without operator insertions, which reduces to the identity map tensoring a single operator insertion of the form tr$[O\rho]$ where $\rho \propto I$. We can then decompose the operator O into a part that is proportional to the identity and a part that is traceless. The first part coarse-grains to an operator proportional to the identity; they do not contribute to non-trivial correlations. The tensor contraction of the second part vanishes by tracelessness. Because the network always has EPs in its outer layer, this is sufficient to show that the state generated by the network contains trivial correlation functions.

For completeness, let us also examine operator inserted on VPs. If the boundary operator is inserted on a VP, then either the tensor contracts to 0, when $d > 3$, or it produces a weight 2 operator on the parent layer. The former again is trivial. For the latter case, because the graph is simple, the 2 operators must be passed onto 2 different tensors in the parent layer. At least one of these tensors is on an EP because they are immediate ancestors of a VP. They have a weight 1 insertion on each tensor, which makes the EP tensor contraction vanish also (Figure

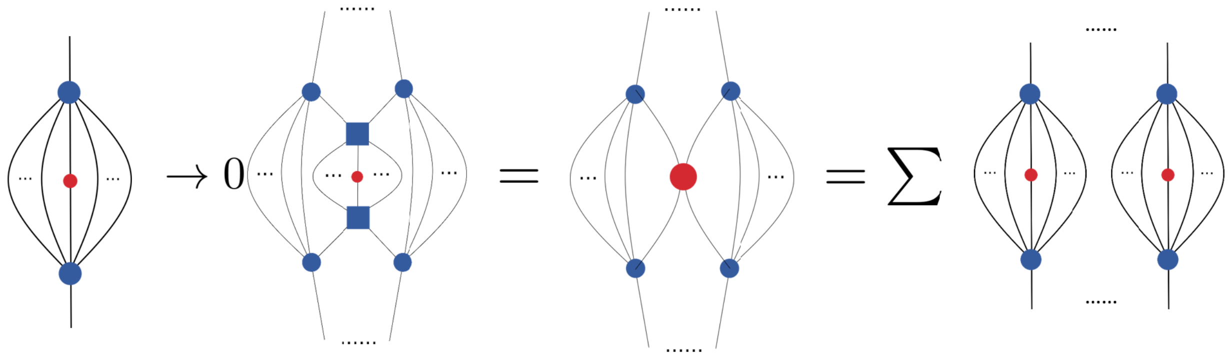

Figure 4.2: Left: for inserted operators not proportional to the identity (red dot), such components are found on EPs and are contracted to 0. Right: an operator inserted on a VP tensor can be coarse-grained to a weight 2 operator insertion. It can then be decomposed as sum over weight 1 operators contracted on EPs.

4.2b). The only non-trivial term from such contractions is if the parent contains only one EP and that an identity operator is pushed to the parent EP while a weight one operator is pushed to the parent VP. However, this cannot always be true because the contraction terminates on a "top tensor" whose descendents are EPs only. Therefore, there must exist a layer for which both parents are EPs. Hence for $q > 3$, we do not have any non-trivial super ascending operator. Therefore a two-point function is trivial as long as the two insertions are sufficiently far apart on the boundary.

Case 2 ($q = 3$): By construction, each descendent of the central tile is immediately adjacent to two others in the same layer. Therefore, for a tensor network on this tiling to be contractible at all, it has to be at least a 3-isometry. Again, we drop the bulk indices for convenience. Adding the completely regularity condition, this implies $d \geq 4$. Thus for any operator inserted on a VP, which has only 2 edges facing inwards, insertion on these sites will vanish. Because there are VPs in this tiling, there will be two-point functions that are trivial.

□

In other words, if one constructs a tensor network out of a single type of code that corrects erasures exactly and demands it to be efficiently contractible, then some correlation functions of this network must be trivial.

Indeed, we see that this is true for both the hyper-invariant tensor network and MERA where at least two types of tensors are used in its construction. This is also true for the pentagon and the heptagon code. In fact, we see that there are trivial correlation functions in [52] even for localized two-point function and that the (pairs of) sites with non-trivial correlators are sparse in the infinite-layer limit[51].

Note that here we have only focused on locally contractible completely regular HMERAs. It is in general possible to allow a completely regular HMERA to still be efficiently contractible by taking groups of tensors to contract to an isometry. We call such tensor networks quasi-locally contractible. One may worry that the local contractibility is too restrictive a requirement, and that there may be quasi-locally contractible networks that are completely regular. However, if a completely regular HMERA is quasi-locally contractible, then we can group the tensors into isometries. If the grouping produces another uniform tiling of the hyperbolic space, then it is simply a locally contractible uniform HMERA but with a different component tensor. By the above theorem it cannot have non-trivial correlations. If the network admits grouping of tensors into different isometries which correspond to a non-regular tessellation of the hyperbolic plane, then it is equivalent to an HMERA with multiple component tensors similar to MERA or the hyper-invariant tensor network, which are not completely regular.

The intuition of the above result is essentially that one has put too much “isometric-ness” into the network. By requiring the tensor network to be completely regular we force each tensor to be permutation invariant. This then forces every two-site subsystem on each tensor to be maximally mixed. As we have mentioned above, such properties prevent a non-trivial two-point function. It is clear that we then need to dial down the amount of "isometric-ness" in the network to avoid this no-go result.

One can achieve this by removing different restricting clauses in the theorem while still having a satisfactory HMERA. For instance, this is possible by relaxing a completely regular network to a regular one. In doing so, we may relinquish some of the local symmetries of the tensor by not requiring permutation invariance. Such tensors can only be isometries when contracted in certain directions (e.g. the isometries in MERA). Alternatively, we can allow more than one type of tensor in the network while still demanding that all types have the same degree. For such kind of networks, one can selectively reduce the "isometric-ness" of some tensors such that we still maintain local contractibility. Of course, we also give up some symmetries in the network. Or, one can take a combination of these two approaches. The latter will be the approach we take in the next section.

Going beyond regular and locally contractible HMERA, one can give up regularity entirely by going to semi-regular or k-uniform tessellations where different shaped tiles can map to different tensors. Local contractibility can also be relaxed to quasi-local contractibility, *e.g.*, in the hyper-invariant tensor network, while still retaining an exactly contractible ansatz.

4.3 HMERA model

4.3.1 General Construction Guidelines

In this section, we consider a construction that uses more than one type of tensors while preserving a regular tessellation. Although it can be tricky to prepare a tensor network with desired properties using only one type of tensor, it is much easier with two or more.

Let us begin with a regular tiling of the hyperbolic plane with Schlafli symbol $\{p, q\}$. We choose p, q such that the suitable isometries which we will describe in more detail later exist. In addition, all tiles except the one at the center can be divided into two types: the polygons with one edge facing the center, or edge polygons (EP), and polygons with a vertex/two edges facing the center, or vertex polygons (VP)[2].

Correspondingly, we need two types of isometries, the $1(+k_1)$-isometries of degree $p+k_1$, which we assign to the EPs, and $2(+k_2)$-isometries of degree $p+k_2$, which are assigned to the VPs. For the top tensor living in the central tile, we assign a k_0-isometry which encodes k_0 qudits into p qudits. From the error correction perspective, the top tensor does not exactly correct any erasure errors, but it may correct them approximately. By construction, we will assume that p, q are suitably chosen such that these types of isometries exist (we will give an example of such a choice in the next paragraph). $k_0, k_1, k_2 \geq 0$ are the number of "bulk" or logical degrees of freedom we want to assign to each tile. For the tensor network to be a non-trivial code, we want $k_0 + k_1 + k_2 > 0$. We then orient the remaining p tensor legs such that each leg is perpendicular to the polygon edges. The bulk legs will be left uncontracted while the two

[2] This construction method will not apply to the cases where some polygons are neither EP nor VP, e.g. when q is odd. However, for $q \geq 5$, one can circumvent this difficulty by preferentially designating such polygons to be either VPs or EPs. For $q = 3$ the situation is much worse and it is unclear if such a simple modification is sufficient.

in-plane legs of each tensors that lie on the same edge of a polygon will be contracted through the usual tensor contraction procedure[27, 31, 33]. This then produces a tensor network that maps the bulk degrees of freedom onto the boundary degrees of freedom. For the sake of convenience, when we refer to isometries from now on we will automatically drop the $(+k)$ bulk degrees of freedom and only consider in-plane legs unless otherwise specified.

For a slightly more concrete example, consider the $\{5, 4\}$ tiling of the hyperbolic plane by pentagons in Figure (4.5), where the VPs are labelled by squares and EPs are labelled by disks. The top tensor, a (0(+1))-isometry of degree 6, is denoted by a pentagon. Then for each VP, we can assign a (2(+1))-isometry and for each EP a (1(+1))-isometry, both of degree 6. This will allocate $k_0 = k_1 = k_2 = 1$ bulk qubit degree of freedom for each pentagonal tile. Such isometries clearly exist. One example is to take a $[[5, 1, 3]]$ code for the VP and a $[[5, 1, 2]]$ code for the EP. For the top tensor, more generic encoding isometries $V : \mathbb{C}^2 \to (\mathbb{C}^2)^{\otimes 5}$ would suffice. For example, we can turn a non-additive $[[6, 0, 2]]$ code into a $[[5, 1]]$ code which does not correct any erasure error by taking one of the tensor legs to be the bulk leg. Of course, while these isometries satisfy the necessary conditions we outlined, they need not be sufficient.

The error-correction properties of the code, e.g. the physical representations of logical operators, can also be easily derived using operator pushing. See [31, 33] for details. The pushing rules follow from the isometric properties of the tensors, where an ℓ-isometry of degree p can push any operator supported on ℓ legs to the remaining $p - \ell$ legs. Therefore, the support of each logical operators can also be derived by following these local pushing rules in the tensor network. See Figure (4.3) for an example in the $\{5, 4\}$ tiling where the relevant isometries are given by the $[[5, 1, 2]]$ and $[[5, 1, 3]]$ stabilizer codes[3].

[3] The operator pushing in Figure (4.3) also holds for the approximate code we construct in Section (4.3.2). How-

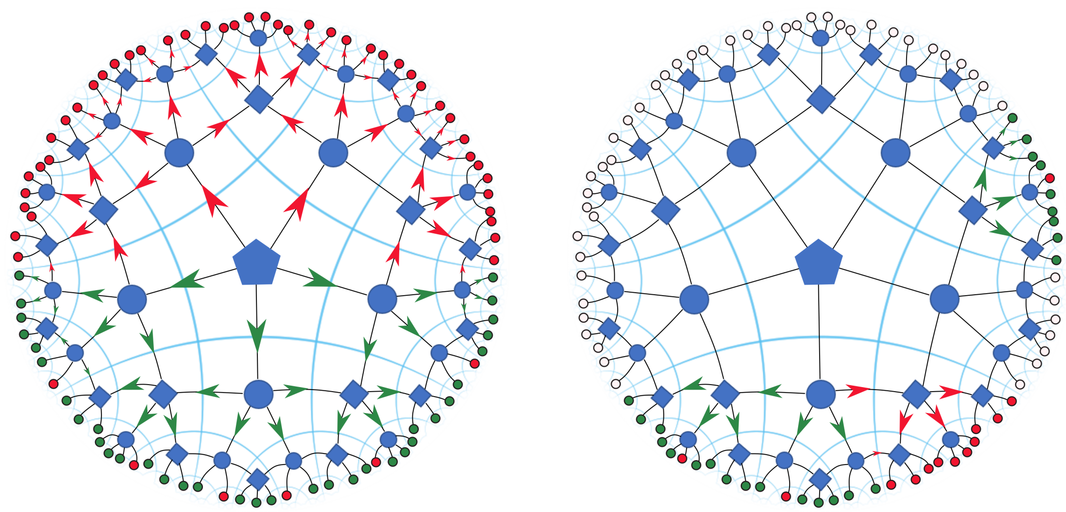

Figure 4.3: Left: a logical operator on the central (top) tensor is supported on all boundary degrees of freedom (red and green nodes). However, if one constructs a code that approximates the HaPPY code, then a logical operator can be pushed along the green arrows to a subregion of the boundary (green nodes) with a small error. Right: a similar pushing for certain logical operators closer to the boundary produce operators that are supported on a subregion. The logical operator can be reconstructed approximately on green nodes and can be reconstructed exactly on the union of green and red nodes.

Conversely, if all logical operators of some bulk region can be "cleaned" off of a boundary subregion, *i.e.* there exists a representation of the logical operators such that they act trivially on said subregion, then the erasure of this subregion also does not affect the encoded logical information in that bulk region. Specific code properties will, of course, depend on the details of the isometries and the network one uses.

Furthermore, because these isometries are QECCs that correct no more than e erasure errors, where $e = 1$ for EPs and $e = 2$ for VPs, they will not (exactly) correct any erasure errors on the boundary. Equivalently, this implies that an inserted weight one operator (such as a Pauli error) on the boundary will generally coarse-grain to a non-trivial (not zero or identity) operator on the more coarse-grained layers. This allows us to define non-trivial ascending/descending su-

ever, in Figure (4.3)b, only the logical Z operator can be supported on 4 legs of the imperfect code.

peroperators in a way similar to that of the MERA[100]. These are mappings that take operators to operators, corresponding to coarse/fine-graining a particular operator along the renormalization group direction. However, a key difference is that these superoperators can be different on different layers. Therefore we only take them to be similar to their MERA counterparts in an average sense. Suppose such a coarse-graining (ascending) superoperator averaged over the layers is given by $\bar{S}(\cdot)$ which admits spectral decomposition with eigenvalues $\bar{\lambda}_\alpha$ and corresponding eigen-operators $\bar{\psi}_\alpha$, then, we can reuse the same argument as is used to derive the MERA power-law correlation functions. See Section 3 of[100] for example.

Consider inserting operators $\bar{\psi}_\alpha, \bar{\psi}_\beta$ on the boundary sites indexed by i, j. Then the correlation function is expected to behave as

$$\langle \bar{\psi}_\alpha(i)\bar{\psi}_\beta(j)\rangle \approx C_{\alpha\beta}\bar{\lambda}^l_\alpha \bar{\lambda}^l_\beta = \frac{C_{\alpha\beta}}{|i-j|^{\Delta_\alpha+\Delta_\beta}}. \tag{4.3}$$

Here $C_{\alpha\beta} = \mathrm{tr}[\bar{\Psi}(\alpha,\beta)\bar{\rho}]$ is the expectation value of a localized coarse-grained operator $\bar{\Psi}(\alpha,\beta)$ evaluated against the reduced state $\bar{\rho}$ supported on a few sites which is approximately a fixed point[4] of the coarse-graining $\bar{S}(\bar{\rho}) \approx \bar{\rho}$, and under its dual fine-graining descending superoperator $\bar{S}^*(\bar{\rho}) \approx \bar{\rho}$. Equivalently, one can keep coarse-graining the operators $\bar{\Psi}(\alpha,\beta)$ using the ascending superoperators all the way up to the top tensor then evaluate $C_{\alpha\beta}$ against the top tensor[5]. $l \sim \log|i-j|$ is the number of layers of coarse-graining needed before $\bar{\psi}_\alpha\bar{\psi}_\beta$ becomes localized, and $\Delta_\alpha = \log\bar{\lambda}_\alpha$. The specifics of these super-operators will depend on both the network structure

[4]The existence of a fixed point is an additional assumption we make for the model. It seems physically reasonable that, for such a tensor network with a large number of layers with the same average ascending/descending superoperators, there should be a fixed point.

[5]The top tensor may encode global information of the state[101], but its impact on a few-site reduced state is washed out by the ascending/descending superoperators, so we expect that ((4.3)) should not depend on the choice of top tensor.

and the tensor isometries we use.

Note that this heuristic argument, by itself, does not imply the model can be used to approximate the ground states of CFTs whereby Δ are fit to the correct primary operators. Our statement is simply that such networks should support power-law correlations, as opposed to other completely regular HMERAs which Theorem (4.2.1) ensures do not.

Thus far, the method described constructs a quantum code which, in general, does not correct for erasures of subregions. In addition, the logical operators are not necessarily represented transversally. While such properties are not desirable for fault-tolerance, the latter is not a concern for models of AdS/CFT[6]. As for the former, holographic codes in general should correct for erasures of boundary subregions, at least approximately, in the large N limit. Therefore, if one wants more similarity with holography, it is not enough for such tensor networks to simply be a "bad code", rather it also has to be "close" to a good holographic code with proper erasure correction properties like [31]. To this end, we have to take a bit more care in constructing the isometric tensors such that they are also close to good erasure correction codes with larger code distances.

4.3.2 An Explicit Construction

We now present a concrete example of HMERA that is both efficiently contractible and permits non-trivial boundary correlations on all sites. We will construct isometries using a tunable parameter θ such that the code reduces to two copies of the $[[5,1,3]]$ "perfect" code when $\theta = 0$. It well approximates the HaPPY code when θ small, but can now produce power-law decaying

[6]In fact, it would be extremely unusual if all bulk operators can be represented transversally on the boundary, i.e. that they are simple tensor products of boundary operators acting on disjoint subregions, because the smearing function is highly non-trivial.

correlations and can in principle sustain a non-flat entanglement spectrum. We base our model on a tensor product of two copies of the HaPPY pentagon code. To circumvent the no-go theorem (4.2.1), we substitute some of the perfect codes in the network with imperfect codes which we now construct.

First we construct a $1(+0)$-isometry tensor associated with the edge polygons which we call the imperfect code. The imperfect code is illustrated graphically in Figure (4.4). This is but one way of constructing such isometries which are manifestly close to a perfect code for some parameters. In practice, one can easily construct other tensors over larger bond dimensions with more variational parameters. However, we choose this simple construction for the sake of clarity.

The imperfect code is a superposition of the double copy perfect tensor together with weight-2 Z-type errors inserted[7]. A weight-1 Z error is inserted in each copy, but no two errors are inserted on the same leg of different copies. Here $i, j = 1, 2, ..., 5$ are labelling legs in which errors are inserted. All different possible insertion configurations are summed up. To have this imperfect tensor be a 1-isometry (see Definition (4.1.2)), the parameters should satisfy the following relation:

$$\cos\theta^2 + \sum_{i\neq j} \sin\theta_{ij}^2 = 1. \tag{4.4}$$

To retain the original symmetry of the perfect tensor, we usually choose the parameterization $\sin\theta_{ij} = \frac{\sin\theta}{\sqrt{20}}$. Both the perfect and the imperfect tensor being isometries guarantees the efficiently contractible property of our HMERA model.

Treating each leg as a qudit, we can show that this imperfect tensor defines a $[[5, 0, 2]]_4$ code but approximates two copies of the perfect code (Appendix (C.3)). It exactly reduces to

[7] The added terms with Z errors help tilt the perfect code away from a stabilizer code. In doing so, it adds magic, which is necessary at all scales of the tensor network to produce a low energy state of a CFT[102].

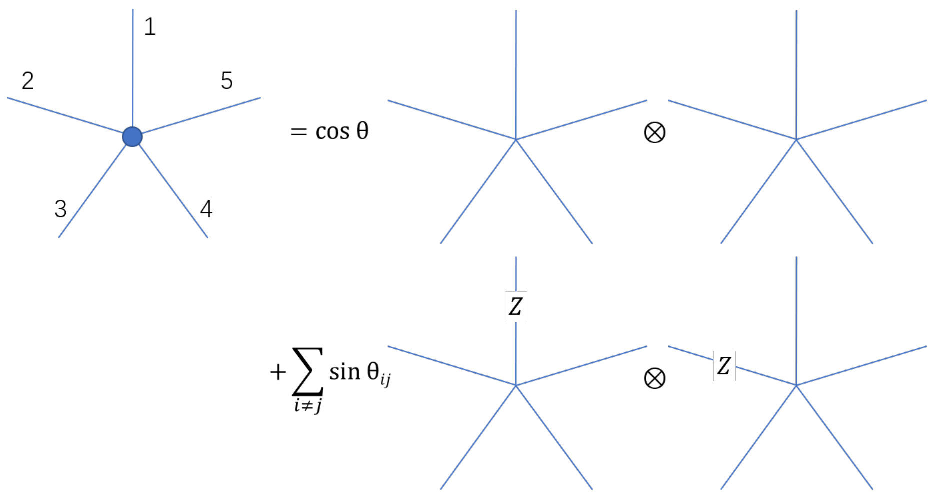

Figure 4.4: The construction of the imperfect code where each line on the left hand side represents two physical qubits. Each 5-pronged diagram on the right hand side is a perfect code. In the second line i, j label the legs in which Z errors are inserted on each copy respectively.

two copies of the 5 qubit perfect code when $\theta = 0$, and therefore inherits all its error correction properties approximately when θ is small. In the tensor network notation, each leg has bond dimension 4 and the code sub-algebra is supported on any three legs of this tensor when $\theta = 0$. However, when θ small but nonzero, it only approximates the double-copy perfect code.

We can also construct the top tensor in a similar fashion by super-imposing the same codes with different choices of the code subspace. For instance, let V be the perfect code encoding isometry, then we may construct a tensor that approximates the perfect code for small $\phi_{i\neq 0}$ with encoding map V_T such that,

$$V_T = \cos\phi_0 V + \sum_{i=1}^{5} \sin\phi_i P_i V \tag{4.5}$$

where $\cos^2\phi_0 + \sum_i \sin^2\phi_i = 1$ and $P_i \in \{X, Y, Z\}$ are the same Pauli operators acting on site i. For the sake of symmetry, let us choose $\phi_i = \phi_0 = \phi$. We can then take two tensor copies of this code as the top tensor we use in the network.

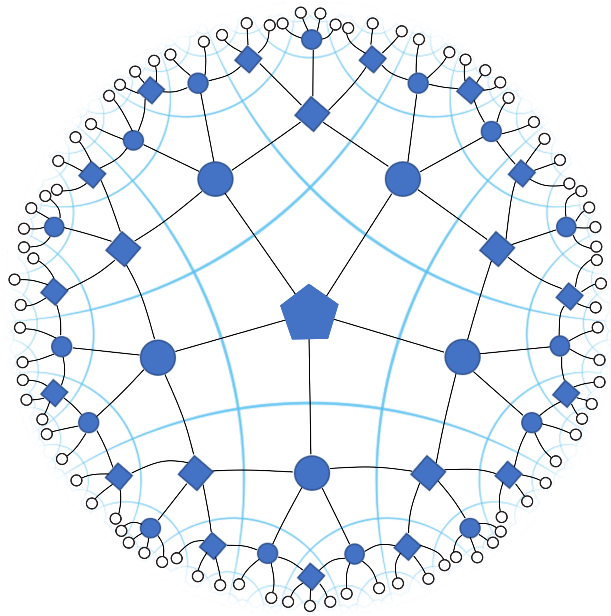

Figure 4.5: The illustration of the HMERA tensor network. The first several layers of substitution is explicitly shown. The circles represent the imperfect tensors defined in Figure (4.4), while the squares represent the tensor product of two perfect tensors.

To construct the full tensor network, we specify the positions of the substitution and replace those perfect codes with their imperfect counterparts. This is explicitly shown in Figure (4.5). First we choose a pentagon as the origin and replace it by an imperfect double copy top tensor ((4.5)). From the origin we can label each pentagon uniquely by the number of edges we need to cross to reach it from the origin. The collection of pentagons that are assigned to the same number a is called a “layer”. Apart from the top tensor, if a particular pentagon tile has only one edge connected to the previous layer, we replace the two tensor copies of the perfect code on it by the imperfect code (Figure (4.4)).

The variational parameters of this model are given by the logical degrees of freedom, the top tensor skewing parameter ϕ, and θ_τ where in principle each imperfect code is labelled by τ. For a more symmetric construction, we can set $\theta_\tau = \theta, \forall \tau$.

This network again supports a power-law decaying correlation function. Heuristically, it should contain at least one type of scaling operator with $\Delta \approx \log \bar{\lambda}$, where $\bar{\lambda}$ as the average of the dominant eigenvalue of the coarse-graining super operators over the layers:

$$\bar{\lambda} \approx \prod_{a} \lambda_a^{p_a}. \tag{4.6}$$

The index a labels different types of super operators and p_a denotes the probability of type a super operator contributing to the coarse-graining process. It can be shown that one can choose the variational parameters such that $\lambda_a < 1$. The detail distributions of p_a and the details on the different superoperators can be found in Appendix (C).

This HMERA model effectively "interpolates" between the usual MERA (or hyper-invariant tensor network model) and the HaPPY code model of holographic quantum error correction codes. By tuning these variational parameters, it mimics the former by introducing some variational parameters, power-law correlation functions while reproduces the approximate code properties of latter in reconstructing bulk operators on the boundary. Furthermore, because it is an approximate holographic quantum error correction code for small θ, ϕ, it also approximately retains all properties of the HaPPY code such as the Ryu-Takayanagi formula, entanglement wedge reconstruction, and other error correction properties.

4.4 Summary

In this chapter, we have examined some general properties needed to construct a holographic quantum error correction code that can support power-law decaying correlation functions. By also demanding the network to be locally contractible, we found that it is impossible to satisfy both these requirements simultaneously in a completely regular HMERA. Instead, one has to introduce more than one type of tensors in order to construct a satisfactory variational ansatz that is also exactly contractible. This statement also coincide with the general observation that so far all the MERA-like variational ansatze presented contain at least two types of tensors. We have also provided general guidelines for constructing approximate holographic quantum error correction codes with the aforementioned properties. In particular, we gave one explicit construction where the tensor network approximated two copies of the HaPPY pentagon code in certain regimes of the parameter space.

It is also desirable, both from AdS/CFT and from many-body physics, for such an ansatz to capture the CFT entanglement spectrum. We have not investigated this in detail, but we can provide some general speculations using heuristic arguments. As shown in Appendix (C.2), cuts through any edge of a perfect tensor have a tendency to flatten the entanglement spectrum while cuts through more than one edge of the imperfect tensors tend to be the opposite. As the entanglement of a subregion is tied to minimal cuts through the tensor network, for large enough boundary regions, we expect such a cut to contain both types of edges after averaging over the different types of tensors that can be contained in the bulk region affecting the given bulk subregion. Therefore, the overall entanglement spectrum should be somewhere in between the behaviour shown in Figure (C.6) and Figure (C.7). Thus the tensor network should be able to accommodate non-flat spectrums.

Chapter 5: Summary and Outlook

5.1 Summary

In this dissertation, I present three scenarios where recovery methods are applied to different quantum systems. They are the perfect recovery in Gaussian fermionic systems in Chapter (2), the approximate recovery in quantum field theory in Chapter (3), and the approximate QECC in the context of AdS/CFT in Chapter (4). The logic behind this arrangement is to develop from finite systems to infinite systems, from perfectly recoverable to approximately recoverable, trying to capture nature more and more realistically.

In Chapter (2), I deal with the perfect recovery in Gaussian fermionic systems. When both the channel and the reference state are Gaussian, using the Lagrangian representation of Gaussian linear maps, the Petz recovery map can be expressed in terms of the covariance matrix of the reference state, and the matrices A, B that encode the information of the Gaussian quantum channel in Eq. (2.36). A similar expression for the rotated Petz map is obtained in Eq. (2.41). As a side product, a new formula for the fidelity of two arbitrary fermionic Gaussian states is derived in terms of their covariance matrices, shown in Eq. (2.43).

In Chapter (3), the main effort is put to generalize the results of the approximate reversibility of quantum channels in [2] from a type-I von Neumann algebra setting to general von Neumann algebras. This is stated as Theorem (3.1.2). This chapter concentrates on the sub-algebra case where the corresponding channel is called an inclusion. A strengthened version of the monotonicity [21] of relative entropy, stated in Theorem (3.1.1), guarantees the existence of such an approximate channel. To prepare for the proof of the main theorems, a regularization method, stated as Theorem (3.2.2), is developed to produce states with finite relative entropy. It also allows for continuous extrapolation of relative entropy when removing the regulator. Theorem (3.2.2) is at the core of the proof of Theorem (3.1.1) because it leads to extended domains of holomorphy so that derivatives can be performed at the domain which is otherwise on the boundary of holomorphic regions.

In Chapter (4), the goal is to clarify the general properties needed to construct a holographic quantum error correction code that can support power-law decaying correlation functions. It turns out that it is impossible to be both locally contractible and have power-law decaying correlation functions in a completely regular HMERA. This is summarized as a no-go theorem in Theorem (4.2.1). We provide general guidelines for circumventing this no-go theorem and constructing approximate holographic quantum error correction codes with the aforementioned properties. In particular, one explicit construction is given where the tensor network approximates two copies of the HaPPY pentagon code in certain regimes of the parameter space of the building block isometries. Some general speculations are also provided to argue that our HMERA model can capture entanglement spectra of generic CFTs in Appendix (C.2). The entanglement entropy of a CFT for a single region takes a universal form depending on the central charege of the theory.

5.2 Outlook

The results in this dissertation have various implications and applications . At the same time, the subjects presented here leave much to be explored and to be extended to further research.

The results in Chapter (2) should be useful for studying error correction in Majorana fermion systems (e.g. [103]), or for constructing fermionic recovery maps in experiments. Also, it is desirable to generalize the formula to approximate Gaussian states as a step towards interacting systems. An important interacting Majorana model is the Sachdev-Ye-Kitaev (SKY) model (e.g.[104]). It is conjectured to have a dual gravity description of 2 dimensional AdS spacetime. At the same time, the methods of obtaining the A, B matrices are of particular use. This is an efficient way to describe the channels in large systems. For example, it could be used to study the purification or thermalization problems of fermionic Gaussian systems. One particularly interesting channel is the so-called "modular flow", which is the unitary group generated by the operator logarithm of the density matrices. It is of general interest to discuss in which circumstances modular flows are local. The Gaussian fermion system provides a simple and neat playground and the methods of representing the action of modular flows have been partially obtained during the calculation of the rotated Petz map.

The results in Chapter (3) have profound implications for both entanglement structures of quantum field theories and the constraints on interacting dynamic systems. As stated in the main text, the quantum null energy condition is related to the strengthened monotonicity inequality, which is illustrated in Section (3.4.2). It is interesting to investigate the implications of this inequality in the context of AdS/CFT, for example, whether the particular form of the recovery channel or the informational quantity of fidelity has a certain geometric interpretation. It is also of research interest to examine the relation between this strengthened inequality and the monogamy of mutual information (MMI). The latter is an informational inequality that is only valid for semi-classical holographic states, thus defining the so-called holographic entropy cone [105]. It turns out MMI can be saturated for certain holographic states, so that the remainder term of the inequality obtained in this chapter is always supershaowed by that in the MMI inequality in the context of holography. It is a feasible question to ask the reason for this in holography, and whether this observation can have geometric implications.

The HMERA network constructed in Chapter (4) can in principle serve as a variational ansatz, but much work is needed to establish its utility. In particular, one would need to develop an optimization algorithm and analyze its complexity in a similar procedure to [100]. This is left for future work. I am optimistic that the construction methods described in this dissertation can be generalized to create other HMERA-like variational ansatze which are also QECCs. In particular, because AdS/CFT is tied to AQECCs, we hope that such HMERA models can provide computable examples that help us understand some aspects of holography beyond leading order. They may also serve as useful tools for intuition building for small N, where the tensor network remains valid and well-defined despite being in the regime where gravity is strongly coupled and highly quantum.

The idea of quantum recovery definitely goes beyond the three scenarios presented in this dissertation. From a pure informational theoretical point, it is always desirable to construct universal approximate channels that can achieve better recovery results. From an applicational point of view, ideas of the recovery channel can be applied to gravitational theories to address some of the most concerning questions in science. For example, it would be of great interest to see if the information encoded in the Hawking radiation can be recovered to reveal the characteristics of matter before falling into the balck hole. As addressed at the very beginning of the dissertation, my major motivation was using ideas of quantum recovery in AdS/CFT duality. Specifically, applying the recovery channel to a subregion in the AdS spacetime might enable us to construct explicit examples of the entanglement wedge reconstruction, thus revealing more details of the microscopic theories of gravity[7]. An intersting scenario is how to express the operators in the region inside the entanglement wedge but outside the causal wedge, considering the perturbations around the classical geometry. A promising playground is the aforementioned SYK model. With the techniques of calculating fermionic systems studied in Chapter (2), as well as the quantum recovery techniques studied throughout this dissertation, obtaining the explicit bulk reconstruction in the SYK/AdS_2 duality should be achievable in the near future.

Appendix A: Supplementary materials of Chapter 2

A.1 Grassmann Calculus Identities

We list some useful formula for Grassmann integral in this section. The integral of a single Grassmann variable is defined as follows:

$$\int d\theta \equiv 0, \quad \int \theta d\theta \equiv 1. \tag{A.1}$$

For multiple Grassmann variables,

$$\int \theta_1 \theta_2 ... \theta_{2n} d\theta_{2n} ... d\theta_2 d\theta_1 = 1. \tag{A.2}$$

The integral is performed from the interior to the exterior.

One usually abbreviates the integral measure $D\theta \equiv d\theta_{2n}...d\theta_2 d\theta_1$. Commonly one writes $\theta = (\theta_1, ..., \theta_n)^T$ for multiple variables so

$$\theta^T A \eta \equiv \sum_{j,k=1}^{2n} \theta_j A_{jk} \eta_k. \tag{A.3}$$

If one makes the following changes of variables

$$\eta_i = \sum_j R_{ij}\theta_j, \tag{A.4}$$

the corresponding measure changes as

$$D\eta = \det(R)^{-1} D\theta. \tag{A.5}$$

One can obtain it by requiring that Eq. (A.2) still holds for the set of variables η_i's.

The following formula are useful for the calculation:

$$\text{tr}(XY) = (-2)^n \int D\theta D\mu e^{\theta^T \mu} X(\theta) Y(\mu), \tag{A.6a}$$

$$\int D\theta \exp\left(\frac{i}{2}\theta^T M \theta\right) = i^n \text{Pf}(M), \tag{A.6b}$$

$$\int D\theta \exp\left(\frac{i}{2}\theta^T M \theta + \eta^T B \theta\right) = i^n \text{Pf}(M) \exp\left(-\frac{i}{2}\eta^T B M^{-1} B^T \eta\right) \tag{A.6c}$$

where Pf stands for the Pfaffian. Pfaffian is a polynomial defined for an anti-symmetric matrix A such that Pf$(A)^2 = \det(A)$. For the odd dimensional case, Pf$(A) \equiv 0$ since $\det(A) = 0$. For the even dimensional case, the Pfaffian for a $2n \times 2n$ anti-symmetric matrix B is defined as

$$\text{Pf}(B) \equiv \frac{1}{2^n n!} \sum_{\sigma \in S_{2n}} \text{sign}(\sigma) \prod_{i=1}^{n} B_{\sigma_{2i-1}, \sigma_{2i}}, \tag{A.7}$$

where σ stands for a certain permutation as an element of the permutation group S_{2n}, and sign(σ) denotes the parity of the given permutation.

Note that Eq. (A.6c) holds when M is invertible. However, if M is not invertible, there is a well-defined limit of the right hand side that makes the equality holds. We show this by an explicit calculation.

We work in the bases where the covariance matrix G is in its block diagonal form

$$M = \text{diag}\left(\lambda_1, ..\lambda_p, 0, ..., 0\right) \otimes \begin{pmatrix} 0 & 1 \\ -1 & 0 \end{pmatrix} \tag{A.8}$$

where the diagonal matrix is n dimensional so it has $(n-p)$ zero Williamson eigenvalues. For simplicity, we take $B = I$, while general B can be transformed into this form by redefining $\tilde{\eta} = B^T \eta$.

Calculating the Grassmann integral explicitly gives

$$\begin{aligned} &\int D\theta \exp\left(\eta^T\theta + \frac{i}{2}\theta^T M\theta\right) \\ =&(-1)^n \sum_{k=1}^{p} i^k \sum_{\sigma_1,\ldots,\sigma_k} \left(\prod_{i=1}^{k} \lambda_{\sigma_i}\right) \eta_{2\bar{\sigma}_{k+1}-1}\eta_{2\bar{\sigma}_{k+1}} \ldots \eta_{2\bar{\sigma}_p-1}\eta_{2\bar{\sigma}_p} \left(\prod_{i=p+1}^{n} \eta_{2i-1}\eta_{2i}\right), \end{aligned} \tag{A.9}$$

where $\sigma_1, ..., \sigma_k$ label a certain choice of k items from a total number of p and $\bar{\sigma}_{k+1}, ..., \bar{\sigma}_p$ are the corresponding left $(p-k)$ items.

Consider

$$M(\epsilon) = \text{diag}\left(\lambda_1, ..\lambda_p, \epsilon_{p+1}, ..., \epsilon_n\right) \otimes \begin{pmatrix} 0 & 1 \\ -1 & 0 \end{pmatrix}, \tag{A.10}$$

where all $\epsilon_{p+1}, ..., \epsilon_n \neq 0$. Now $M(\epsilon)$ is invertible so we can use Eq. (A.6c) to get

$$\begin{aligned}
&\int D\theta \exp\left(\eta^T\theta + \frac{i}{2}\theta^T M(\epsilon)\theta\right) \\
&= i^n \text{Pf}(M(\epsilon)) \exp\left(-\frac{i}{2}\eta^T M^{-1}(\epsilon)\eta\right) \\
=&(-1)^n i^n \prod_{i=1}^{p} \lambda_i \left(1 - i\lambda_i^{-1}\eta_{2i-1}\eta_{2i}\right) \prod_{j=p+1}^{n} \epsilon_j \left(1 - i\epsilon_j^{-1}\eta_{2j-1}\eta_{2j}\right) \\
=&(-1)^n i^n \prod_{i=1}^{p} (\lambda_i - i\eta_{2i-1}\eta_{2i}) \prod_{j=p+1}^{n} (\epsilon_j - i\eta_{2j-1}\eta_{2j}) \,.
\end{aligned} \tag{A.11}$$

We can now take the limit $\epsilon_{p+1}, ..., \epsilon_n \to 0$ and it is straight forward to verify

$$\begin{aligned}
&(-1)^n i^n \prod_{i=1}^{p} (\lambda_i - i\eta_{2i-1}\eta_{2i}) \prod_{i=p+1}^{n} (-i\eta_{2i-1}\eta_{2i}) \\
=&(-1)^n \sum_{k=1}^{p} i^k \sum_{\sigma_1,...,\sigma_k} \left(\prod_{i=1}^{k} \lambda_{\sigma_i}\right) \eta_{2\bar{\sigma}_{k+1}-1}\eta_{2\bar{\sigma}_{k+1}} \cdots \eta_{2\bar{\sigma}_p-1}\eta_{2\bar{\sigma}_p} \left(\prod_{i=p+1}^{n} \eta_{2i-1}\eta_{2i}\right) .
\end{aligned} \tag{A.12}$$

This limit does not depend how $(\epsilon_{p+1}, ..., \epsilon_n)$ approaches $(0, 0, ..., 0)$ in a $(n-p)$ dimensional space, so it is well-defined. We have verified that

$$\lim_{(\epsilon_{p+1},...,\epsilon_n)\to(0,0,...,0)} \int D\theta \exp\left(\eta^T\theta + \frac{i}{2}\theta^T M(\epsilon)\theta\right) = \int D\theta \exp\left(\eta^T\theta + \frac{i}{2}\theta^T M\theta\right) . \tag{A.13}$$

So if M is not invertible in Eq. (A.6c), we can still write the right hand side formally, which is understood as the unique value obtained by a perturbing and limiting procedure described above and is independent of how we perform the perturbation. Formally, the integration in Eq. (A.6c) can be viewed as a matrix-valued function of M, and the above derivation shows that this function is continuous when M is singular.

A.2 Calculation Details

A.2.1 Two relations for matrix function

We show two matrix function relations whose arguments are anti-symmetric matrices. They are similar to those matrix functions for bosons found in [60].

Consider an odd function $f : \mathbb{R} \to \mathbb{R}$ and an even function $g : \mathbb{R} \to \mathbb{R}$ whose Talyor series exist at $x = 0$. The corresponding function acting on a matrix M is defined via Talyor series. Due to the odd/even property of the function f and g, only the odd powers of f and the even powers of g in the Talyor series remain.

Let an anti-symmetric matrix be the argument of the function

$$X = O^T \left(\chi \otimes \begin{pmatrix} 0 & -1 \\ 1 & 0 \end{pmatrix} \right) O, \tag{A.14}$$

where $O \in SO(2n)$ and $\chi = \text{diag}\,(\chi_1, \chi_2, ..., \chi_n)$.

Now define the induced functions f_* and g_* acting on a matrix such that if X takes the form of (A.14),

$$f_*(X) \equiv O^T \left(f(\chi) \otimes \begin{pmatrix} 0 & -1 \\ 1 & 0 \end{pmatrix} \right) O, \;\; g_*(X) \equiv O^T \left(g(\chi) \otimes I_2 \right) O. \tag{A.15}$$

Here $f(\chi) = \text{diag}\,(f(\chi_1), ..., f(\chi_n))$, $g(\chi) = \text{diag}\,(g(\chi_1), ..., g(\chi_n))$.

We want to show

$$f_*(X) = -if(iX), \quad g_*(X) = g(iX). \tag{A.16}$$

Direct calculation gives

$$\begin{aligned}
&-if(iX) \\
=&\sum_{k=0}^{\infty} \frac{-i}{(2k+1)!} f^{(2k+1)}(0) \left(iO^T \left(\chi \otimes \begin{pmatrix} 0 & -1 \\ 1 & 0 \end{pmatrix} \right) O \right)^{2k+1} \\
=&\sum_{k=0}^{\infty} \frac{(-1)^k}{(2k+1)!} f^{(2k+1)}(0) O^T \left(\chi^{2k+1} \otimes \begin{pmatrix} 0 & -1 \\ 1 & 0 \end{pmatrix}^{2k+1} \right) O \\
=&\sum_{k=0}^{\infty} \frac{1}{(2k+1)!} f^{(2k+1)}(0) O^T \left(\chi^{2k+1} \otimes \begin{pmatrix} 0 & -1 \\ 1 & 0 \end{pmatrix} \right) O \\
=&O^T \left(f(\chi) \otimes \begin{pmatrix} 0 & -1 \\ 1 & 0 \end{pmatrix} \right) O = f_*(X).
\end{aligned} \tag{A.17}$$

The same calculation gives the second formula in Eq.(A.16).

A.2.2 Construction of $\mathcal{N}_1, \mathcal{N}_3$

We present the calculation details for the construction of $\mathcal{N}_3$ in this part, while that for $\mathcal{N}_1$ follows in a similar way so is largely omitted.

One can write the ansatz for $\sigma^{\frac{1}{2}}$:

$$\sigma^{\frac{1}{2}} = \prod_{i=1}^{n} c_i \left(\hat{I} - i\lambda_i^{(\sigma^{\frac{1}{2}})} \tilde{\gamma}_{2i-1} \tilde{\gamma}_{2i} \right). \tag{A.18}$$

c_i and $\lambda_i^{(\sigma^{\frac{1}{2}})}$ are obtained by requiring $\sigma^{\frac{1}{2}} \sigma^{\frac{1}{2}} = \sigma$. So

$$c_i^2 = \frac{1}{2\left(1 + \lambda_i^{(\sigma^{\frac{1}{2}})2}\right)}, \quad \frac{\lambda^{(\sigma)}}{2} = 2c_i^2 \lambda^{(\sigma^{\frac{1}{2}})}. \tag{A.19}$$

One can solve to get Eq. (2.26) and Eq. (2.27).

Note that Eq. (2.27) has a well defined limit

$$\lim_{\lambda^{(\sigma)} \to 0} \lambda^{(\sigma^{\frac{1}{2}})} = 0. \tag{A.20}$$

It indeed gives the right answer when $\lambda^{(\sigma)} = 0$. So we will not single out this seemingly singular case in the following derivation.

The Choi-Jamiolkowski dual of $\mathcal{N}_3$ is

$$
\begin{aligned}
&\sigma^{\frac{1}{2}}\rho_I\sigma^{\frac{1}{2}} \otimes_f \hat{I} \\
=&\frac{1}{2^{3n}}\prod_{i=1}^{n}\frac{1}{1+\left(\lambda_i^{(\sigma^{\frac{1}{2}})}\right)^2}\left(\hat{I}-i\lambda_i^{(\sigma^{\frac{1}{2}})}\tilde{\gamma}_{2i-1}\tilde{\gamma}_{2i}\right)\left(\hat{I}+i\tilde{\gamma}_{2i-1}\tilde{\gamma}_{2i-1+2n}\right) \\
&\times\left(\hat{I}+i\tilde{\gamma}_{2i}\tilde{\gamma}_{2i+2n}\right)\left(\hat{I}-i\lambda_i^{(\sigma^{\frac{1}{2}})}\tilde{\gamma}_{2i-1}\tilde{\gamma}_{2i}\right) \\
=&\frac{1}{2^{3n}}\prod_{i=1}^{n}\hat{I}+i\left(1-\lambda_i^{(\sigma^{\frac{1}{2}})2}\right)\left(1+\lambda_i^{(\sigma^{\frac{1}{2}})2}\right)^{-1}\left(\tilde{\gamma}_{2i-1}\tilde{\gamma}_{2i-1+2n}+\tilde{\gamma}_{2i}\tilde{\gamma}_{2i+2n}\right) \\
&-\left(2i\lambda_i^{(\sigma^{\frac{1}{2}})}\right)\left(1+\lambda_i^{(\sigma^{\frac{1}{2}})2}\right)^{-1}\left(\tilde{\gamma}_{2i-1}\tilde{\gamma}_{2i}-\tilde{\gamma}_{2i-1+2n}\tilde{\gamma}_{2i+2n}\right)+\tilde{\gamma}_{2i-1}\tilde{\gamma}_{2i}\tilde{\gamma}_{2i-1+2n}\tilde{\gamma}_{2i+2n} \\
=&\frac{1}{2^{3n}}\prod_{i=1}^{n}\hat{I}+i\sqrt{1-\lambda_i^{(\sigma)2}}\left(\tilde{\gamma}_{2i-1}\tilde{\gamma}_{2i-1+2n}+\tilde{\gamma}_{2i}\tilde{\gamma}_{2i+2n}\right)-i\lambda_i^{(\sigma)}\left(\tilde{\gamma}_{2i-1}\tilde{\gamma}_{2i}-\tilde{\gamma}_{2i-1+2n}\tilde{\gamma}_{2i+2n}\right) \\
&+\tilde{\gamma}_{2i-1}\tilde{\gamma}_{2i}\tilde{\gamma}_{2i-1+2n}\tilde{\gamma}_{2i+2n}.
\end{aligned}
\tag{A.21}
$$

The second equality is obatined by expanding the product into 16 terms, doing contractions using the anti-commutation rules and rearrangement.

Substitute γ_i with θ_i, γ_{i+2n} with η_i and let $\tilde{\theta}_{2i} \equiv \sum_a O_{2i,a}\theta_a$, $\tilde{\eta}_{2i} \equiv \sum_a O_{2i,a}\eta_a$, etc. One can write

$$
\begin{aligned}
&\left(\sigma^{\frac{1}{2}}\rho_I\sigma^{\frac{1}{2}}\right)(\theta,\eta) \\
=&\frac{1}{2^{3n}}\prod_{i=1}^{n}\left(\hat{I}-i\lambda_i^{(\sigma)}\tilde{\theta}_{2i-1}\tilde{\theta}_{2i}\right)\left(1+i\lambda_i^{(\sigma)}\tilde{\eta}_{2i-1}\tilde{\eta}_{2i}\right)\left(1+i\sqrt{1-\left(\lambda_i^{(\sigma)}\right)^2}\tilde{\theta}_{2i-1}\tilde{\eta}_{2i-1}\right) \\
&\times\left(1+i\sqrt{1-\left(\lambda_i^{(\sigma)}\right)^2}\tilde{\theta}_{2i}\tilde{\eta}_{2i}\right).
\end{aligned}
\tag{A.22}
$$

Comparing with (2.18), (2.23) and making use of (A.16), one can read out that the linear map $\mathcal{N}_3 : X \mapsto \sigma^{\frac{1}{2}} X \sigma^{\frac{1}{2}}$ corresponds to the Grassmann integral representation in Eq. (2.28).

One can also obtain $\sigma^{-\frac{1}{2}}$ by writing down an ansatz and calculating $\sigma^{-\frac{1}{2}}\sigma^{\frac{1}{2}} = I$. The result is

$$\sigma^{-\frac{1}{2}} = 2^{\frac{n}{2}} \prod_{i=1}^{n} \left(\sqrt{1 - \left(\lambda_i^{(\sigma)}\right)^2} \right)^{-\frac{1}{2}} \left(\sqrt{1 + \left(\lambda_i^{(\sigma^{\frac{1}{2}})}\right)^2} \right)^{-\frac{1}{2}} \left(1 + i\lambda_i^{(\sigma^{\frac{1}{2}})} \tilde{\gamma}_{2i-1}\tilde{\gamma}_{2i}\right). \quad \text{(A.23)}$$

After a similar calculation, one can verify that $\mathcal{N}_1 : X \mapsto \mathcal{N}(\sigma)^{-\frac{1}{2}} X \mathcal{N}(\sigma)^{-\frac{1}{2}}$ has the Grassmann integral representation which is specified in Eq. (2.29).

A.2.3 Construction of $\mathcal{N}_2$

In this part we construct $\mathcal{N}_2$, which is the adjoint map of a given Gaussian quantum channel $\mathcal{N}$. We first consider the case when $\mathcal{N}$ is just a Gaussian map. If $\mathcal{N}$ is specified by matrices

A, B, D and complex number C, one can explicitly write

$$
\begin{aligned}
&\operatorname{tr}(X^\dagger \mathcal{N}(Y)) \\
=&C(-2)^n \int D\theta D\mu e^{\theta^T \mu} X(\theta) \int \exp[S(\mu,\eta) + i\eta^T \xi] Y(\xi) D\eta D\xi \\
=&C(-2)^n \int D\theta D\mu D\eta D\xi \exp[\theta^T \mu + i\eta^T \xi + \frac{i}{2}\mu^T A \mu + \frac{i}{2}\eta^T D\eta + i\mu^T B\eta] X^\dagger(\theta) Y(\xi) \\
=&C(-2)^n \int D\theta D\mu D\eta D\xi \exp[-i\theta^T \tilde{\mu} + \tilde{\eta}^T \xi - \frac{i}{2}\tilde{\mu}^T A\tilde{\mu} - \frac{i}{2}\tilde{\eta}^T D\tilde{\eta} - i\tilde{\mu}^T B\tilde{\eta}] X^\dagger(\theta) Y(\xi) \\
=&C(-2)^n \int D\theta D\tilde{\mu} D\tilde{\eta} D\xi \exp[-i\theta^T \tilde{\mu} + \tilde{\eta}^T \xi - \frac{i}{2}\tilde{\mu}^T A\tilde{\mu} - \frac{i}{2}\tilde{\eta}^T D\tilde{\eta} - i\tilde{\mu}^T B\tilde{\eta}] X^\dagger(\theta) Y(\xi) \\
=&(-2)^n \int D\tilde{\eta} D\xi e^{\tilde{\eta}^T \xi} \left(C \int \exp[i\tilde{\mu}^T \theta - \frac{i}{2}\tilde{\mu}^T A\tilde{\mu} - \frac{i}{2}\tilde{\eta}^T D\tilde{\eta} - i\tilde{\mu}^T B\tilde{\eta}] X^\dagger(\theta) D\tilde{\mu} D\theta \right) Y(\xi) \\
\equiv&\operatorname{tr}(\mathcal{N}^*(X)^\dagger Y).
\end{aligned}
\tag{A.24}
$$

In the third line we relabel $\tilde{\mu}_i = i\mu_i$, $\tilde{\eta}_i = i\eta_i$. The third line goes to the fourth because the measure is changed by a factor $i^{-4n} = 1$. Note that $\exp[S(\mu,\eta) + i\eta^T \xi]$ and integral measures are even in Grassmann numbers, so $X^\dagger(\theta)$ is interchangeable with these pieces. However $X^\dagger(\theta)$ and $Y(\xi)$ are arbitrary operators, so are not interchangeable.

The Grassmann variables are mapped from Majorana operators which are hermitian, so they should be real. Since $(D\theta)^\dagger = d\theta_1 \ldots d\theta_{2n} = (-1)^{n(2n-1)} D\theta$, the hermitian conjugate of $D\tilde{\mu} D\theta$ gives an overall factor of $(-1)^{2n(2n-1)} = 1$. One gets

$$
\begin{aligned}
\mathcal{N}^*(X)(\tilde{\eta}) &= \left(C \int \exp[i\tilde{\mu}^T \theta - \frac{i}{2}\tilde{\mu}^T A\tilde{\mu} - \frac{i}{2}\tilde{\eta}^T D\tilde{\eta} - i\tilde{\mu}^T B\tilde{\eta}] X^\dagger(\theta) D\tilde{\mu} D\theta \right)^\dagger \\
&= C^\dagger \int \exp[i\tilde{\mu}^T \theta + \frac{i}{2}\tilde{\mu}^T A^\dagger \tilde{\mu} + \frac{i}{2}\tilde{\eta}^T D^\dagger \tilde{\eta} + i\tilde{\eta}^T B^\dagger \tilde{\mu}] X(\theta) D\tilde{\mu} D\theta.
\end{aligned}
\tag{A.25}
$$

Comparing with Eq. (2.17) and Eq. (2.18), we get

$$A_{\mathcal{N}^*} = D^\dagger, B_{\mathcal{N}^*} = B^\dagger, C_{\mathcal{N}^*} = C^\dagger, D_{\mathcal{N}^*} = A^\dagger. \tag{A.26}$$

According to Eq. (2.32), $\mathcal{N}^*$ as the adjoint of a quantum channel is obviously unital as $A_2 = 0$, $C_2 = 1$. To see it is completely positive, note

$$N_2 = \begin{pmatrix} 0 & B^T \\ -B & -A \end{pmatrix} = \begin{pmatrix} 0 & 1 \\ 1 & 0 \end{pmatrix} \begin{pmatrix} -A & -B \\ B^T & 0 \end{pmatrix} \begin{pmatrix} 0 & 1 \\ 1 & 0 \end{pmatrix} = -JNJ \tag{A.27}$$

where $J \equiv \begin{pmatrix} 0 & 1 \\ 1 & 0 \end{pmatrix}$,

$$N_2^T N_2 = JN^T NJ \leq J^2 = I. \tag{A.28}$$

So the adjont map of a completely positive map is still completely positive.

A.2.4 Composition of three maps

Substitute Eq. (2.33) into Eq. (2.35), one explicitly gets

$$
\begin{aligned}
A_{2\circ 1} &= -B^T \left(A + \left(G^{(\sigma)}\right)^{-1}\right)^{-1} B, \\
B_{2\circ 1} &= B^T \left(A + \left(G^{(\mathcal{N}(\sigma))}\right)^{-1}\right)^{-1} \left(G^{(\mathcal{N}(\sigma))}\right)^{-1} \sqrt{I_{2n} + \left(G^{(\mathcal{N}(\sigma))}\right)^2}, \\
C_{2\circ 1} &= 2^n \det\left(I_{2n} + \left(G^{(\mathcal{N}(\sigma))}\right)^2\right)^{-\frac{1}{2}} (-1)^n \mathrm{Pf}\left(-G^{(\mathcal{N}(\sigma))}\right) \mathrm{Pf}\left(-A - \left(G^{(\mathcal{N}(\sigma))}\right)^{-1}\right), \\
D_{2\circ 1} &= G^{(\mathcal{N}(\sigma))} - \sqrt{I_{2n} + \left(G^{(\mathcal{N}(\sigma))}\right)^2} A \left(A + \left(G^{(\mathcal{N}(\sigma))}\right)^{-1}\right)^{-1} \left(G^{(\mathcal{N}(\sigma))}\right)^{-1} \sqrt{I_{2n} + \left(G^{(\mathcal{N}(\sigma))}\right)^2}.
\end{aligned}
\tag{A.29}
$$

The following pieces are useful for further calculations:

$$
\begin{aligned}
-D_3 - A_{2\circ 1}^{-1} &= \left(B^T \left(A + \left(G^{(\mathcal{N}(\sigma))}\right)^{-1}\right)^{-1} B\right)^{-1} + G^{(\sigma)} \\
&= B^{-1} \left(A + \left(G^{(\mathcal{N}(\sigma))}\right)^{-1} + B G^{(\sigma)} B^T\right) \left(B^T\right)^{-1} \\
&= B^{-1} \left(\left(G^{(\mathcal{N}(\sigma))}\right)^{-1} + G^{(\mathcal{N}(\sigma))}\right) \left(B^T\right)^{-1}, \\
A_{2\circ 1}^{-1} B_{2\circ 1} &= -B^{-1} \left(A + \left(G^{(\mathcal{N}(\sigma))}\right)^{-1}\right) \left(B^T\right)^{-1} B^T \left(A + \left(G^{(\mathcal{N}(\sigma))}\right)^{-1}\right)^{-1} \\
&\times \left(G^{(\mathcal{N}(\sigma))}\right)^{-1} \sqrt{I_{2n} + \left(G^{(\mathcal{N}(\sigma))}\right)^2} \\
&= -B^{-1} \left(G^{(\mathcal{N}(\sigma))}\right)^{-1} \sqrt{I_{2n} + \left(G^{(\mathcal{N}(\sigma))}\right)^2}.
\end{aligned}
\tag{A.30}
$$

One can then explicitly calculate

$$
\begin{aligned}
A_{\mathcal{P}} &= A_3 + B_3 \left(D_3 + A_{2\circ 1}^{-1}\right)^{-1} B_3^T \\
&= G - \sqrt{I_{2n} + \left(G^{(\sigma)}\right)^2} B^T \left(\left(G^{(\mathcal{N}(\sigma))}\right)^{-1} + G^{(\mathcal{N}(\sigma))}\right)^{-1} B \sqrt{I_{2n} + \left(G^{(\sigma)}\right)^2}, && \text{(A.31a)} \\
B_{\mathcal{P}} &= B_3 \left(D_3 + A_{2\circ 1}^{-1}\right)^{-1} A_{2\circ 1}^{-1} B_{2\circ 1} = \sqrt{I_{2n} + \left(G^{(\sigma)}\right)^2} B^T \left(\sqrt{I_{2n} + \left(G^{(\mathcal{N}(\sigma))}\right)^2}\right)^{-1}, && \text{(A.31b)} \\
C_{\mathcal{P}} &= \det \left(I_{2n} + \left(G^{(\mathcal{N}(\sigma))}\right)^2\right)^{-\frac{1}{2}} \mathrm{Pf}\left(-G^{(\mathcal{N}(\sigma))}\right) \\
&\times \mathrm{Pf}\left(-A - \left(G^{(\mathcal{N}(\sigma))}\right)^{-1}\right) \mathrm{Pf}\left(-B^T \left(A + \left(G^{(\mathcal{N}(\sigma))}\right)^{-1}\right)^{-1} B\right) \\
&\times \mathrm{Pf}\left(\left(-B^T \left(A + \left(G^{(\mathcal{N}(\sigma))}\right)^{-1}\right)^{-1} B\right)^{-1} - G^{(\sigma)}\right), && \text{(A.31c)} \\
D_{\mathcal{P}} &= D_{2\circ 1} + B_{2\circ 1}^T D_3 \left(D_3 + A_{2\circ 1}^{-1}\right)^{-1} A_{2\circ 1}^{-1} B_{2\circ 1} \\
&= G^{(\mathcal{N}(\sigma))} - \sqrt{I_{2n} + \left(G^{(\mathcal{N}(\sigma))}\right)^2} A \left(A + \left(G^{(\mathcal{N}(\sigma))}\right)^{-1}\right)^{-1} \left(G^{(\mathcal{N}(\sigma))}\right)^{-1} \sqrt{I_{2n} + \left(G^{(\mathcal{N}(\sigma))}\right)^2} \\
&- \sqrt{I_{2n} + \left(G^{(\mathcal{N}(\sigma))}\right)^2} \left(I_{2n} + A G^{(\mathcal{N}(\sigma))}\right)^{-1} B G^{(\sigma)} B^T \left(\sqrt{I_{2n} + \left(G^{(\mathcal{N}(\sigma))}\right)^2}\right)^{-1} \\
&= -\left(G^{(\mathcal{N}(\sigma))}\right)^{-1} + \sqrt{I_{2n} + \left(G^{(\mathcal{N}(\sigma))}\right)^2} \left(G^{(\mathcal{N}(\sigma))}\right)^{-1} \left(A + \left(G^{(\mathcal{N}(\sigma))}\right)^{-1}\right)^{-1} \\
&\times \left(G^{(\mathcal{N}(\sigma))}\right)^{-1} \sqrt{I_{2n} + \left(G^{(\mathcal{N}(\sigma))}\right)^2} \\
&- \sqrt{I_{2n} + \left(G^{(\mathcal{N}(\sigma))}\right)^2} \left(G^{(\mathcal{N}(\sigma))}\right)^{-1} \left(A + \left(G^{(\mathcal{N}(\sigma))}\right)^{-1}\right)^{-1} \left(G^{(\mathcal{N}(\sigma))} - A\right) \\
&\times \left(I_{2n} + \left(G^{(\mathcal{N}(\sigma))}\right)^2\right)^{-1} \sqrt{I_{2n} + \left(G^{(\mathcal{N}(\sigma))}\right)^2} \\
&= -\left(G^{(\mathcal{N}(\sigma))}\right)^{-1} + \sqrt{I_{2n} + \left(G^{(\mathcal{N}(\sigma))}\right)^2} \left(G^{(\mathcal{N}(\sigma))}\right)^{-1} \left(I_{2n} + \left(G^{(\mathcal{N}(\sigma))}\right)^2\right)^{-1} \sqrt{I_{2n} + \left(G^{(\mathcal{N}(\sigma))}\right)^2} \\
&= 0. && \text{(A.31d)}
\end{aligned}
$$

$C_{\mathcal{P}}$ can be calculated by first calculating its square as $\mathrm{Pf}\,(A)^2 = \det(A)$. It's straightforward then that $C_{\mathcal{P}}^2 = 1$. We choose $C_{\mathcal{P}} = 1$ because the composition of completely positive maps should still be completely positive. So one can verify that $A_{\mathcal{P}}$, $B_{\mathcal{P}}$, $C_{\mathcal{P}}$ and $D_{\mathcal{P}}$ are indeed as specified in Eq. (2.36). With $C_{\mathcal{P}} = 1$ and $D_{\mathcal{P}} = 0$, it is explicit that the Petz recovery map is trace preserving.

A.2.5 Fidelity calculation

We can obtain the Grassmann representation of $\sigma^{\frac{1}{2}}\rho\sigma^{\frac{1}{2}}$ by direct calculation,

$$\begin{aligned}\sigma^{\frac{1}{2}}\rho\sigma^{\frac{1}{2}}(\theta) =& C\int \exp[S(\theta,\eta) + i\eta^T\mu]\frac{1}{2^n}\exp\left(\frac{i}{2}\mu^T G^{(\rho)}\mu\right) D\eta D\mu \\ =& \frac{(-1)^n}{2^{2n}}\text{Pf}(G^{(\rho)})\text{Pf}(G^{(\rho)-1} - G^{(\sigma)})\exp\left(\frac{i}{2}\theta^T G^{(\sigma^{\frac{1}{2}}\rho\sigma^{\frac{1}{2}})}\theta\right),\end{aligned} \tag{A.32}$$

in which S, C are specified in Eq. (2.28) and

$$G^{(\sigma^{\frac{1}{2}}\rho\sigma^{\frac{1}{2}})} \equiv G^{(\sigma)} + \sqrt{I + G^{(\sigma)2}}\left(G^{(\rho)-1} - G^{(\sigma)}\right)^{-1}\sqrt{I + G^{(\sigma)2}}. \tag{A.33}$$

Note that

$$\begin{aligned}&\sqrt{I_{2n} + (G^{(\sigma)})^2}\left(G^{(\rho)-1} - G^{(\sigma)}\right)^{-1}\sqrt{I_{2n} + (G^{(\sigma)})^2} + G^{(\sigma)} \\ =&\sqrt{I_{2n} + (G^{(\sigma)})^2}\left(\left(G^{(\rho)-1} - G^{(\sigma)}\right)^{-1} + \left(G^{(\sigma)} + (G^{(\sigma)})^{-1}\right)^{-1}\right)\sqrt{I_{2n} + (G^{(\sigma)})^2} \\ =&\sqrt{I_{2n} + (G^{(\sigma)})^2}\left(G^{(\sigma)} + (G^{(\sigma)})^{-1}\right)^{-1}\left((G^{(\rho)})^{-1} + (G^{(\sigma)})^{-1}\right)\left((G^{(\rho)})^{-1} - G^{(\sigma)}\right)^{-1}\sqrt{I_{2n} + (G^{(\sigma)})^2} \\ =&\left(\sqrt{I_{2n} + (G^{(\sigma)})^2}\right)^{-1}\left(G^{(\sigma)} + G^{(\rho)}\right)\left(I_{2n} - G^{(\sigma)}G^{(\rho)}\right)^{-1}\sqrt{I_{2n} + (G^{(\sigma)})^2}.\end{aligned} \tag{A.34}$$

We denote $\delta \equiv \sqrt{\sigma^{\frac{1}{2}}\rho\sigma^{\frac{1}{2}}}$, so

$$\delta(\theta) = \left(\frac{(-1)^n}{2^{2n}}\mathrm{Pf}(G^{(\rho)})\mathrm{Pf}(G^{(\rho)-1} - G^{(\sigma)})\right)^{\frac{1}{2}} \prod_{i=1}^{n} \frac{1}{\sqrt{1+\lambda^{(\delta)2}}} \exp\left(\frac{i}{2}\theta^T G^{(\delta)}\theta\right). \tag{A.35}$$

By applying Eq. (A.16) to Eq. (2.27), we get

$$G^{(\delta)} = \left(G^{(\sigma^{\frac{1}{2}}\rho\sigma^{\frac{1}{2}})}\right)^{-1}\left(\sqrt{I + \left(G^{(\sigma^{\frac{1}{2}}\rho\sigma^{\frac{1}{2}})}\right)^2} - I\right). \tag{A.36}$$

The fidelity of two states ρ and σ is merely the trace of the operator δ. Since only the coefficient of $\hat{I}$ in Eq. (2.7) or (2.9) contributes to the trace via $\alpha_X = 2^{-n}\mathrm{tr}X$, we focus on that coefficient

$$\begin{aligned}
&\left(\frac{(-1)^n}{2^{2n}}\mathrm{Pf}(G^{(\rho)})\mathrm{Pf}(G^{(\rho)-1} - G^{(\sigma)})\right)^{\frac{1}{2}} \prod_{i=1}^{n} \frac{1}{\sqrt{1+\lambda^{(\delta)2}}} \\
=&\frac{1}{2^n}\det(I - G^{(\rho)}G^{(\sigma)})^{\frac{1}{4}} \det\left(I - G^{(\delta)2}\right)^{-\frac{1}{4}} \\
=&\frac{1}{2^n}\det(I - G^{(\rho)}G^{(\sigma)})^{\frac{1}{4}} \det\left(\frac{1}{2}\left(I + \sqrt{I + \left(G^{(\sigma^{\frac{1}{2}}\rho\sigma^{\frac{1}{2}})}\right)^2}\right)\right)^{\frac{1}{4}} \\
=&\frac{1}{2^n}\det(I - G^{(\rho)}G^{(\sigma)})^{\frac{1}{4}} \det\left(\frac{1}{2}\left(I + \sqrt{I + \left(\tilde{G}^{(\sigma\rho)}\right)^2}\right)\right)^{\frac{1}{4}}.
\end{aligned} \tag{A.37}$$

The last line makes use of Eq. (A.34). Noting that the dimension of I is $2n$, we arrive at the final result in Eq. (2.43).

A.3 Treatment of Singular Matrices

As part of the construction of the Petz recovery map and the derivation of the fidelity formula, the inverses of several matrices appear. In the calculations in Appendix (A.2), we assumed all relevant matrices to be invertible. Here these assumptions are analyzed.

A.3.1 Singular matrices in the construction of Petz recovery map

As discussed in Section.(2.2), we assume

$$G^{(\mathcal{N}(\sigma))},\ A+\left(G^{(\mathcal{N}(\sigma))}\right)^{-1},\ B^T\left(A+\left(G^{(\mathcal{N}(\sigma))}\right)^{-1}\right)^{-1}B,\ \left(B^T\left(A+\left(G^{(\mathcal{N}(\sigma))}\right)^{-1}\right)^{-1}B\right)^{-1}+G^{(\sigma)} \tag{A.38}$$

are invertible ($1'-4'$). We claimed $1'-4'$ is equivalent to assuming

$$G^{(\mathcal{N}(\sigma))},\quad A+\left(G^{(\mathcal{N}(\sigma))}\right)^{-1},\quad B,\quad I+\left(G^{(\mathcal{N}(\sigma))}\right)^{2} \tag{A.39}$$

are invertible ($1-4$). The equivalence between $1-3$ and $1'-3'$ is obvious. Eq. (A.30) shows $1'-4'$ implies that $\left(G^{(\mathcal{N}(\sigma))}+\left(G^{(\mathcal{N}(\sigma))}\right)^{-1}\right)$ is invertible, which is equivalent to 4 with the help of $1'$. One can show $1-4$ implies $4'$ just by reversing the derivation in Eq. (A.30). So $1'-4'$ and $1-4$ are equivalent. We work with $1-4$ hereafter.

We next show that $1,3$ or $1,4$ imply 2. A neccessary condition for $\mathcal{N}$ to be completely positive is $A^TA+BB^T\leq I$. If B is invertible, then we have $A^TA<I-BB^T<I$, so $||A||<1$. However, since $||G^{(\mathcal{N}(\sigma))}||\leq 1$, $||\min\lambda^{\left(G^{(\mathcal{N}(\sigma))}\right)^{-1}}||\geq 1$, $A+\left(G^{(\mathcal{N}(\sigma))}\right)^{-1}$ can not have zero eigenvalue so it is invertible. In general $||A||\leq 1$, and $||\min\lambda^{\left(G^{(\mathcal{N}(\sigma))}\right)^{-1}}||>1$

when $I+\left(G^{(\mathcal{N}(\sigma))}\right)^2$ is invertible. So $A+\left(G^{(\mathcal{N}(\sigma))}\right)^{-1}$ is invertible for the same reason. So the independent assumptions are $1, 3$ and 4.

We first assume that $I+\left(G^{(\mathcal{N}(\sigma))}\right)^2$ is invertible. The construction of the Petz recovery map, i.e., given $G^{(\sigma)}$, A, B(or equivalently $G^{(\sigma)}$, B, $G^{(\mathcal{N}(\sigma))}$), find $A_{\mathcal{P}}$, $B_{\mathcal{P}}$, $C_{\mathcal{P}}$ and $D_{\mathcal{P}}$, can be viewed as a function $\mathbb{R}^{12n^2} \to \mathbb{R}^{4n^2}$ for $A_{\mathcal{P}}$, $B_{\mathcal{P}}$, $D_{\mathcal{P}}$ and $\mathbb{R}^{12n^2} \to \mathbb{R}$ for $C_{\mathcal{P}}$. The matrix multiplication is continuous in its entries just by the continuity of multiplication and adddition. The matrix inverse is known to be continuous when the inverse exists[106].[1] So the function $\left(G^{(\sigma)}, B, G^{(\mathcal{N}(\sigma))}\right) \to (A_{\mathcal{P}}, B_{\mathcal{P}}, C_{\mathcal{P}}, D_{\mathcal{P}})$ is continuous when $I+\left(G^{(\mathcal{N}(\sigma))}\right)^2$ is invertible. This continuity guarantees that if we do perturbation $G^{(\mathcal{N}(\sigma))} \to G^{(\mathcal{N}(\sigma))}(\epsilon_1)$, $B \to B(\epsilon_2)$ so that $G^{(\mathcal{N}(\sigma))}(\epsilon_1)$ and $B(\epsilon_2)$ are invertible, then carry on the derivation in Appendix (A.2.4), and finally take the limit $\epsilon_1 \to 0$ and $\epsilon_2 \to 0$, we will get a well-defined result as in Eq. (2.36).

We then turn to the assumption 4. As is shown in Eq.(A.23), if 4 does not apply, $\mathcal{N}(\sigma)^{-\frac{1}{2}}$ is not well-defined and $\mathcal{N}(\sigma)$ can be written as $\mathcal{N}(\sigma)_A \otimes |\psi^{(\mathcal{N}(\sigma))}\rangle\langle\psi^{(\mathcal{N}(\sigma))}|_{\bar{A}}$. Here A is some region in the full Hilbert space $\mathcal{H}$ while $\bar{A}$ is its complement. In this case $\mathcal{N}(\sigma)$ only have support on A. This contradicts with the assumption in [11, 12] that the state $\mathcal{N}(\sigma)$ is faithful, which means $\operatorname{tr}(\mathcal{O}\mathcal{N}(\sigma)) = 0$ does not imply $\mathcal{O} = 0$. So usually we assume that $\mathcal{N}(\sigma)^{-\frac{1}{2}}$ is well-defined. If $\mathcal{N}(\sigma)$ takes the form of $\mathcal{N}(\sigma)_A \otimes |\psi^{(\mathcal{N}(\sigma))}\rangle\langle\psi^{(\mathcal{N}(\sigma))}|_{\bar{A}}$, we can still determine the form of the Petz recovery map on A.[9, 17]

One might worry that if $I+\left(G^{(\mathcal{N}(\sigma))}\right)^2$ approaches a singular limit, then $B_{\mathcal{P}}$ or $A_{\mathcal{P}}$ could be unbounded in Eq. (2.36). Actually $B_{\mathcal{P}}$ will still be bounded, as well as $A_{\mathcal{P}}$. This can be argued by the complete positive of the composite of completely positivity maps. We give a

[1] By continuity of matrix calculation we mean that each entry of the output matrix when viewed as a multivariable function of the entries of the input matrices is continuous.

detailed analysis here. To simplify the discussion, when $I + \left(G^{(\mathcal{N}(\sigma))}\right)^2$ is singular, we take $\mathcal{N}(\sigma) = |\psi^{(\mathcal{N}(\sigma))}\rangle\langle\psi^{(\mathcal{N}(\sigma))}|_{\mathcal{H}}$ and the discussion can be easily generalized. We first consider the case that σ has full support on $\mathcal{H}$.[2] We can show that a valid quantum channel that takes such σ to $\mathcal{N}(\sigma)$ can only be a swap, i.e. $B = 0$ and $A = G^{(\mathcal{N}(\sigma))}$. Consider the monotonicity of the relative entropy. $S(\rho||\sigma) \geq S(\mathcal{N}(\rho)||\mathcal{N}(\sigma))$ actually implies that if supp$(\rho) \subseteq$ supp(σ), then supp$(\mathcal{N}(\rho)) \subseteq$ supp$(\mathcal{N}(\sigma))$. Because otherwise the RHS is $+\infty$ while the LHS is finite so the inequality does not hold. However, since $\mathcal{N}(\sigma) = |\psi^{(\mathcal{N}(\sigma))}\rangle\langle\psi^{(\mathcal{N}(\sigma))}|_{\mathcal{H}}$ is pure, for any ρ with supp$(\rho) \subseteq$ supp(σ), $\mathcal{N}(\rho) = \mathcal{N}(\sigma)$. Since ρ is arbitrary, we can conclude that the only quantum channel that does the job is the swap described above. So in the formula for $B_{\mathcal{P}}$, B^T is strictly a zero matrix so $B_{\mathcal{P}} = 0$ regardless of the singularity of $I + \left(G^{(\mathcal{N}(\sigma))}\right)^2$. If σ is a different pure state from $\mathcal{N}(\sigma)$, then B is an orthogonal matrix with $BB^T = I$. A proper limiting procedure (for example as described in the last part of Appendix (A.1)) shows that $B_{\mathcal{P}} = B^T$, which means that the recovery map rotates the state back. If σ and $\mathcal{N}(\sigma)$ are two identical pure states, we can still show that for each mode $B_{\mathcal{P}} = B^T, A_{\mathcal{P}} = 0$ or $B_{\mathcal{P}} = 0, A_{\mathcal{P}} = G^{(\mathcal{N}(\sigma))}$. So in any case $B_{\mathcal{P}}$ is bounded and so is $A_{\mathcal{P}}$.

A.3.2 Singular matrices in the derivation of fidelity formula

As presented in (A.2.5), in the derivation of the fidelity formula, we assume that $G^{(\rho)}$ and $I - G^{(\sigma)}G^{(\rho)}$ are invertible. If we make use of Eq. (A.34), we might as well assume that $G^{(\sigma)}$ and $\sqrt{I + (G^{(\sigma)})^2}$ are invertible. However, as discussed in Eq. (A.13) and in (A.3.1), the continuity property of the Grassmann integral and the final form guarantees that Eq. (2.43) is well-defined

[2] This depends on the choice of the family of states θ discussed in the introduction. We can always choose σ to be the state with the largest support in the family θ. If σ is mixed in some region in Hilbert space A, and pure in its complementary $\bar{A}$, then the considerations below apply for A and $\bar{A}$ respectively and $B_{\mathcal{P}}$ is still bounded.

by a limiting treatment if $G^{(\sigma)}$, $G^{(\rho)}$ or $\sqrt{I + (G^{(\sigma)})^2}$ are singular. So the physical one is the singularity of the matrix $I - G^{(\sigma)}G^{(\rho)}$.[3]

We can show that $I - G^{(\sigma)}G^{(\rho)}$ being singular implies the fidelity $F(\rho, \sigma) = 0$. One can make use of the trace formula Eq. (A.6a) to calculate

$$
\begin{aligned}
&\mathrm{tr}(\rho\sigma) \\
=&\frac{(-2)^n}{2^{2n}} \int D\theta D\mu e^{\theta^T \mu} \exp\left(\frac{i}{2}\theta^T G^{(\rho)}\theta\right) \exp\left(\frac{i}{2}\mu^T G^{(\sigma)}\mu\right) \\
=&\frac{1}{2^n}\mathrm{Pf}(G^{(\rho)})\mathrm{Pf}(G^{(\rho)-1} - G^{(\sigma)}) = \frac{1}{2^n}\det\left(I - G^{(\rho)}G^{(\sigma)}\right)^{\frac{1}{2}}.
\end{aligned}
\tag{A.40}
$$

So when $I - G^{(\sigma)}G^{(\rho)}$ is singular, we have $\mathrm{tr}(\rho\sigma) = 0$. However $\mathrm{tr}(\rho\sigma) = \mathrm{tr}(\sigma^{\frac{1}{2}}\rho\sigma^{\frac{1}{2}})$ and $\sigma^{\frac{1}{2}}\rho\sigma^{\frac{1}{2}}$ is a positive semidefinite operator so all its eigenvalues $\lambda_i^{(\sigma^{\frac{1}{2}}\rho\sigma^{\frac{1}{2}})} \geq 0$. So $\mathrm{tr}(\sigma^{\frac{1}{2}}\rho\sigma^{\frac{1}{2}}) = 0$ implies that $\sigma^{\frac{1}{2}}\rho\sigma^{\frac{1}{2}} = 0$ since the only case is that all its eigenvalues are 0. Then naturally its square root is 0 so the fidelity $F(\rho, \sigma) = 0$.

[3]Equivalently $I - G^{(\rho)}G^{(\sigma)}$, as they share the same spectrum.

Appendix B: Supplementary materials of Chapter 3

B.1 Isometric embedding

We work with $\sigma \in \mathcal{A}_\star$ faithful which implies that $\sigma \circ \iota \in \mathcal{B}_\star$ is faithful. Thus the corresponding vectors $|\xi_\sigma^{\mathcal{A}}\rangle, |\xi_\sigma^{\mathcal{B}}\rangle$ in the natural cones are cyclic and separating. By a trivial calculation, one sees that V_σ defined in (3.16) is a norm-preserving (densely defined) map from $\mathscr{K}$ to $\mathscr{H}$. So the map extends to the full Hilbert space as an isometric embedding $V_\sigma^* V_\sigma = 1_{\mathscr{K}}$. A similar argument shows that:

$$V_\sigma V_\sigma^* = \pi_{\mathscr{K}} \in B(\mathscr{H}) \tag{B.1}$$

where this equation applies on the subspace of $\mathscr{H}$ that is generated by $\mathcal{B}$:

$$\overline{\iota(\mathcal{B})\,|\xi_\sigma^{\mathcal{A}}\rangle} = \pi_{\mathscr{K}}\mathscr{H} \equiv \pi^{\mathcal{B}'}(\sigma)\mathscr{H} \tag{B.2}$$

In other words, $|\xi_\sigma^{\mathcal{A}}\rangle$ is not cyclic for $\iota(\mathcal{B})$ and $\pi^{\mathcal{B}'}(\sigma)$ defines the associated support projector for the commutant algebra.

The embedding satisfies:

$$V_\sigma b\,|\chi\rangle = bV_\sigma\,|\chi\rangle\ , \qquad \chi \in \mathscr{K}\ , \qquad b \in \mathcal{B} \tag{B.3}$$

since we can approximate any $|\chi\rangle = \lim_n c_n \left|\xi_\sigma^{\mathcal{B}}\right\rangle \in \mathscr{K}$ for suitable $c_n \in \mathcal{B}$, and take the limit on both sides of:

$$V_\sigma b c_n \big|\xi_\sigma^{\mathcal{B}}\big\rangle = \iota(bc_n)\,|\xi_\sigma\rangle = \iota(b)\iota(c_n)\,|\xi_\sigma\rangle = \iota(b)V_\sigma c_n\big|\xi_\sigma^{\mathcal{B}}\big\rangle. \tag{B.4}$$

Thus,

$$\langle\chi_1|\, V_\sigma^* \iota(b) V_\sigma\, |\chi_2\rangle = \langle\chi_1|\, V_\sigma^* V_\sigma b\, |\chi_2\rangle = \langle\chi_1|\, b\, |\chi_2\rangle \tag{B.5}$$

for all vectors $|\chi_{1,2}\rangle \in \mathscr{K}$, or:

$$V_\sigma^* \iota(\mathcal{B}) V_\sigma = \mathcal{B}. \tag{B.6}$$

The commutant satisfies:

$$V_\sigma^* \mathcal{A}' V_\sigma \subset \mathcal{B}' \tag{B.7}$$

which can be verified via a short calculation for $a' \in \mathcal{A}'$ and $b \in \mathcal{B}$:

$$[V_\sigma^* a' V_\sigma, b] = [V_\sigma^* a' V_\sigma, V_\sigma^* \iota(b) V_\sigma] = V_\sigma^* \left[\pi_{\mathscr{K}} a' \pi_{\mathscr{K}}, \iota(b)\right] V_\sigma = 0 \tag{B.8}$$

where we used the fact that $\pi_{\mathscr{K}} \in \iota(\mathcal{B})'$ and $\mathcal{A}' \subset \iota(\mathcal{B})'$.

B.2 Fidelity

B.2.1 Proof of Lemma 3.2.1 (Fidelity and the Araki-Masuda norm)

Proof. (1) In this proof, all L_1 norms are taken relative to the commutant $\mathcal{A}'$ as in

$$\|\phi\|_{1,\psi} = \inf_{\chi \in \mathscr{H} : \|\chi\| = 1, \pi'(\chi) \geq \pi'(\phi)} \|(\Delta'_{\chi,\psi})^{-1/2}\phi\|, \tag{B.9}$$

from (3.59), and we want to relate this to the fidelity,

$$F(\omega_\psi, \omega_\phi) = \sup_{x' \in \mathcal{A}' : \|x\| \leq 1} |\langle\psi| \, x' \, |\phi\rangle| \tag{B.10}$$

where ϕ, ψ are normalized vectors. This relation is proven in [70], lem. 5.3 for a cyclic and separating vector $|\psi\rangle$. We will now remove this condition. The linear functional that appears in (B.10) $\mathcal{A}'$ can be written using a polar decomposition

$$\langle\psi| \cdot |\phi\rangle = \langle\xi| \; \cdot \; u' \, |\xi\rangle \tag{B.11}$$

for some ξ in the natural cone and a partial isometry u' with initial support $(u')^* u' = \pi'(\xi)$. This polar decomposition has the property that the largest projector in $\mathcal{A}'$ that satisfies $\langle\xi| \, x'p'u' \, |\xi\rangle = 0$ for all x' is $p' = 1 - \pi'(u'\xi) = 1 - u'(u')^*$.[1] Thus:

$$\langle\psi| \, x'(1 - u'(u')^*) \, |\phi\rangle = 0 \,, \quad \forall x' \in \mathcal{A}' \tag{B.12}$$

and since $\overline{\mathcal{A}' \, |\psi\rangle} = \pi(\psi)\mathscr{H}$ we derive that the final support projector satisfies:

$$(1 - u'(u')^*) \, |\phi\rangle \in (1 - \pi(\psi))\mathscr{H} \tag{B.13}$$

[1] Proof: Certainly $1 - u'(u')^*$ satisfies this. Suppose p' is larger and still satisfies this. Pick $x' = (u')^*$, then $\langle\xi| \, (u')^* p' u' \, |\xi\rangle = 0$, but then $p' \leq 1 - \pi'(u'\xi)$ which is a contradiction. Note that the largest projector in $\mathcal{A}'$ that satisfies $\langle\xi| \, p'x'u' \, |\xi\rangle = 0$ for all x' is $p' = 1 - \pi'(\xi) = 1 - (u')^* u'$.

Consider

$$
\begin{aligned}
((x')^* |\psi\rangle , (u')^* |\phi\rangle) &= (|\xi\rangle , \pi'(\psi)x'\pi'(\xi) |\xi\rangle) = (|\xi\rangle , \pi'(\psi)x' |\xi\rangle) \\
&= \big(J(\Delta'_{\xi,\psi})^{1/2} |\psi\rangle , J(\Delta'_{\xi,\psi})^{1/2}(x')^* |\psi\rangle\big) \\
&= \big((\Delta'_{\xi,\psi})^{1/2}(x')^* |\psi\rangle , (\Delta'_{\xi,\psi})^{1/2} |\psi\rangle\big)
\end{aligned} \tag{B.14}
$$

where in the second line we used (3.6) and in the third we used the anti-unitarity of J. The above relation can be rewritten as:

$$
((x')^* |\psi\rangle + |\zeta\rangle , \pi(\psi)(u')^* |\phi\rangle) = \big((\Delta'_{\xi,\psi})^{1/2}((x')^* |\psi\rangle + |\zeta\rangle), (\Delta'_{\xi,\psi})^{1/2} |\psi\rangle\big) \tag{B.15}
$$

where we have freely added $\zeta \in (1 - \pi(\psi)\pi'(\xi))\mathscr{H}$ since $\pi(\psi)(u')^* |\phi\rangle$ is in the subspace $\pi(\psi)\pi'(\xi)\mathscr{H}$, and this subspace is also the support of $\Delta'_{\xi,\psi}$. Now since the vector on the left of (B.15) is dense: $\pi'(\xi)\overline{\mathcal{A} |\psi\rangle} + (1 - \pi(\psi)\pi'(\xi))\mathscr{H} = \mathscr{H}$ we learn that $(\Delta'_{\xi,\psi})^{1/2} |\psi\rangle$ is in the domain of $(\Delta'_{\xi,\psi})^{1/2}$ and

$$
\Delta'_{\xi,\psi} |\psi\rangle = \pi(\psi)(u')^* |\phi\rangle , \tag{B.16}
$$

so that

$$
u'\Delta'_{\xi,\psi} |\psi\rangle = \pi(\psi)u'(u')^* |\phi\rangle = \pi(\psi) |\phi\rangle , \tag{B.17}
$$

where we used (B.13). The next step is to show that

$$
\|\phi\|_{1,\psi} = \|\pi(\psi)\phi\|_{1,\psi} = \|u'\Delta'_{\xi,\psi}\psi\|_{1,\psi} = \|\xi\|^2, \tag{B.18}
$$

which implies that

$$\|\phi\|_{1,\psi} = \sup_{x' \in \mathcal{A}' : \|x'\| \leq 1} |\langle \xi | x' | \xi \rangle| = \sup_{x' \in \mathcal{A}' : \|x'\| \leq 1} |\langle \psi | x' | \phi \rangle| = F(\omega_\psi, \omega_\phi). \tag{B.19}$$

This is what we wanted to derive.

The later equality in (B.18) is fairly standard, but for completeness we go through this. Without loss of generality we take χ in (B.9) such that $u'\Delta'_{\xi,\psi} |\psi\rangle$ is in the domain of $(\Delta'_{\chi,\psi})^{-1/2}$ and also such that $\pi'(\chi) \geq \pi'(u'\Delta'_{\xi,\psi} |\psi\rangle) = \pi'(u'\xi)$ and $\| |\chi\rangle \| = 1$. We would like to use the following result that we will justify later (for now the reader should feel free to verify this for type-I algebras with density matrices):

$$(\Delta'_{\chi,\psi})^{-1/2} u' \Delta'_{\xi,\psi} |\psi\rangle = (\Delta'_{\chi,\xi})^{-1/2} u' |\xi\rangle = (\Delta'_{\chi,\xi})^{-1} j(u')^* |\chi\rangle \tag{B.20}$$

where $j(u') = Ju'J$ and all the domains in the above equation are appropriate. Now apply the Cauchy-Schwarz inequality:

$$\|\xi\|^2 = \|\pi'(\chi) u' \xi\|^2 = \|\Delta^{1/2}_{\xi,\chi} j(u')^* \chi\|^2 = \langle \chi | j(u') (\Delta'_{\chi,\xi})^{-1} j(u')^* |\chi\rangle \tag{B.21}$$

$$\leq \|(\Delta'_{\chi,\xi})^{-1} j(u')^* \chi\| \|j(u')^* \chi\| \leq \|(\Delta'_{\chi,\psi})^{-1/2} u' \Delta'_{\xi,\psi} \psi\|. \tag{B.22}$$

Taking the infimum over all such χ we find that:

$$\|\xi\|^2 \leq \|u' \Delta'_{\xi,\psi} \psi\|_{1,\psi} = \|\phi\|_{1,\psi}. \tag{B.23}$$

The other inequality is found since the optimal vector in the infimum is $|\chi\rangle = u' |\xi\rangle / \| |\xi\rangle \|$

where (B.20) becomes:

$$(\Delta'_{\chi,\psi})^{-1/2} u' \Delta'_{\xi,\psi} |\psi\rangle = u' |\xi\rangle \|\xi\| \tag{B.24}$$

which implies that:

$$\|\phi\|_{1,\psi} = \|u' \Delta'_{\xi,\psi} \psi\|_{1,\psi} \geq \|\xi\|^2 \tag{B.25}$$

and this establishes equality. We now only need to prove (B.20). To do this we will analytically continue the equation:

$$(\Delta'_{\chi,\psi})^{-z} u' (\Delta'_{\xi,\psi})^{z} |\xi\rangle = \pi(\psi)(\Delta'_{\chi,\xi})^{-z} u' (\Delta'_{\xi,\xi})^{z} |\xi\rangle = \pi(\psi)(\Delta'_{\chi,\xi})^{-z} u' |\xi\rangle \tag{B.26}$$

away from $z = is$ for s real. We simply take an inner product with a dense set of vectors $a |\chi\rangle + |\zeta\rangle$ where $a \in \mathcal{A}$ and $|\zeta\rangle \in (1 - \pi'(\chi))\mathscr{H}$:

$$\left((\Delta'_{\chi,\psi})^{-\bar{z}}(a|\chi\rangle + |\zeta\rangle), u'(\Delta'_{\xi,\psi})^{z} |\xi\rangle\right) = \left((\Delta'_{\chi,\xi})^{-\bar{z}} \pi(\psi)(a|\chi\rangle + |\zeta\rangle), u' |\xi\rangle\right) \tag{B.27}$$

since we know that $|\xi\rangle$ is in the domain of $(\Delta'_{\xi,\psi})^{1/2}$ (since we established that $|\psi\rangle$ is in the domain of $\Delta'_{\xi,\psi}$) it is clear that we can analytically continue the two functions above into the strip $0 < \mathrm{Re} z < 1/2$ with continuity in the closure (using standard results in Tomita-Takesaki theory.) Agreement along $z = is$ implies agreement in the full strip. Setting $z = 1/2$ we have a uniform bound (with $\|a |\chi\rangle \| \leq 1$) on the left hand side since we started with the assumption that the left hand side of (B.20) exists. On the right hand side this establishes the fact that $u' |\xi\rangle$ is in the domain $(\Delta'_{\chi,\xi})^{-1/2}$ and the first equality in (B.20). The second equality in (B.20) is immediate.

We have thus finished the proof that (B.9) and (B.10) are equal.

(2) Our next task is to show that it is sufficient to vary over unitaries in (B.10) and relate this to (3.62). Note that for a bounded operator we have the polar decomposition $x' = u'p'$ where u' is unitary and $\|p'\| \leq 1$. Such a self adjoint operator can always be written as $(v' + (v')^*)/2$ where $v' = p' + i\sqrt{1-(p')^2}$. So:

$$x' = \frac{1}{2}u'v' + \frac{1}{2}u'(v')^* = \frac{1}{2}w' + \frac{1}{2}y' \tag{B.28}$$

for unitaries $w', y' \in \mathcal{A}'$. Then $|\langle\psi| x' |\phi\rangle| \leq \frac{1}{2}(|\langle\psi| w' |\phi\rangle| + |\langle\psi| y' |\phi\rangle|)$. Thus

$$|\langle\psi| x' |\phi\rangle| \leq \sup_{u' \in \mathcal{A}' : u'(u')^* = 1} |\langle\psi| u' |\phi\rangle| \tag{B.29}$$

since the right hand side is larger than both terms with w' and y' above. Taking the sup over the left hand side:

$$\sup_{u' \in \mathcal{A}' : u'(u')^* \leq 1} |\langle\psi| u' |\phi\rangle| \leq \sup_{x' \in \mathcal{A}' : \|x'\| \leq 1} |\langle\psi| x' |\phi\rangle| \leq \sup_{u' \in \mathcal{A}' : u'(u')^* = 1} |\langle\psi| u' |\phi\rangle| \tag{B.30}$$

where the first inequalities is because the set of unitaries is a subset of operators bounded by 1. This implies equality and we see that the L_1 norm is equivalent to the Uhlmann fidelity of two linear functionals:

$$F(\omega_\psi, \omega_\phi) = \|\phi\|_{1,\psi}\,, \quad \omega_\psi = \langle\psi| \cdot |\psi\rangle\,, \quad \omega_\phi = \langle\phi| \cdot |\phi\rangle \in \mathcal{A}_\star. \tag{B.31}$$

Thus it is clear the fidelity is independent of the vector representation. We take the norms of ϕ, ψ to be 1.

(3) Finally, we want to relate the fidelity to the norm of the linear functional difference:

$$||\omega_\psi - \omega_\phi|| \equiv \sup_{x\in\mathcal{A};||x||\leq 1} |\omega_\psi(x) - \omega_\phi(x)| \tag{B.32}$$

Since $\mathcal{A} \subset B(\mathscr{H})$:

$$||\omega_\psi - \omega_\phi|| \leq \sup_{x\in B(\mathscr{H});||x||\leq 1} |\langle\psi| x |\psi\rangle - \langle\phi| (u')^* x u' |\phi\rangle| = 2\sqrt{1 - \left|\left\langle\psi\middle|u'\phi\right\rangle\right|^2} \tag{B.33}$$

We calculate the last equality as follows. The two normalized vectors $\psi, u'\phi$ live in a two dimensional subspace, which without loss of generality can be chosen as:

$$|\psi\rangle = \cos(\theta/2)\,|0\rangle + \sin(\theta/2)\,|1\rangle\ , \qquad u'\left|\phi\right\rangle = e^{i\varphi}(\sin(\theta/2)\,|0\rangle + \cos(\theta/2)\,|1\rangle) \tag{B.34}$$

where $\left\langle\psi\middle|u'\phi\right\rangle = e^{i\varphi}\sin(\theta)$. We can then take x to be an operator in this subspace. Note that:

$$|\psi\rangle\langle\psi| - \left|u'\phi\right\rangle\left\langle u'\phi\right| = \cos\theta\sigma_3 \tag{B.35}$$

such that the maximum is achieved for $x = \sigma_3 = \mathrm{diag}(1,-1)$ which has an operator norm of 1. So the norm of this linear functional is $2\cos\theta$, giving the last equality in (B.33). Taking the $\inf$ over u' in (B.33), we have:

$$||\omega_\psi - \omega_\phi|| \leq 2\sqrt{1 - F(\omega_\psi, \omega_\phi)^2}. \tag{B.36}$$

In the other direction we can pick ϕ and ψ to live in the natural cone without loss of generality, and then we have $\|\omega_\psi - \omega_\phi\| \geq |\,|\phi\rangle - |\psi\rangle\,|^2 = 2(1 - \langle\psi|\,\phi\rangle)$ where the later quantity is real since both vectors are in the cone. We use the inequality (3.69) for $p = 1$ that we reproduce here:

$$\|\phi\|_{1,\psi} \geq \langle\phi|\,(\Delta'_{\psi,\phi})^{1/2}\,|\phi\rangle = \langle\phi|\,\psi\rangle\,, \tag{B.37}$$

so

$$\frac{1}{2}\|\omega_\psi - \omega_\phi\| \geq 1 - F(\omega_\psi, \omega_\phi) \tag{B.38}$$

Altogether, we have

$$1 - F(\omega_\psi, \omega_\phi) \leq \frac{1}{2}\|\omega_\psi - \omega_\phi\| \leq \sqrt{1 - F(\omega_\psi, \omega_\phi)^2}. \tag{B.39}$$

Note that the fidelity lies between 0 and 1 and:

$$0 \leq \|\omega_\psi - \omega_\phi\| \leq 2 \tag{B.40}$$

where equality is achieved on the left iff the two linear functionals are the same and on the right if the support of the two linear functionals are orthogonal. We can see this as follows. Note that for $\|x\| \leq 1$:

$$|\omega_\psi(x)| \leq \|x\|\omega_\psi(1) \leq 1 \tag{B.41}$$

so that $|\omega_\psi(x) - \omega_\phi(x)|$ lies between 0 and 2. Equality is achieved for $x = \pi(\psi) - \pi(\phi)$ with orthogonal support. $\square$

B.2.2 Proof of Lemma B.2.1 (Continuity of fidelity)

In this section, all L_1 norms refer to the commutant algebra $\mathcal{A}'$, as in (lem. 3.2.1):

$$\|\psi\|_{1,\phi} = F(\omega_\psi, \omega_\phi) \equiv \sup_{u' \in \mathcal{A}'} |\langle\psi| \, u' \, |\phi\rangle| \,, \tag{B.42}$$

where the supremum is over partial isometries u'.

Lemma B.2.1. For a v. Neumann algebra $\mathcal{A}$ in standard form acting on a Hilbert space $\mathscr{H}$ and any $|\psi_i\rangle, |\phi_i\rangle \in \mathscr{H}$,

$$\Big| \, \|\psi_1\|_{1,\phi_1} - \|\psi_2\|_{1,\phi_2} \Big| \leq \|\phi_1 - \phi_2\| + \|\psi_1 - \psi_2\| \,. \tag{B.43}$$

Proof. The variational expression (B.42) immediately allows one to deduce the triangle inequality for the L_1-norms. Note that:

$$\sup_{u' \in \mathcal{A}'} |\langle\psi_1| \, u' \, |\psi_2\rangle| \leq \sup_{u \in B(\mathscr{H})} |\langle\psi_1| \, u \, |\psi_2\rangle| = \|\psi_1\| \, \|\psi_2\| \,, \tag{B.44}$$

and that $\|\psi\|_{1,\phi} = \|\phi\|_{1,\psi}$ are further trivial consequences of the variational definition. For normalized vectors $\psi_1, \psi_2, \phi_1, \phi_2$ we derive for the L_1-norms relative to $\mathcal{A}'$:

$$\begin{aligned} \Big| \, \|\psi_1\|_{1,\phi_1} - \|\psi_2\|_{1,\phi_2} \Big| &\leq \Big| \, \|\psi_1\|_{1,\phi_1} - \|\psi_1\|_{1,\phi_2} \Big| + \Big| \, \|\psi_1\|_{1,\phi_2} - \|\psi_2\|_{1,\phi_2} \Big| \\ &\leq \|\phi_1 - \phi_2\|_{1,\psi_1} + \|\psi_1 - \psi_2\|_{1,\phi_2} \leq \|\phi_1 - \phi_2\| + \|\psi_1 - \psi_2\| \end{aligned} \tag{B.45}$$

where to go to the second line we used the reverse triangle inequality twice, and in the last step we used (B.44). □

B.3 Proof of lemma 3.2.7 (Hirschman's improvement)

Proof. (1) First assume that ω_ψ is faithful and we may assume $|\psi\rangle \in \mathscr{P}^\natural_\mathcal{M}$ by invariance of the L_p-norms. Then $|\psi\rangle$ is cyclic and separating and the standard theory developed in [70] applies. We use the notation $\mathbb{S}_{1/2} = \{0 < \mathrm{Re} z < 1/2\}$.

Denote the dual of a Hölder index p by p', defined so that $1/p + 1/p' = 1$. [70] have shown that the non-commutative $L^p(\mathcal{M}, \psi)$-norm of a vector $|\zeta\rangle$ relative to $|\psi\rangle$ can be characterized by (dropping the superscript on the norm)

$$\|\zeta\|_{p,\psi} = \sup\{|\langle\zeta|\zeta'\rangle| : \ \ \|\zeta'\|_{p',\psi} \le 1\}. \tag{B.46}$$

They have furthermore shown that when $p' \ge 2$, any vector $|\zeta'\rangle \in L^{p'}(\mathcal{M}, \psi)$ has a unique generalized polar decomposition, i.e. can be written in the form $|\zeta'\rangle = u\Delta^{1/p'}_{\phi,\psi}|\psi\rangle$, where u is a unitary or partial isometry from $\mathcal{M}$. Furthermore, they show that $\|\zeta'\|_{p',\psi} = \|\phi\|^{p'}$. We may thus choose a u and a normalized $|\phi\rangle$, so that

$$\|G(\theta)\|_{p(\theta),\psi} = \langle u\Delta^{1/p(\theta)'}_{\phi,\psi}\psi|G(\theta)\rangle, \tag{B.47}$$

perhaps up to a small error which we can let go zero in the end. Now we define p_θ as in the statement, so that

$$\frac{1}{p'_\theta} = \frac{1-2\theta}{p'_0} + \frac{2\theta}{p'_1}, \tag{B.48}$$

and we define an auxiliary function $f(z)$ by

$$f(z) = \langle u\Delta_{\phi,\psi}^{2\bar{z}/p_1'+(1-2\bar{z})/p_0'}\psi|G(z)\rangle, \tag{B.49}$$

noting that

$$f(\theta) = \|G(\theta)\|_{p_\theta,\psi} \tag{B.50}$$

by construction. By Tomita-Takesaki-theory, $f(z)$ is holomorphic in $\mathbb{S}_{1/2}$. For the values at the boundary of the strip $\mathbb{S}_{1/2}$, we estimate

$$\begin{aligned}
|f(it)| &= |\langle u\Delta_{\phi,\psi}^{-2it(1/p_1'-1/p_0')}\Delta_{\phi,\psi}^{1/p_0'}\psi|G(it)\rangle| \\
&\leq \|u\Delta_{\phi,\psi}^{-2it(1/p_1'-1/p_0')}\Delta_{\phi,\psi}^{1/p_0'}\psi\|_{p_0',\psi}\|G(it)\|_{p_0,\psi} \\
&\leq \|\Delta_{\phi,\psi}^{-2it(1/p_1'-1/p_0')}\Delta_{\phi,\psi}^{1/p_0'}\psi\|_{p_0',\psi}\|G(it)\|_{p_0,\psi} \\
&\leq \|\phi\|^{p_0'}\|G(it)\|_{p_0,\psi} \\
&\leq \|G(it)\|_{p_0,\psi}.
\end{aligned} \tag{B.51}$$

Here we used the version of Hölder's inequality proved by [70], we used $\|a^*\zeta\|_{p_0',\psi} \leq \|a\|\|\zeta\|_{p_0',\psi}$ for any $a \in \mathcal{A}$, see [70], lem. 4.4, and we used $\|\Delta_{\phi,\psi}^{-2it(1/p_1'-1/p_0')}\Delta_{\phi,\psi}^{1/p_0'}\psi\|_{p_0',\psi} \leq \|\phi\|^{p_0'}$ which we prove momentarily. A similar chain of inequalities also gives

$$|f(1/2+it)| \leq \|G(1/2+it)\|_{p_1,\psi}. \tag{B.52}$$

To prove the remaining claim, let $|\zeta'\rangle = \Delta_{\phi,\psi}^{z}|\psi\rangle$ and $z = 1/p' + 2it$. Then we have, using the variational characterization by [70] of the $L^{p'}(\mathcal{M},\psi)$-norm when $p' \geq 2$:

$$\begin{aligned}
\|\zeta'\|_{p',\psi} &= \sup_{\|\chi\|=1} \|\Delta_{\chi,\psi}^{1/2-1/p'}\Delta_{\phi,\psi}^{z}\psi\| \\
&= \sup_{\|\chi\|=1} \|\Delta_{\chi,\psi}^{1/2-1/p'-2it}\Delta_{\phi,\psi}^{1/p'+2it}\psi\| \\
&= \sup_{\|\chi\|=1} \|\Delta_{\chi,\psi}^{1/2-1/p'}(D\chi : D\phi)_{2t}\pi^{\mathcal{M}}(\phi)\Delta_{\phi,\psi}^{1/p'}\psi\| \\
&\leq \sup_{\|\chi\|=1, a\in\mathcal{A}, \|a\|=1} \|\Delta_{\chi,\psi}^{1/2-1/p'}a\Delta_{\phi,\psi}^{1/p'}\psi\| \\
&\leq \sup_{a\in\mathcal{A},\|a\|=1} \|a\Delta_{\phi,\psi}^{1/p'}\psi\|_{p',\psi}.
\end{aligned} \tag{B.53}$$

Using [70], lem. 4.4, we continue this estimation as

$$\leq \sup_{a\in\mathcal{A},\|a\|=1} \|a\|\|\Delta_{\phi,\psi}^{1/p'}\psi\|_{p',\psi} = \|\phi\|^{p'}, \tag{B.54}$$

which gives the desired result.

Next, we use the Hirschman improvement of the Hadamard three lines theorem [107, 108].

Lemma B.3.1. Let $g(z)$ be holomorphic on the strip $\mathbb{S}_{1/2}$, continuous and uniformly bounded at the boundary of $\mathbb{S}_{1/2}$. Then for $\theta \in (0, 1/2)$,

$$\ln|g(\theta)| \leq \int_{-\infty}^{\infty} \left(\beta_\theta(t)\ln|g(1+it)|^{2\theta} + \alpha_\theta(t)\ln|g(it)|^{1-2\theta}\right) \mathrm{d}t, \tag{B.55}$$

where $\alpha_\theta(t), \beta_\theta(t)$ are as in lem. 3.2.7.

Applying this to $g = f$ gives the statement of the theorem.

(2) Let us now extend this result to the case where $\rho = \omega_\psi$ is not faithful. We employ the

following common trick where we use case (1) above for the modified functional

$$\rho_\epsilon \equiv (1-\epsilon)\rho + \epsilon\sigma, \tag{B.56}$$

where σ is any faithful normal state, which exists since $\mathcal{M}$ is assumed to be sigma-finite. Then ρ_ϵ in (B.56) with $0 < \epsilon < 1$ is now a faithful state. We take the unique cyclic and separating vector representative in the natural cone and denote it as $|\psi_\epsilon\rangle$.

Lemma B.3.2. For $1 \leq p \leq 2$ and ρ_ϵ the family of states (B.56), we have $\lim_{\epsilon\to 0^+} \|\zeta\|_{p,\psi_\epsilon} = \|\zeta\|_{p,\psi}$.

Proof. Since $\rho_\epsilon/(1-\epsilon) > \rho$, it follows that $\Delta_{\psi_\epsilon,\chi} \geq (1-\epsilon)\Delta_{\psi,\chi}$. Therefore, by standard properties of the modular operator, $\Delta^{-1}_{\chi,\psi_\epsilon} \geq (1-\epsilon)\Delta^{-1}_{\chi,\psi}$. By Löwner's theorem [109] applied to the operator monotone (for $1 \leq p \leq 2$) function $f(x) = x^{1/p-1/2}$, we have

$$\Delta^{1/2-1/p}_{\chi,\psi_\epsilon} \geq (1-\epsilon)^{1/p-1/2}\, \Delta^{1/2-1/p}_{\chi,\psi}. \tag{B.57}$$

Taking the infimum on (B.57) gives

$$\|\zeta\|_{p,\psi} \leq \inf_{\substack{\chi\in\mathscr{H}:\|\chi\|=1,\pi(\chi)\geq\pi(\zeta)\\ \zeta\in\mathscr{D}(\Delta^{1/2-1/p}_{\chi,\psi_\epsilon})}} \|\Delta^{1/2-1/p}_{\chi,\psi}\zeta\| \leq (1-\epsilon)^{1-2/p}\,\|\zeta\|_{p,\psi_\epsilon}. \tag{B.58}$$

The first inequality holds because the domain restriction gives a smaller class of states over which one takes the infimum and the second inequality is (B.57). We therefore obtain

$$\|\zeta\|^2_{p,\psi} - \|\zeta\|^2_{p,\psi_\epsilon} \leq O(\epsilon). \tag{B.59}$$

Now we use a variational characterization of the L_p-norms proven in paper II, prop. 1, for $1 \leq p \leq 2$.

$$\|\zeta\|_{p,\psi}^2 = -\frac{\sin(2\pi/p)}{\pi} \inf_{x:\mathbb{R}_+\to\mathcal{M}'} \int_0^\infty [\|x(t)\zeta\|^2 + t^{-1}F_{\mathcal{M}'}(y(t)\omega'_\zeta y(t)^*, \omega'_\psi)^2] t^{-2/p'} \mathrm{d}t, \quad \text{(B.60)}$$

where $y(t) = 1 - x(t)$, the infimum is taken over all step functions $x : \mathbb{R}_+ \to \mathcal{M}'$ with finite range such that $x(t) = 1$ for $t \in [0, c]$ for some $c > 0$, and $x(t) = 0$ for sufficiently large t. We also use the notation $(x\omega x^*)(b) = \omega(x^*ax)$. For any fixed $\delta > 0$ a step function may be chosen so that the infimum is achieved up to δ. It follows that, with this choice,

$$\begin{aligned}
&\|\zeta\|_{p,\psi_\epsilon}^2 - \|\zeta\|_{p,\psi}^2 \\
&\leq \delta - \frac{\sin(2\pi/p)}{\pi} \int_c^\infty [F_{\mathcal{M}'}(y(t)\omega'_\zeta y(t)^*, \rho'_\epsilon)^2 - F_{\mathcal{M}'}(y(t)\omega'_\zeta y(t)^*, \rho')^2] t^{-1-2/p'} \mathrm{d}t \qquad \text{(B.61)} \\
&\leq \delta + \mathrm{sinc}(2\pi/p')\, c^{-2/p'} \left(\sup_{t \geq c} \|y(t)\zeta\|^2 \right) \|\rho - \rho_\epsilon\|^{1/2} \leq \delta + O(\epsilon^{1/2}),
\end{aligned}$$

using the continuity of the fidelity, lem. B.2.1 together with $(1/2)\|\rho' - \rho'_\epsilon\| \leq \|\psi - \psi_\epsilon\| \leq \|\rho - \rho_\epsilon\|^{1/2}$ from (3.4) in the second step, and using (B.56) in the third step. If we chose ϵ so small that the ϵ-dependent terms in (B.59), (B.61) are each less than δ, we get $|\,\|\zeta\|_{p,\psi_\epsilon}^2 - \|\zeta\|_{p,\psi}^2| < 2\delta$. Therefore, since $\delta > 0$ can be arbitrarily small, the lemma is proven. $\square$

Using this lemma in conjunction with [70], lem. 6 (2) gives $\|\zeta\|_{p,\psi} \leq \|\zeta\|$. Then, since $|G(z)\rangle$ is assumed to be bounded in the Hilbert space norm, we have $\|G(z)\|_{p,\psi} \leq C$ inside the closed strip $\{0 \leq \mathrm{Re} z \leq 1\}$. Now taking the limit $\epsilon \to 0$ of case (1) for the vector $|\psi_\epsilon\rangle$ using the lemma and the dominated convergence theorem to take the limit under the integral in (3.141) concludes the proof of (2). $\square$

Appendix C: Supplementary materials of Chapter 4

This appendix provides the details of the HMERA model constructed in Section (4.3).

C.1 Super-operators

Recall that tensor networks of this type can yield a power-law decaying correlation as shown in (4.3) where the scaling dimensions are given by Eq. (4.6). To preview the results of this subsection, the different types of superoperators are depicted in Figure (C.4) and their corresponding probabilities are presented in Eq. (C.8). As long as we show that (1) the only eigen-operator for eigenvalue 1 is the identity operator; (2) for each type of superoperator all the other eigenvalues indeed have absolute value less than 1, we can conclude it produces a decaying connected two-point function that is roughly a power law.

We start by investigating the properties of each tensor individually, as the superoperators interpolating between layers are composed of them. The perfect tensor defines a 2-isometry depending on the state of the logical qubit. See the left panel of Figure (C.1). As the two copies form a direct product, studying a single copy suffices. Most generally, we initialize the logical qubit in the state $|\phi\rangle = \cos\alpha|0\rangle + e^{i\beta}\sin\alpha|1\rangle$ and denote the corresponding isometry as W_p. By distinguishing the inward 2 legs from the others, the original rotational symmetry breaks down to the reflection symmetry $1 \leftrightarrow 2,\ 3 \leftrightarrow 5$. Except for the top few layers, the incoming operator of W_p will at most be weight 2, and will have support either on $3, 4$ or $4, 5$. This motivates us to view $W_p(\cdot)W_p^\dagger$ as a super-operator sending a weight 2 operator to another weight 2 operator. Studying the case in which operators have support on legs 3 and 4 would suffice because of the reflection symmetry. If the operator is weight 1, say X_3, we view it as a weight 2 operator $X_3 I_4$, etc. The identity operators together with Pauli matrices on both legs form a set of bases of weight 2 operators. The super-operator can be viewed as a 16×16 matrix in such bases. The right panel of Figure (C.1) illustrates how to determine one entry of the super operator. One can easily calculate the eigen-operators and the eigenvalues of this superoperator. It turns out that there is only one eigenvalue with norm 1, whose eigen-operator is the identity operator, as expected. All the other eigenvalues, though complex, have norm less than 1. This is manifestly seen in Figure (C.2). Since for the tensor product of two matrices, the eigenvalues are pairwise products of each matrix, we conclude that for the double copy of 2-isometries, all but one eigenvalue have norm less than 1 as well.

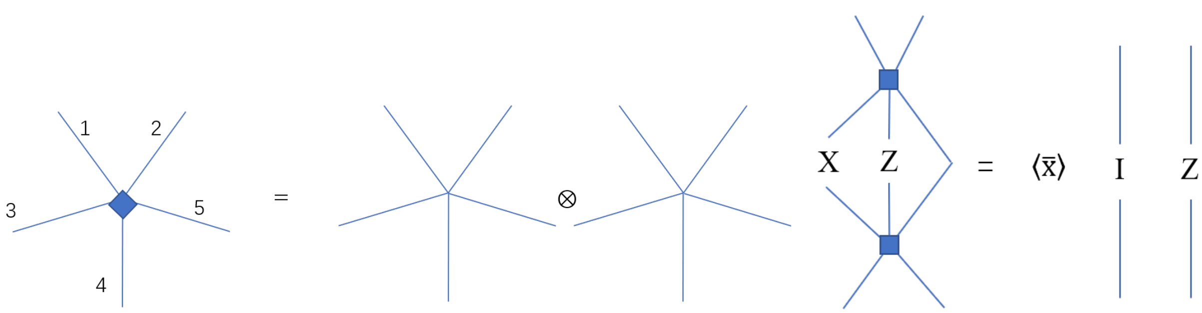

Figure C.1: Left: The perfect tensor on the pentagon defines a 2-isometry. Right: An example of how the super-operator defined by $W_p(\cdot)W_p^\dagger$ acting on a weight 2 operator. The prefactor $\langle \bar{X} \rangle$ is the expectation value of the logical $\bar{X}$ operator in state $|\phi\rangle$.

We then investigate the properties of the imperfect code defined in Figure (4.4). This defines a 1-isometry. We denote the isometry as W_I. In this case, the original five-fold rotational symmetry breaks down to the reflection symmetry $2 \leftrightarrow 5,\ 3 \leftrightarrow 4$. It turns out that one can have

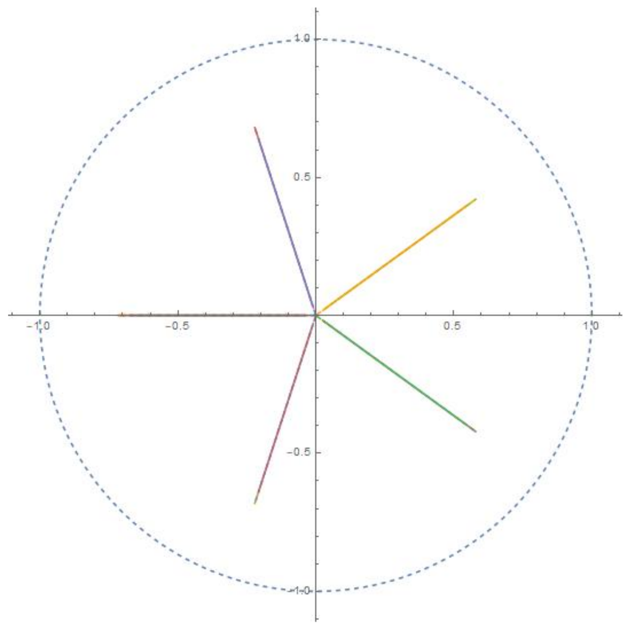

Figure C.2: Eigenvalues of the super-operator defined by $W_p(\cdot)W_p^\dagger$. This is depicted on the complex plane with parameter $\alpha = \frac{\pi}{3},\ \beta \in (0, 2\pi)$. The outer dashed one is the unit circle. This manifestly shows that all but one eigenvalues have norm less than 1.

weight 1 or 2 operator fed into the super-operator defined by $W_I(\cdot)W_I^\dagger$. In the weight 1 case, one can solve for its eigenvalues and eigen-operators. In the weight 2 case, operators can have support on leg $2, 3$ or $3, 4$ or $4, 5$. In this case no eigen-operator can be defined because the operator weight changes. Instead, we calculate the operator norm after applying the super-operator $W_I(\cdot)W_I^\dagger$. The identity operator together with Pauli matrices of one qubit forms the bases of operators. For weight 2 operators, this is a Hilbert space of 256 dimensions. Since the bases operators all have norm 1, to show that the super-operator $W_I(\cdot)W_I^\dagger$ result in decaying two point functions, we show the resulting operators have norm less than 1, except for the identity operators on 4 qubits. For operators inserted on leg $2, 3$, numerical results in Figure (C.3) explicitly verifies this property. Inserting the operators in legs $3, 4$ turns out to produce the same figure. Inserting the operators in legs $4, 5$ is the same as inserting in $2, 3$ by symmetry.

With the properties of perfect and imperfect codes above, we can already conclude that our

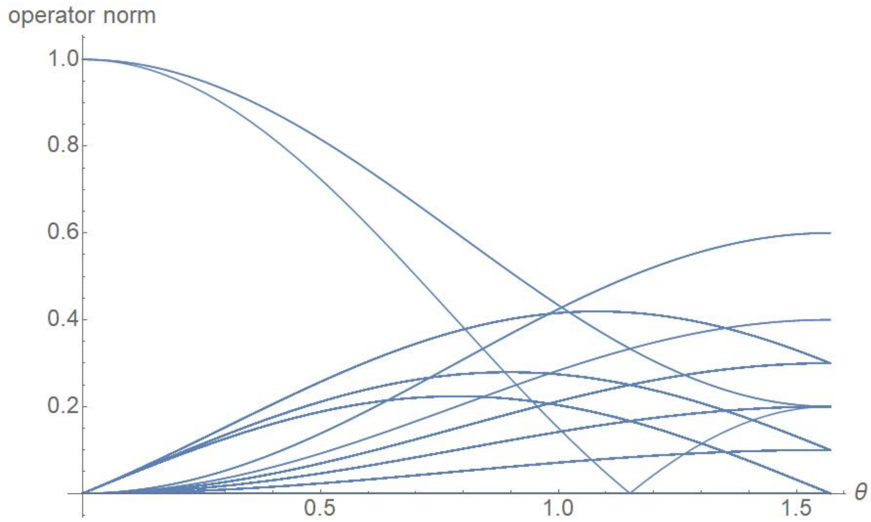

Figure C.3: The norms of weight 2 operators inserted on leg $2, 3$ with respect to the parameter θ in the range $\theta \in (0, \frac{\pi}{2})$. We plot all 255 bases after the action of super-operator $W_I(\cdot)W_I^\dagger$. This explicitly shows that they have norm strictly less than 1 when $\theta > 0$.

model can produce decaying yet non-vanishing two point correlations. Furthermore, we would like to identify different types of super-operators. They are collectively depicted in Figure (C.4). We draw the dual graph so that the isometries are on the nodes. We summarize them in the following. A weight 1 operator can be coarse-grained either into a weight 1 operator via an imperfect code (panel 1), or into a weight 2 operator via a perfect tensor (panel 2). A weight 2 operator can be coarse-grained into a weight 1 operator via an imperfect tensor (panel 3), or into a weight 2 operator via a product of imperfect tensors (panel 4), or into a weight 3 tensor via a product of perfect and imperfect tensor (panel 5). A weight 3 operator may remain "stable" as weight 3 (panel 6 and 7), or "shrink" to weight 2 (panel 8).

Since the operator weight may change, it is not feasible to solve for the eigen-operators of super operators defined on an individual layer. It is possible to calculate the eigenvalue and the eigen-operators for the procedure during which a weight 1 operator increases to weight 3 then decreases to weight 1, i.e., defining a super-operator across multiple layers. However the number

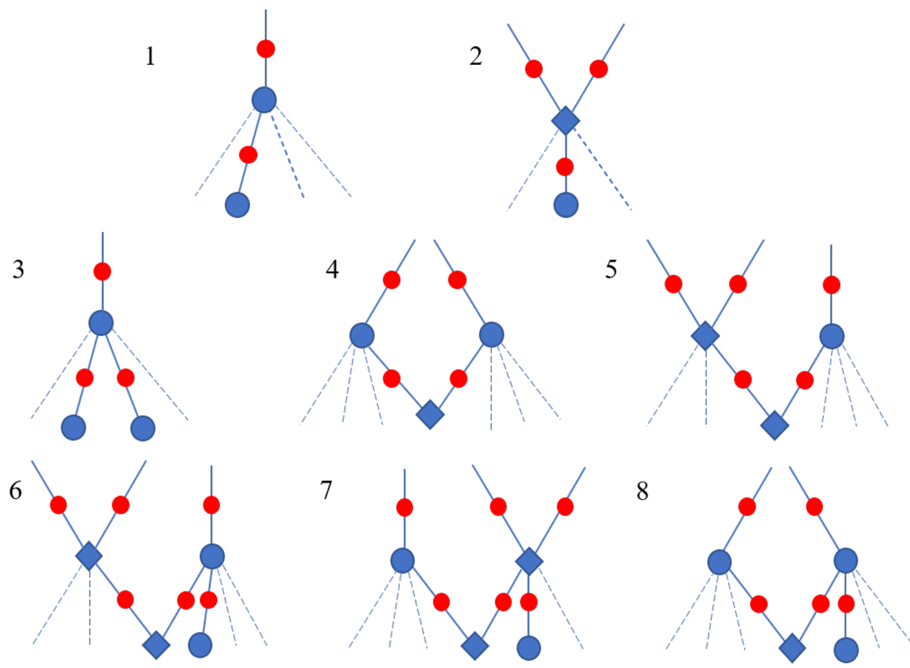

Figure C.4: This shows the different superoperators during the coarse-graining process. The coarse-graining goes from bottom to top in each panel. Blue circles and diamonds represent imperfect and perfect tensors respectively. The red circles mark the legs on which the operators act. The irrelevant legs are depicted in dashed lines. The first row shows the cases of weight 1 operators, the second row for weight 2 and the third for weight 3.

of layers involved depends largely on particular processes. We adopt a different strategy to calculate the probability of each type of super-operator appearing in a typical coarse graining process. For a given insertion point, the total coarse-graining process is fixed. We randomize the insertion point at the boundary for a generic operator so we can calculate these probabilities as an average over different coarse-graining processes[1]. An assumption is that the two operators inserted at the cut-off boundary are well-separated, i.e., $N \sim \log|i-j| \gg 1$, so the two insertions will be coarse-grained separately before they meet at the top few layers. It is this part that contributes to the long range behaviour of the correlation. Also, the notion of taking the average super-operator with said probability distribution make more sense when N is large.

The types of super-operators and their corresponding probabilities depend primarily on the graph structure of the tensor network. We start by reviewing the formulae for the number of perfect tensors $g(n)$ and imperfect tensors $f(n)$ in each layer. One node is chosen as the center and is labelled layer 0. Then if we need to go across a minimal number of n edges to reach from the center to a particular node, it is assigned to layer n. The labelling procedure is unique and unambiguous in this model. This setup is familiar in the literature [31] and we reproduce its result here for readability:

$$\begin{aligned} f(n) &= \frac{5-\sqrt{5}}{2}\Big(\frac{3+\sqrt{5}}{2}\Big)^n\Big[1+O\Big(\Big(\frac{3-\sqrt{5}}{3+\sqrt{5}}\Big)^n\Big)\Big], \\ g(n) &= \frac{3\sqrt{5}-5}{2}\Big(\frac{3+\sqrt{5}}{2}\Big)^n\Big[1+O\Big(\Big(\frac{3-\sqrt{5}}{3+\sqrt{5}}\Big)^n\Big)\Big]. \end{aligned} \tag{C.1}$$

We work in the case where n is large so we can set the factors in the square brackets to 1. The

[1] This is similar to the strategy in [100], where the authors averaged over the super-operators, which can also be viewed as an averaging over different coarse-graining processes.

number of total layers N can be calculated more precisely as

$$N \approx \frac{\log|i-j|}{\log(\frac{3+\sqrt{5}}{2})}. \tag{C.2}$$

Now we are able to calculate the probability of a weight 1 operator expanding to weight 2. There are two situations. If the weight 1 operator is at the start of the coarse-graining process, the probability of it spreading is the same as the probability of inserting an operator on legs that are directly connected to a perfect code.

$$P_0(1 \to 2) = \frac{3g(n)}{4f(n)+3g(n)} = 3 - \frac{6}{\sqrt{5}},\ P_0(1 \to 1) = \frac{4f(n)}{4f(n)+3g(n)} = \frac{6}{\sqrt{5}} - 2. \tag{C.3}$$

This only affects the initial step and does not impact the final result in Eq. (C.8). If the weight 1 operator appears during coarse-graining process, then it has a different probability. The reason is that the weight 1 operator necessarily came from the superoperator of an imperfect code. See Figure (C.5) for an illustration. So this is the conditional probability of connecting to a perfect code at layer n, given that it is connected to imperfect code at layer $n+1$.

$$P(1 \to 2|1) = \frac{g(n)}{2f(n)+g(n)} = \sqrt{5} - 2,\ P(1 \to 1|1) = \frac{2f(n)}{2f(n)+g(n)} = 3 - \sqrt{5}. \tag{C.4}$$

If the operator is weight 2, then its behaviour is more complicated as it depends on the previous two coarse-graining steps. Suppose an operator has just expanded from weight 1 to 2 by passing through a perfect code, it may either remain weight 2, shrink to weight 1, or expand to weight 3. The illustrations are depicted in the second row of Figure (C.4). Ignoring the case where the operator weight remains constant, as it does not involve any transitions, from the graph

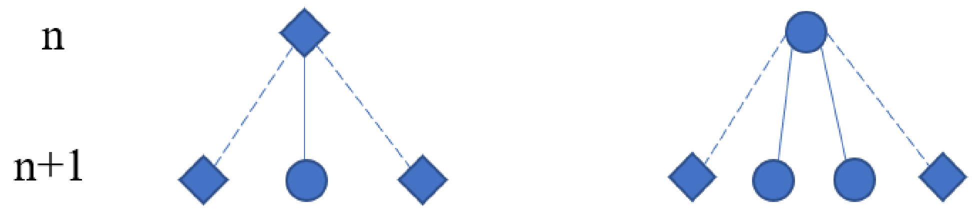

Figure C.5: These figures illustrate the possible insertions of weight 1 operators. If the operator is inserted at the boundary, it can appear on any leg randomly. If it is a result of the coarse-graining, it can only appear on solid lines which connect to imperfect tensor in the layer $n+1$. It can not appear on dashed lines while being weight 1 in generic cases.

one finds that when looking at layer n, there are $f(n-2)$ cases that corresponds to the panel 3 of Figure (C.4) and $2g(n-1)$ cases that corresponds to the panel 5 of Figure (C.4). So this leads to the conditional probabilities:

$$P(2\to 2|1\to 2)=\frac{f(n-2)}{g(n)}=\sqrt{5}-2,\ P(2\to 3|1\to 2)=\frac{2g(n-1)}{g(n)}=3-\sqrt{5}. \quad \text{(C.5)}$$

If an operator has just shrunk from weight 3 or stayed as weight 2, it will necessarily shrink to weight 1. This is illustrated in panel 3, 4, 8 in Figure: (C.4).

$$P(2\to 1|2\to 2)=P(2\to 1|3\to 2)=1. \quad \text{(C.6)}$$

For a weight 3 operator, it is similar to the behaviour of weight 1 operator. It may stay weight 3 or shrink to weight 2 then to weight 1. This depends on which tensor these legs connect to in the next layer. Similar to weight 2 cases, if they both connect to imperfect tensors, the weight would shrink to 2; if they connect to 1 perfect and 1 imperfect tensor, the weight would remain to be 3. The illustrations are collected in the third row of Figure (C.4). So we have the following conditional probabilities:

$$P(3 \to 2|3) = \frac{f(n-2)}{g(n)} = \sqrt{5} - 2,\ P(3 \to 3|3) = \frac{2g(n-1)}{g(n)} = 3 - \sqrt{5}. \tag{C.7}$$

With all these conditional probabilities, we are able to calculate the unconditional probabilities of different types of super-operators appearing in a sufficiently long and typical coarse-graining process. We take $p(1 \to 1) = x,\ p(3 \to 3) = y$. Then $p(1 \to 2) = \frac{p(1\to 2|1)}{p(1\to 1|1)}x$ from the conditional probabilities in Eq. (C.4). Similarly $p(3 \to 2) = \frac{p(3\to 2|3)}{p(3\to 3|3)}y$ from Eq. (C.7). Next we have $p(2 \to 1) = p(1 \to 2)$ and $p(2 \to 3) = p(3 \to 2)$. This is because when the total number of the layers N is large enough and intermediate coarse-graining processes dominate. If an operator remains weight 1 through several layers, it always begins with a transition $2 \to 1$ and ends with a transition $1 \to 2$. The same happens for the weight-3 case. The remaining unknown $p(2 \to 2)$ can be obtained from the normalization condition and from the conditional probability in Eq. (C.5), such that $p(2 \to 2) = \frac{p(2\to 2|1\to 2)}{p(2\to 3|1\to 2)}p(2 \to 3)$. This yields two equations of $x,\ y$ and we can solve for them to obtain Eq. (C.8).

The resulting probabilities are,

$$\begin{aligned}
&p(1 \to 1) = \frac{3\sqrt{5}}{5} - 1 \approx 34.16\%,\ p(1 \to 2) = 1 - \frac{2\sqrt{5}}{5} \approx 10.56\%,\\
&p(2 \to 1) = 1 - \frac{2\sqrt{5}}{5} \approx 10.56\%,\ p(2 \to 2) = \frac{9\sqrt{5}}{5} - 4 \approx 2.49\%,\ p(2 \to 3) = 5 - \frac{11\sqrt{5}}{5} \approx 8.07\%,\\
&p(3 \to 2) = 5 - \frac{11\sqrt{5}}{5} \approx 8.07\%,\ p(3 \to 3) = \frac{14\sqrt{5}}{5} - 6 \approx 26.10\%.
\end{aligned} \tag{C.8}$$

When N is sufficiently large, there are approximately $p(i \to j)N$ layers in which the coarse-graining operation is sending a weight-i operator to weight-j. These are precisely the probabilities p_a's in Eq. (4.6).

In summary, we have shown that each super-operator has a dominant singular value 1 with only the identity operator as its sole eigen-operator; all other singular values are less than 1. By averaging such super-operators, our HMERA model produces power-law decaying correlation functions. The probabilities of each type of super operator are further calculated in Eq. (C.8). This allows us to estimate the average eigenvalue $\bar{\lambda}$ that appears in in Eq. (4.3) and (4.6).

C.2 Non-flat entanglement spectrum

It was pointed out in [110, 111] that, to leading order, the density matrix obtained from the gravitational path integral evaluated with fixed area RT surface has a flat entanglement spectrum. This implies that the Renyi entropies of the resulting density matrix is identical to all orders. It is consistent with the existing QECC constructions [31, 32], yet in contradiction to any real CFT models [112]. In this section, we show that the tensor sub-networks in our proposed approximate QECC model can obtain non-flat entanglement spectra.

Here we consider two examples. In Figure (C.6) and (C.7) we calculate explicitly the eigenvalues of some reduced density matrices of three sites at the boundary. As each leg represents a qudit or a pair of qubits, the density matrices are of dimension 64. With two legs contracted, they both have rank 16. If the θ parameter is 0, the eigenvalues are indeed flat, i.e. all the non-zero ones are $1/16$. In the figures we turn on θ to a generic random non-zero value and the spectrum is no longer flat. While they are insufficient to show that the entanglement spectrum is non-flat for all subsystems in the actual HMERA, we can gain some intuition from such toy examples.

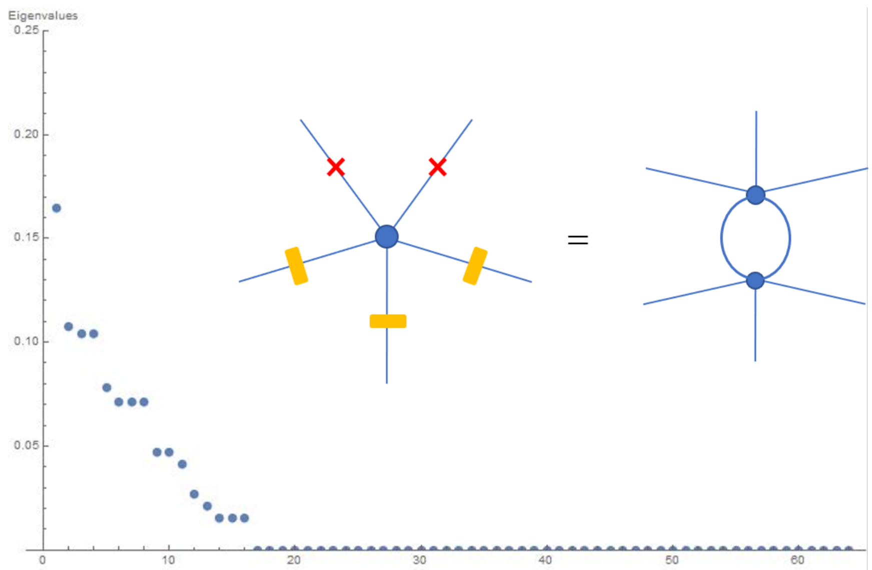

Figure C.6: The reduced density matrix of the sites labelled by yellow rectangle are calculated. Its corresponding Schimdt coefficients are plotted on the left. The legs that are labelled by red crosses are contracted to compute the reduced density matrix in the tensor network.

C.3 Imperfect Tensor Properties

The imperfect tensor itself is an approximate quantum error correction code that inherits the code properties of two copies of the $[[5,1,3]]$ code in the small θ regime. For any value of $\theta \neq 0$, it is also an exact 1-isometry when the logical qubits are fixed to be the $|\overline{00}\rangle$ state. While its isometric properties can be verified by showing all single-qudit (single-leg) reduced density matrices are maximally mixed, they can also be verified through tensor contraction. The latter technique also generalizes to other stabilizer codes without matrix computations.

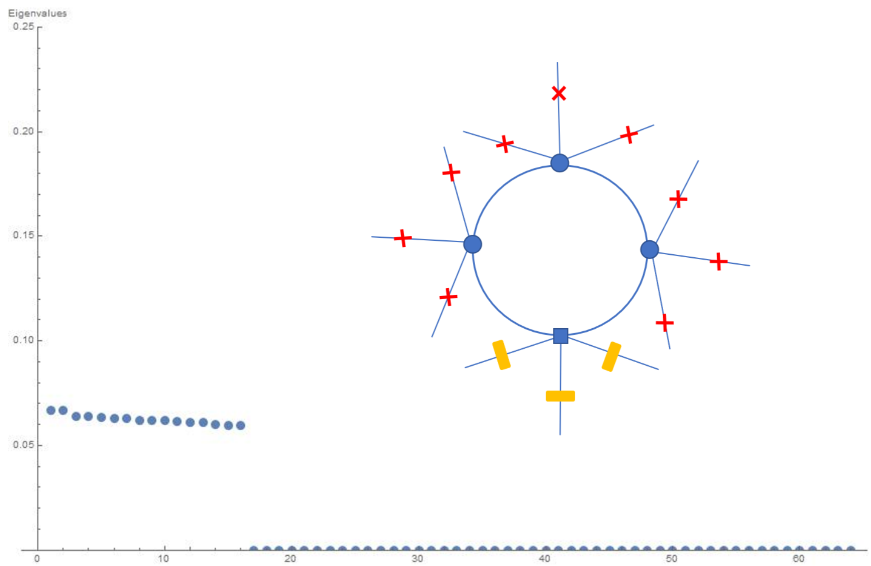

Figure C.7: The eigenvalues of another reduced density matrix. The legends are the same as those in Figure. (C.6).

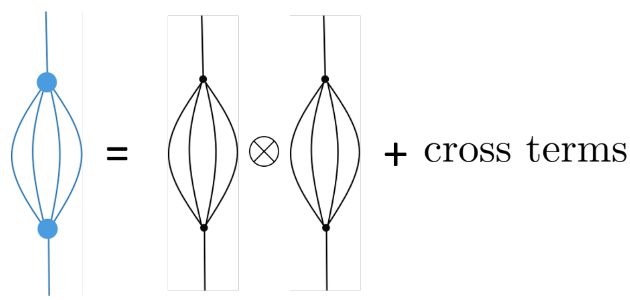

Figure C.8: Contraction of two imperfect tensors (blue, left) with their logical states fixed in $|\bar{0}\rangle$ can be decomposed into contractions of perfect tensors with non-trivial operator insertions in the cross terms.

Proof. The imperfect tensor can be expanded as the sum over diagonal terms and cross terms (Figure (C.8)). Because we have chosen the coefficients to be normalized, the diagonal terms sum to the identity operator. It remains to show that the cross terms vanish.

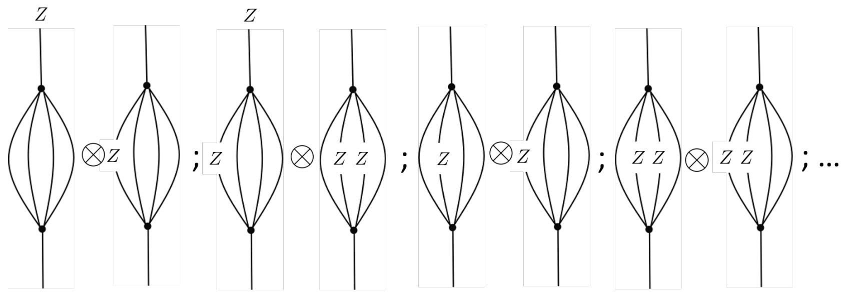

Figure C.9: Examples of cross terms that are present in the contraction. The four diagrams shown here represent the four types of terms that are relevant to us. All other terms are variations of these terms with Z operators in different places.

The cross terms consist of the type of tensor contractions shown in Figure (C.9). All of them contain factors of the following two types: ones with a single Z insertion (type-1) and ones with weight-2 ZZ insertions (type-2).

The stabilizer group of the double copy perfect code is $\langle S_i \otimes I, I \otimes S_j \rangle$, where $S_i, i \in \{1, \ldots, 4\}$ are the original 5 qubit code stabilizer generators. Suppose we can find a stabilizer element, $S = S' \otimes I$, that only acts non-trivially on the 4 contracted legs and anti-commute with the inserted operator O, then by the commutation relation in Figure (C.10), the terms in Figure (C.9) will vanish.

Indeed, this can be trivially done for terms of type-1 — let us treat the uncontracted leg(s) and the one potential Pauli Z error insertion within the contraction as two located errors. Because the 5 qubit code detects two errors, there must exist stabilizers of the 5 qubit code that anticommute with any insertion of $P_i \otimes P_j$ where $P \in \{I, X, Y, Z\}$. Therefore, all terms in Figure (C.9) vanish except for the last one where both of them are type-2 factors.

For type-2 contraction with ZZ insertions, the above argument no longer works because

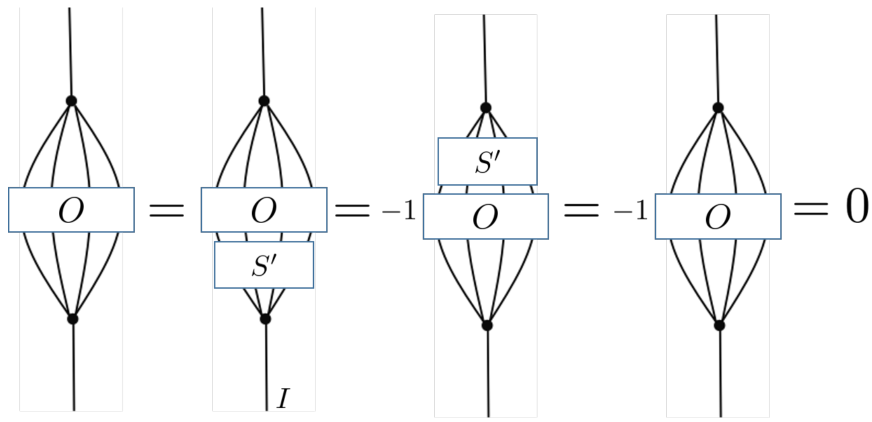

Figure C.10: If $S = S' \otimes I$ and $\{S', O\} = 0$, then the tensor contraction with operator O inserted is trivial.

the code doesn't detect any three errors. To show that it vanishes, we do an exhaustive search of all stabilizers that will anti-commute with the terms with ZZ insertions.

The stabilizer group of the 5 qubit code is

$$\mathcal{S} = \langle XZZXI, IXZZX, XIXZZ, ZXIXZ \rangle. \tag{C.9}$$

Without loss of generality, let the first qubit be the uncontracted leg of the perfect tensor, then the only stabilizer elements from the 5 qubit code that act trivially on the uncontracted legs are $IXZZX, IYXXY, IZYYZ$ where we ignore the potential minus signs. These anti-commute with all weight-2 Z insertions except $IZIIZ, IIZZI$. However, recall that the state $|\bar{0}\rangle$ is also stabilized by $\bar{Z} = ZZZZZ$. A representation of $\bar{Z}$ is $IIYZY$, which anti-commutes with both $IZIIZ$ and $IIZZI$. Therefore all cross-terms vanish.

Note that other logical states are not stabilized by both $\bar{Z}\bar{I}$ and $\bar{I}\bar{Z}$. As there are no other stabilizers that anti-commute with $IZIIZ, IIZZI$, the tensor is not a 1-isometry when it is in other logical states.

$\square$

Because the imperfect code in the $|\overline{00}\rangle$ state is a 1-isometry, any two qubits associated with one leg must be maximally entangled with the rest of the system. Because any leg is maximally mixed, it contains no information of the logical state. Thus, the code corrects any one qudit erasure error; it is a $[[5,0,2]]_4$ code on dimension-4 qudits.

List of Publications Related to the Dissertation

[1] Swingle, Brian G., and Yixu Wang. Recovery map for fermionic Gaussian channels. *Journal of Mathematical Physics*, 60.7 (2019): 072202.
[2] Thomas Faulkner, Stefan Hollands, Brian Swingle, and Yixu Wang. Approximate Recovery and Relative Entropy I: General von Neumann Subalgebras. *Communications in Mathematical Physics*, (2022): 1-49.
[3] Cao, ChunJun, Jason Pollack, and Yixu Wang. Hyperinvariant multiscale entanglement renormalization ansatz: Approximate holographic error correction codes with power-law correlations. *Physical Review D*, 105.2 (2022): 026018.

Bibliography

[1] Brian Swingle and Yixu Wang. Recovery Map for Fermionic Gaussian Channels. *Journal of Mathematical Physics*, 60(7):072202, 2019.

[2] Marius Junge, Renato Renner, David Sutter, Mark M Wilde, and Andreas Winter. Universal recovery maps and approximate sufficiency of quantum relative entropy. *Annales Henri Poincaré*, 19(10):2955–2978, 2018.

[3] Thomas Faulkner, Stefan Hollands, Brian Swingle, and Yixu Wang. Approximate Recovery and Relative Entropy I: General von Neumann Subalgebras. *Communications in Mathematical Physics*, pages 1–49, 2022.

[4] ChunJun Cao, Jason Pollack, and Yixu Wang. Hyperinvariant Multiscale Entanglement Renormalization Ansatz: Approximate Holographic Error Correction Codes with Power-law Correlations. *Physical Review D*, 105(2):026018, 2022.

[5] Emanuel Knill, Raymond Laflamme, and Lorenza Viola. Theory of Quantum Error Correction for General Noise. *Phys. Rev. Lett.*, 84:2525–2528, Mar 2000.

[6] H. Barnum and E. Knill. Reversing Quantum Dynamics with Near-optimal Quantum and Classical Fidelity. *Journal of Mathematical Physics*, 43(5):2097–2106, 2002.

[7] Jordan Cotler, Patrick Hayden, Geoffrey Penington, Grant Salton, Brian Swingle, and Michael Walter. Entanglement wedge reconstruction via universal recovery channels. *Physical Review X*, 9(3):031011, 2019.

[8] T. Faulkner, R. G. Leigh, O. Parrikar, and H. Wang. Modular Hamiltonians for Deformed Half-spaces and the Averaged Null Energy Condition. *Journal of High Energy Physics*, 9:38, September 2016.

[9] P. Hayden, R. Jozsa, D. Petz, and A. Winter. Structure of States which Satisfy Strong Subadditivity of Quantum Entropy with Equality. *Communications in Mathematical Physics*, 246:359–374, 2004.

[10] B. Swingle and J. McGreevy. Mixed s-sourcery: Building Many-body States Using Bubbles of Nothing. *Physical Review B*, 94(15):155125, October 2016.

[11] Dnes Petz. Sufficient Subalgebras and the Relative Entropy of States of a von Neumann Algebra. *Comm. Math. Phys.*, 105(1):123–131, 1986.

[12] Dnes Petz. Sufficiency of Channels over von Neumann Algebras. *The Quarterly Journal of Mathematics*, 39(1):97–108, 1988.

[13] Mark M Wilde. Recoverability in quantum information theory. *Proc. R. Soc. A*, 471(2182):20150338, 2015.

[14] Fikret Ceyhan and Thomas Faulkner. Recovering the QNEC from the ANEC. *Communications in Mathematical Physics*, 377(2):999–1045, 2020.

[15] Marlan O. Scully and M. Suhail Zubairy. *Quantum Optics*. Cambridge University Press, 1997.

[16] Hans-Albert Bachor and Timothy C Ralph. *A Guide to Experiments in Quantum Optics*. Wiley, 2004.

[17] L. Lami, S. Das, and M. M. Wilde. Approximate Reversal of Quantum Gaussian Dynamics. *Journal of Physics A Mathematical General*, 51(12):125301, March 2018.

[18] Daniel Gottesman. An introduction to quantum error correction. In *Proceedings of Symposia in Applied Mathematics*, volume 58, pages 221–236, 2002.

[19] Claude Crépeau, Daniel Gottesman, and Adam Smith. Approximate Quantum Error-Correcting Codes and Secret Sharing Schemes. In Ronald Cramer, editor, *Advances in Cryptology – EUROCRYPT 2005*, pages 285–301, Berlin, Heidelberg, 2005. Springer Berlin Heidelberg.

[20] Rudolf Haag. *Local Quantum Physics: Fields, Particles, Algebras*. Springer Science & Business Media, 2012.

[21] A. Uhlmann. Relative entropy and the Wigner-Yanase-Dyson-Lieb concavity in an interpolation theory. *Commun. Math Phys*, 54(1):21–32, 1977.

[22] Thomas Faulkner and Stefan Hollands. Approximate recoverability and relative entropy II: 2-positive channels of general von Neumann algebras. *Letters in Mathematical Physics*, 112, 2022.

[23] David D Blanco, Horacio Casini, Ling-Yan Hung, and Robert C Myers. Relative entropy and holography. *Journal of High Energy Physics*, 2013(8):1–65, 2013.

[24] Thomas Faulkner, Monica Guica, Thomas Hartman, Robert C Myers, and Mark Van Raamsdonk. Gravitation from entanglement in holographic CFTs. *Journal of High Energy Physics*, 2014(3):1–41, 2014.

[25] R. Bousso, Z. Fisher, J. Koeller, S. Leichenauer, and A. Wall. Proof of the Quantum Null Energy Condition. *Phys. Rev. D*, 93:024017, 2016.

[26] Srivatsan Balakrishnan, Thomas Faulkner, Zuhair U Khandker, and Huajia Wang. A general proof of the quantum null energy condition. *Journal of High Energy Physics*, 2019(9):1–86, 2019.

[27] Román Orús. A Practical Introduction to Tensor Networks: Matrix Product States and Projected Entangled Pair States. *Annals Phys.*, 349:117–158, 2014.

[28] Román Orús. Tensor networks for complex quantum systems. *APS Physics*, 1:538–550, 2019.

[29] Brian Swingle. Entanglement Renormalization and Holography. *Phys. Rev. D*, 86:065007, 2012.

[30] Goffredo Chirco, Daniele Oriti, and Mingyi Zhang. Group field theory and tensor networks: towards a Ryu–Takayanagi formula in full quantum gravity. *Class. Quant. Grav.*, 35(11):115011, 2018.

[31] Fernando Pastawski, Beni Yoshida, Daniel Harlow, and John Preskill. Holographic quantum error-correcting codes: Toy models for the bulk/boundary correspondence. *Journal of High Energy Physics*, 06:149, 2015.

[32] Patrick Hayden, Sepehr Nezami, Xiao-Liang Qi, Nathaniel Thomas, Michael Walter, and Zhao Yang. Holographic duality from random tensor networks. *Journal of High Energy Physics*, 11:009, 2016.

[33] ChunJun Cao and Brad Lackey. Approximate Bacon-Shor code and holography. *Journal of High Energy Physics*, 2021(5):1–110, 2021.

[34] Andrew J. Ferris and David Poulin. Tensor Networks and Quantum Error Correction. *Physical Review Letters*, 113(3):030501, July 2014.

[35] Robert J. Harris, Nathan A. McMahon, Gavin K. Brennen, and Thomas M. Stace. Calderbank-Shor-Steane holographic quantum error-correcting codes. *Phys. Rev. A*, 98:052301, Nov 2018.

[36] Terry Farrelly, Robert J. Harris, Nathan A. McMahon, and Thomas M. Stace. Tensor-network codes. 9 2020.

[37] ChunJun Cao and Brad Lackey. Quantum Lego: Building Quantum Error Correction Codes from Tensor Networks. *arXiv preprint arXiv:2109.08158*, 2021.

[38] G. Vidal. Class of Quantum Many-Body States That Can Be Efficiently Simulated. *Physical Review Letters*, 101(11):110501, September 2008.

[39] Ahmed Almheiri, Xi Dong, and Daniel Harlow. Bulk locality and quantum error correction in AdS/CFT. *Journal of High Energy Physics*, 2015(4):1–34, 2015.

[40] Zhao Yang, Patrick Hayden, and Xiao-Liang Qi. Bidirectional holographic codes and sub-AdS locality. *Journal of High Energy Physics*, 01:175, 2016.

[41] Fernando Pastawski and John Preskill. Code Properties from Holographic Geometries. *Physical Review X*, 7(2):021022, April 2017.

[42] Ning Bao, Geoffrey Penington, Jonathan Sorce, and Aron C. Wall. Beyond Toy Models: Distilling Tensor Networks in Full AdS/CFT. *Journal of High Energy Physics*, 19:069, 2020.

[43] Tamara Kohler and Toby Cubitt. Toy Models of Holographic Duality between local Hamiltonians. *Journal of High Energy Physics*, 08:017, 2019.

[44] Alexander Jahn and Jens Eisert. Holographic tensor network models and quantum error correction: A topical review. 2 2021.

[45] Isaac H. Kim and Michael J. Kastoryano. Entanglement renormalization, quantum error correction, and bulk causality. *Journal of High Energy Physics*, 04:040, 2017.

[46] Cedric Beny. Causal structure of the entanglement renormalization ansatz. *New J. Phys.*, 15:023020, 2013.

[47] Bartlomiej Czech, Lampros Lamprou, Samuel McCandlish, and James Sully. Tensor Networks from Kinematic Space. *Journal of High Energy Physics*, 07:100, 2016.

[48] Ning Bao, ChunJun Cao, Sean M. Carroll, and Aidan Chatwin-Davies. De Sitter Space as a Tensor Network: Cosmic No-Hair, Complementarity, and Complexity. *Phys. Rev. D*, 96(12):123536, 2017.

[49] Ning Bao, ChunJun Cao, Sean M. Carroll, Aidan Chatwin-Davies, Nicholas Hunter-Jones, Jason Pollack, and Grant N. Remmen. Consistency conditions for an AdS multiscale entanglement renormalization ansatz correspondence. *Phys. Rev. D*, 91:125036, Jun 2015.

[50] Glen Evenbly. Hyperinvariant Tensor Networks and Holography. *Physical Review Letters*, 119(14):141602, October 2017.

[51] Elliott Gesteau and Monica Jinwoo Kang. The infinite-dimensional HaPPY code: entanglement wedge reconstruction and dynamics. 5 2020.

[52] Alexander Jahn, Zoltán Zimborás, and Jens Eisert. Tensor network models of AdS/qCFT. *arXiv e-prints*, page arXiv:2004.04173, April 2020.

[53] L. Banchi, P. Giorda, and P. Zanardi. Quantum Information-geometry of Dissipative Quantum Phase Transitions. *Physical Review E*, 89(2):022102, February 2014.

[54] Sergey Bravyi. Lagrangian Representation for Fermionic Linear Optics. *Quantum Information & Computation*, 5(3):216–238, 2005.

[55] F. Caruso, J. Eisert, V. Giovannetti, and A. S. Holevo. Multi-mode Bosonic Gaussian Channels. *New Journal of Physics*, 10(8):083030, August 2008.

[56] Christian Weedbrook, Stefano Pirandola, Raúl García-Patrón, Nicolas J. Cerf, Timothy C.

Ralph, Jeffrey H. Shapiro, and Seth Lloyd. Gaussian Quantum Information. *Rev. Mod. Phys.*, 84:621–669, May 2012.

[57] Xiang-Bin Wang, Tohya Hiroshima, Akihisa Tomita, and Masahito Hayashi. Quantum Information with Gaussian States. *Physics reports*, 448(1-4):1–111, 2007.

[58] Eliska Greplova. Quantum Information with Fermionic Gaussian States. Master's thesis, Ludwig-Maximilians-Universitat Munchen, 2013.

[59] C. V. Kraus, M. M. Wolf, J. I. Cirac, and G. Giedke. Pairing in Fermionic Systems: a Quantum-information Perspective. *Physical Review A*, 79(1):012306, January 2009.

[60] L. Banchi, S. L. Braunstein, and S. Pirandola. Quantum Fidelity for Arbitrary Gaussian States. *Physical Review Letters*, 115(26):260501, December 2015.

[61] Kevin E. Cahill and Roy J. Glauber. Density Operators for Fermions. *Phys. Rev. A*, 59:1538–1555, Feb 1999.

[62] Michael A Nielsen and Isaac L Chuang. *Quantum Computation and Quantum Information*. Cambridge University Press, 2011.

[63] G.-S. Paraoanu and H. Scutaru. Fidelity for Multimode Thermal Squeezed States. *Physical Review A*, 61(2):022306, February 2000.

[64] O. Bratteli and D. W. Robinson. *Operator Algebras and Quantum Statistical Mechanics I*. Springer, 1987.

[65] M. Takesaki. *Theory of operator algebras, I-III*. Springer, 2003.

[66] S. V. Stratila and L. Zsido. *Lectures on von Neumann Algebras, Cambridge II*. Cambridge University Press, 2nd edition, 2019.

[67] U. Haagerup. The standard form of v. Neumann algebras. *Mathematica Scandinavica*, 37(2):271–283, 1975.

[68] Huzihiro Araki. Relative Hamiltonian for Faithful Normal States of a von Neumann Algebra. *Publications of The Research Institute for Mathematical Sciences*, 9:165–209, 1973.

[69] Huzihiro Araki. Relative Entropy of States of von Neumann Algebras. *Publications of The Research Institute for Mathematical Sciences*, 11:809–833, 1975.

[70] Huzihiro Araki and Tetsu Masuda. Positive Cones and L_p-Spaces for von Neumann Algebras. *Publications of The Research Institute for Mathematical Sciences*, 18:759–831, 1982.

[71] D. Petz. Monotonicity of quantum relative entropy revisited. *Rev. Math Phys.*, 15(01):79–91, 2003.

[72] D. Petz. Quasi-entropies for States of a von Neumann Algebra. *RIMS, Kyoto Univ*, 21:787–800, 1985.

[73] M. Ohya and D. Petz. *Quantum entropy and its use*. Berlin, Heidelberg, Theoretical and Mathematical Physics, Springer-Verlag, 1993.

[74] Luigi Accardi and Carlo Cecchini. Conditional Expectations in von Neumann Algebras and a Theorem of Takesaki. *Journal of Functional Analysis*, 45(2):245–273, 1982.

[75] A. Uhlmann. The ‘transition probability’ in the state space of a *-algebra. *Reports on Mathematical Physics*, 9(2):273–279, 1976.

[76] Mario Berta, Marius Lemm, and Mark M Wilde. Monotonicity of Quantum Relative Entropy and Recoverability. *Quantum Information and Computation*, 15(ARTICLE):1333–1354, 2015.

[77] Eric A Carlen and Anna Vershynina. Recovery map stability for the data processing inequality. *Journal of Physics A: Mathematical and Theoretical*, 53(3):035204, 2020.

[78] Anna Jenčová. Preservation of a quantum Rényi relative entropy implies existence of a recovery map. *Journal of Physics A: Mathematical and Theoretical*, 50(8):085303, 2017.

[79] A. Jencova and D. Petz. Sufficiency in quantum statistical inference: A survey with examples. *Infinite Dimensional Analysis, Quantum Probability and Related Topics*, 09(03):331–351, 2006.

[80] D. Sutter, M. Tomamichel, and A. W. Harrow. Strengthened monotonicity of relative entropy via pinched Petz recovery map. *IEEE Transactions on Information Theory*, 62(5):2907–2913, 2016.

[81] M. Berta, V. B. Scholz, and M. Tomamichel. Renyi Divergences as Weighted Non-commutative Vector-valued L_p-spaces. *Annales Henri Poincare*, 19(1843-1867), 2018.

[82] Anna Jenčová. Rényi Relative Entropies and Noncommutative L_p Spaces. 19(8):2513–2542, 2018.

[83] Lawrence C Evans. *Partial Differential Equations*, volume 19. American Mathematical Soc., 2010.

[84] Huzihiro Araki. On an Inequality of Lieb and Thirring. *Letters in Mathematical Physics*, 19:167–170, 1990.

[85] E. Lieb. Gaussian kernels have only Gaussian maximizers. *Invent. Math*, 102:179–208, 1990.

[86] S. Hollands and K. Sanders. Entanglement measures and their properties in quantum field theory. *Springer Briefs in Mathematical Physics*, 2019.

[87] E. M. Stein. Interpolation of linear operators. *Transactions of the AMS*, 83:482–492, 1956.

[88] Ralph Edwin Showalter. Monotone operators in Banach space and nonlinear partial differential equations. 49, 2013.

[89] E. Michael. Continuous selections. I. *Annals of Mathematics Second Series*, 63(2):361–382, 1956.

[90] César R de Oliveira. Unitary evolution groups. *Intermediate Spectral Theory and Quantum Dynamics*, pages 121–144, 2009.

[91] Carlo Cecchini and Dénes Petz. State extensions and a Radon-Nikodỳm theorem for conditional expectations on von Neumann algebras. *Pacific journal of mathematics*, 138(1):9–24, 1989.

[92] H. W. Wiesbrock. Conformal quantum field theory and half-sided modular inclusions of von Neumann algebras. *Comm. Math Phys*, 158:537–543, 1993.

[93] H. W. Wiesbrock. Half-sided modular inclusions of von Neumann algebras. *Comm. Math Phys*, 184:683–685, 1997.

[94] Hans-Jürgen Borchers. On revolutionizing quantum field theory with Tomitas modular theory. *Journal of mathematical Physics*, 41(6):3604–3673, 2000.

[95] F. Verstraete and J. I. Cirac. Renormalization algorithms for Quantum-Many Body Systems in two and higher dimensions. *arXiv e-prints*, pages cond–mat/0407066, July 2004.

[96] Michael Levin and Cody P. Nave. Tensor Renormalization Group Approach to Two-Dimensional Classical Lattice Models. *Physical Review Letters*, 99(12):120601, September 2007.

[97] Peter W. Shor. Scheme for reducing decoherence in quantum computer memory. *Phys. Rev. A*, 52:R2493–R2496, Oct 1995.

[98] Jordan Cotler, Patrick Hayden, Geoffrey Penington, Grant Salton, Brian Swingle, and Michael Walter. Entanglement Wedge Reconstruction via Universal Recovery Channels. *Phys. Rev. X*, 9(3):031011, 2019.

[99] Patrick Hayden and Geoffrey Penington. Learning the Alpha-bits of Black Holes. *Journal of High Energy Physics*, 12:007, 2019.

[100] G. Evenbly and G. Vidal. Algorithms for entanglement renormalization. *Physical Review B*, 79(14):144108, April 2009.

[101] Miguel Aguado and Guifré Vidal. Entanglement Renormalization and Topological Order. *Physical Review Letters*, 100(7):070404, February 2008.

[102] Christopher David White, ChunJun Cao, and Brian Swingle. Conformal field theories are magical. *Physical Review B*, 103(7):075145, 2021.

[103] Sagar Vijay and Liang Fu. Quantum Error Correction for Complex and Majorana Fermion Qubits. *arXiv preprint arXiv:1703.00459*, 2017.

[104] Juan Maldacena and Douglas Stanford. Remarks on the Sachdev-Ye-Kitaev model. *Phys. Rev. D*, 94:106002, Nov 2016.

[105] Ning Bao, Sepehr Nezami, Hirosi Ooguri, Bogdan Stoica, James Sully, and Michael Walter. The Holographic Entropy Cone. *Journal of High Energy Physics*, 09:130, 2015.

[106] G. W. Stewart. On the Continuity of the Generalized Inverse. *SIAM Journal on Applied Mathematics*, 17(1):33–45, 1969.

[107] I. I. Hirschman. A convexity theorem for certain groups of transformations. *J, d'Anal. Math*, 2:209–218, 1952.

[108] Loukas Grafakos. *Classical Fourier Analysis*, volume 2. Springer, 2008.

[109] F. Hansen. The fast track to Löwner's theorem. *Lin Alg. Appl*, 438:4557–4571, 2013.

[110] Xi Dong, Daniel Harlow, and Donald Marolf. Flat entanglement spectra in fixed-area states of quantum gravity. *Journal of High Energy Physics*, 10:240, 2019.

[111] Chris Akers and Pratik Rath. Holographic Renyi Entropy from Quantum Error Correction. *Journal of High Energy Physics*, 05:052, 2019.

[112] Pasquale Calabrese and Alexandre Lefevre. Entanglement spectrum in one-dimensional systems. *Physical Review A*, 78(3):032329, September 2008.